A SYSTEMS STUDY OF VERY SMALL LAUNCH VEHICLES

by

RICHARD J. FRANCIS JR.

Bachelor of Science in Mechanical Engineering
Purdue University, 1998

Submitted to the Department of Aeronautics and Astronautics
in Partial Fulfillment of the Requirements for the Degree of

MASTER OF SCIENCE IN AERONAUTICS AND ASTRONAUTICS
at the
## MASSACHUSETTS INSTITUTE OF TECHNOLOGY

September 1999

Signature of Author: _____
Department of Aeronautics and Astronautics
September 1, 1999

Certified by: _____
Alan H. Epstein
R.C. Macclaurin Professor of Aeronautics and Astronautics
Thesis Supervisor

Accepted by: _____
Nesbitt W. Hagood
Associate Professor of Aeronautics and Astronautics
Chairman, Departmental Graduate Committee

A SYSTEMS STUDY OF VERY SMALL LAUNCH VEHICLES

by
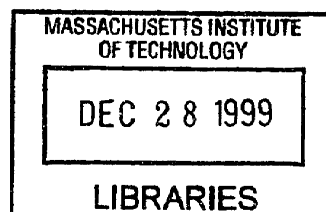
RICHARD J. FRANCIS JR.

Submitted to the Department of Aeronautics and Astronautics
in September 1999 in Partial Fulfillment of the
Requirements for the Degree of
Master of Science in Aeronautics and Astronautics

ABSTRACT

Motivated by the continuing miniaturization of small satellites and ballistic payloads, this thesis studies the performance and feasibility of very small launch vehicles (15 kg – 2000 kg liftoff mass). Gross payload performance for several vehicles was calculated with a commercial three degree of freedom trajectory code. The significance of aerodynamic drag on small vehicles is discussed. Both the options of air and ground-launched vehicles were examined as well as composite configurations with existing motor stages. Parametric analyses were carried out, examining the impact of varying propellant mass fraction, stack fraction, launch conditions (velocity and altitude), and vacuum specific impulse.

All vehicles are based on a version of the MIT microrocket engine, a micro-scale rocket engine fabricated in silicon, and weighing 2 g. The engines use nitrogen tetroxide and hydrazine as propellants which are pump-fed to the engine using micro turbopumps.

Following the performance study, a 77 kg vehicle (w/o gross payload) was carried through a preliminary design. Various subsystems were analyzed, focusing on: vehicle structure, propellant tank design, and propellant pressurization and delivery. The mass of the various vehicle components were analyzed and compared with initial inert mass estimations used to determine gross payload performance.

Thesis Supervisor: Alan H. Epstein
Title: R.C. Macclaurin Professor of Aeronautics and Astronautics

2

TABLE OF CONTENTS

4

ACKNOWLEDGEMENTS

This work is dedicated to my father, Richard J. Francis Sr. His love and support throughout my life has been constant, generous, and indispensable and will always be appreciated.

LIST OF FIGURES

LIST OF TABLES

CHAPTER 1

INTRODUCTION AND PROJECT MOTIVATION

Thundering off the launch pad, the Saturn V was certainly awe inspiring as its five LOX / RP-1 engines generated over 33 million Newtons (7.5 million pounds) of thrust to lift its 2.9 million kilogram (6.4 million pound) mass off the ground. If only required to lift a payload to low earth orbit, the Saturn V could deliver 118,821 kg (262,000 lb_m) to Low Earth Orbit (LEO).[32]

Although the Saturn V was the largest operational vehicle ever built (the Soviet Energia booster runs a close second at 87,982 kg / 194,000 lb_m to LEO), rocket designers of the 1960's had even more grandiose ideas on the drawing board. For example, the Nova booster, an improved version of the Saturn V, was designed to lift up to 1,000,000 pounds (454,000 kg) to LEO.[33] Besides launching men back to the moon and on to Mars, these vehicles would allow the construction literally of "cities" in space.

However, the next 30 years would not see the continued evolution of larger and larger boosters. Instead, the workhorse launchers of the modern era have payload capacities ranging between 500 and 20,000 kg (1,102 and 44,100 lb_m).[33] This range is ideally suited to the primary roles of launch vehicles today, which is as ballistic missiles and for the launch of satellites into earth orbit.

Historically speaking, the last thirty years have seen somewhat of devolution in the size of orbiting satellites and the demand for large launch vehicles. In parallel, the size of electronics and computers has decreased by many orders of
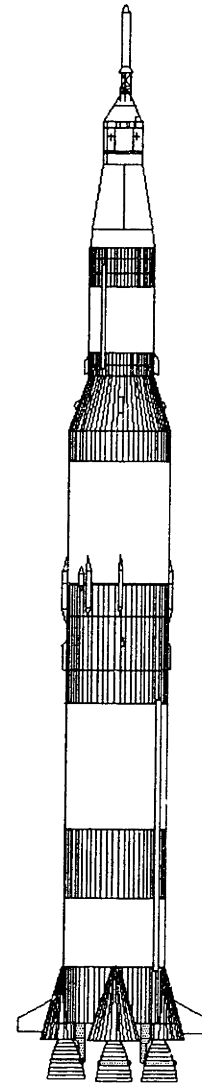
Payload to 200 km	118,821 kg
System Length	102.0 m
Gross Mass	3,038,500 kg

Figure 1.1 – Saturn V Data[32]

magnitude in this time frame, enabling more and more capability to be contained in smaller and smaller packages. The more recent improvements in Micro-Electrical Mechanical Systems (MEMS) are also bringing about the possibility of shrinking mechanisms to the size of today's computer chips, further decreasing the potential size of space systems.

A significant question in today's aerospace industry is whether the launch vehicles and missiles used to deliver orbital and ballistic payloads will shrink with the size of their payloads. Many in the industry contend that as you scale down the size of a launch vehicle, certain factors do not scale down linearly with the mass resulting in difficulty in meeting inert mass and cost targets. However, as this thesis will suggest, there are technologies that show potential for mitigating some of these scale-down effects, and might enable the production of smaller, economical launch vehicles in the near future.

1.1 MODERN LAUNCH VEHICLES

Today's launch vehicles, while smaller than the Saturn V and Energia booster, still are

Table 1.1 -- Launch Vehicle Data[32,33,67]

Vehicle	Country	Length (m)	GLOW (kg)	Payload (kg)	Payload Fraction (%)	Orbital Inc. (deg)	Orbital Alt. (km)	Launch Cost ($ x 10⁶)	Cost Per kg ($ / kg)
Saturn V*	USA	102.0	3,038,500	118,821	3.91%	28.5	200	N/A	N/A
Energia	Russia	97.0	2,524,600	87,982	3.48%	51.6	200	N/A	N/A
Proton D-1	Russia	59.0	669,130	20,860	3.12%	51.6	200	90	$4,314
Ariane V	Europe	53.9	710,000	18,000	2.54%	5.2	185	120	$6,667
Atlas IIAS	USA	47.5	234,000	8,610	3.68%	28.5	185	105	$12,195
Ariane IV (44L)	Europe	58.5	470,000	7,700	1.64%	5.2	185	100	$12,987
Soyuz	Russia	50.6	310,000	7,000	2.26%	51.6	200	35	$5,000
Delta II (7925)	USA	38.1	231,670	4,971	2.15%	28.5	185	52	$10,461
Titan II	USA	42.9	150,530	3,100	2.06%	28.5	185	40	$13,006
Rokot	Russia	22.0	97,170	1,859	1.91%	62.0	300	8	$4,216
Kosmos	Ukraine	26.3	107,500	1,400	1.30%	51.6	400	11	$8,000
Taurus	USA	27.4	73,000	1,300	1.78%	28.5	200	24	$18,462
Conestoga	USA	15.2	87,407	890	1.02%	40.0	463	20	$22,652
Athena	USA	18.9	68,930	794	1.15%	28.5	200	20	$25,189
Pegasus XL	USA	17.5	24,000	460	1.92%	28.5	200	14	$30,444
Shavit	Isreal	15.0	23,400	160	0.68%	143.0	185	N/A	N/A

Notes: *Retired

 *Retired -Variations in Inclination and Altitude will result in differences in perfomance.
 - GLOW = Gross Liftoff Weight -Shavit launch vehicle launches in a retrograde orbit. Posigrade performance would be
 - Launch costs are estimates.   better.
 - Payload Mass does not include -Energia, Shavit, and Conestoga vehicles have not launched since 1988, 1990 and
   fairings.   1995, respectively.

capable of delivering significant payloads to Low Earth Orbit. Table 1.1 shows a sampling of modern launch vehicles and their capabilities to LEO.

As can be seen in Table 1.1, the payload that can be delivered to LEO, when expressed as a fraction of the overall vehicle mass (payload fraction) is on the order of 1% to 4%. This value depends on several things, including: propellant specific impulse, structural efficiency, vehicle size, launch location and method (air or ground), altitude of final orbit, and trajectory to orbit. Looking again at Table 1.1, two trends can be observed. In general, there is a trend toward higher payload fractions as the size of the vehicle increases. The question is whether a significant payload fraction can be maintained with a order-of-magnitude smaller vehicle. The other trend is that the cost per pound of launch tends to increase (disregarding the artificially low Russian booster prices) as vehicle size decreases. This likely is a product of the lowered payload fraction as well as fixed operating costs, etc. that are difficult to reduce on a small scale.

1.2 ROLES FOR A SMALLER LAUNCH VEHICLE

Table 1.2 shows the range of payloads modern launch vehicles are designed to handle. The Shavit, Pegasus XL, Conestoga 1620, and Athena represent some of the smallest of today's

Table 1.2 - New Communication Satellite Networks (1998-2003)

	Data Rate (kbps)	Orbit Altitude (n.mi. / km)		Number of Satellites	Satellite Mass (kg)
ICO	2.4	5,610 /	10,390	12	1925
Teledesic	16.0	378 /	700	288	770
Iridium	2.4	421 /	780	72	700
Globalstar	7.2	761 /	1,410	56	450

vehicles. Interestingly enough, they also are some of the newest vehicles, all developed since 1987. All except for the Pegasus XL were created with an eye toward the rise of large new satellite constellations such as those in Table 1.2. The Shavit and Conestoga have had some difficulties entering regular service, so it is not guaranteed how much of a market share, if any, they will acquire in the future.

Building launchers to serve this demand for LEO telecommunications constellations is proven. However, what about even smaller payloads? Smaller research payloads have been "piggy-backed" onto primary payloads in the past, primarily as small university research projects. This type of launch method limits the mission planners' freedom since the launch profile and conditions will be tailored to the primary payload and the smaller satellite will have to adapt.

What exactly is a small payload? For the purposes of discussion, a few terms will be defined to describe the relative sizes of satellites:

- Conventional Satellites – Mass greater than 1000 kg.
- Small Satellites (Smallsats) – Mass between 100 kg and 1000 kg.
- Micro Satellites (Microsats) – Mass between 10 kg and 100 kg.
- Nano Satellites (Nanosats) – Mass between 0.1 kg and 10 kg.

The majority of satellites launched are in the small or normal ranges. There are many potential possible missions for microsats and nanosats made possible by miniturization technology in the past 20 years. Today's mantra of "faster, better, and cheaper" has caused mission planners to rethink how big a satellite needs to be to accomplish a task. Cost and flexibility are two of the more important factors influencing this way of thinking.

The bottom line in space systems is cost per kilogram to orbit. The last 30 years has not seen much improvement in this metric, and even new proposed reusable launch vehicles don't promise more than a 50% reduction in costs over the Russian boosters on the market[32]. As a result, keeping your payload as small as possible will continue to be the priority of the satellite designer. This favors the use of technologies such as miniaturization of electronics or MEMS to lower satellite mass.

However, cost per kilogram to orbit is based on a launch vehicle lifting its maximum payload to orbit. A launch will costly roughly the same regardless of the payload size. If the payload is smaller than the vehicle's payload capacity, it could be combined with other smaller payloads to reach the payload capacity. Otherwise, the entire launch cost would be divided by the mass of the smaller payload, resulting in a much higher cost per kilogram. In short, if you have a 1 kg nanosatellite and try to launch it on a Pegasus ($13.4 million per launch), you will

actually ring up a cost of \$13.4 million / kg. For smaller satellites, a dedicated small launch system may be the answer.

Micro and nanosat-sized payloads are being planned and developed for a wide range of missions. One of the most promising potential applications for these payloads is orbital servicing and replenishment. Over the next ten years, mainly driven by the telecommunications industry, there will be a great increase in the number of satellites in earth orbit. Commercial companies are developing the majority of these satellites with a focus on cost and profitability. Automated satellites in the 1 to 100 kg range have been suggested to serve as orbital service and

Table 1.3 - Potential Missions For Small Payloads[36,38,66]

	Payload Size	
	(0.1-10 kg)	(10-100 kg)
Commercial Missions		
Satellite Servicing	X	X
Satellite Refueling		X
Satellite Inspection		
Fast Package Delivery (< 90 minutes to any point on the globe)	X	X
Small Deorbiting Tug	X	X
Distributed Satellite Systems for Telecommunication	X	X
Science Missions		
Orbital Debris Simulation / Testing	X	
Distributed Satellite Systems for Atmospheric Measurement and Observation	X	X
Millitary Missions		
Kinetic Energy Kill Weapons	X	X
Ultra-small Survellance Satellites	X	X
Micro Air Vehicle Delivery	X	X
Anti-satellite Weapon	X	X

replenishment vehicles. It is thought that these satellites could perform critical inspection, servicing, repair, and/or refueling functions that could prevent a satellite's failure and/or prolong its life[36]. If this was conducted by a reasonably priced, dedicated launch vehicle, there would be an enormous savings compared with having to replace the aging or failing satellite. Table 1.3 lists more of the potential missions for satellites in the 0.1 kg – 100 kg range (nanosats or microsats).

1.3 CHALLENGES OF SCALING DOWN

Table 1.1 suggests that scaling down a launch vehicle to deliver a 0.1 – 100 kg payload into LEO can be challenging. Costs per kilogram tend to increase, and the vehicle's payload fraction (mass of payload divided by mass of vehicle) seems to decrease. When trying to design a vehicle of this reduced size, it is important to know what the biggest problems that grow more and more significant as you reduce the vehicle's size. The biggest design challenges tend to be :

- Aerodynamic drag reducing performance
- Complexity of creating small components
- Limits on the size of certain components
- Fixed operating costs to launch a small vehicle

Aerodynamic drag is one of the major physical constants that stands in the way of a small launch vehicle delivering a payload into orbit. Taking Konstantin Tsiolkovsky's formulation of Newton's second law (Equations 1.1 and 1.2),[59] we can see the primary loss mechanisms that affect a rocket attempting to make it to orbit. The ΔV terms represent changes in velocity. A rocket going to earth orbit or beyond must acquire enough velocity to either maintain the orbit or escape the pull of gravity from the body it is escaping. Table 1.4 shows various types of missions and the ΔV required to achieve each one. The ΔV term on the left of Equation 1.1 represents the net velocity gain required, which can be found in Table 1.4. Each of the terms on the right side (except $\Delta V_{delivered}$) represent losses from various forces on the vehicle, integrated

Table 1.4 – ΔV Requirements[27]

Mission Type	Ideal ΔV Required (m/s)	Net ΔV Required (m/s)
Earth Orbit	7,500 - 10,000	9,100 - 12,500
Escape from Earth Orbit	11,200	12,900
Earth to Moon (no return)	13,100	16,100
Earth to Mars (no return)	17,500	20,000
Earth to Moon (return)	15,900	18,600
Earth to Mars (return)	22,900	27,000
* Ideal ΔV is without losses (drag, steering)		
* Net ΔV includes major losses		

over the flight path. $\Delta V_{gravity}$ is the integrated velocity loss imparted by the force of gravity on the vehicle during flight. ΔV_{drag} is the same integrated velocity loss from the fluidic retarding effects of the atmosphere. $\Delta V_{steering}$ is the loss from inefficiently pointing the thrust vector of the vehicle away from the velocity vector to create pitching moments on the vehicle for trajectory control. $\Delta V_{delivered}$ is a way of expressing the integrated propulsive force from the engine on the vehicle. It is the sum of the ΔV_{net} required to place the payload in the desired orbit plus all of the other ΔV loss terms.

$$\Delta V_{net} = \Delta V_{delivered} - \Delta V_{gravity} - \Delta V_{drag} - \Delta V_{steering} \qquad \textbf{Equation 1.1}$$

$$\Delta V_{net} = g_0 I_{sp} \ln \frac{m_{initial}}{m_{final}} - \int_0^{t_{bo}} g \cos\theta - \int_0^{t_{bo}} \frac{C_d A_{ref} \frac{1}{2} \rho_{atm} V^2}{m} dt - \int_0^{t_{bo}} \frac{F}{m}(1 - \cos\alpha') dt \qquad \textbf{Equation 1.2}$$

By the expanded ΔV_{drag} term in Equation 1.2, it is possible to see the difficulties with scaling down the vehicle. The A_{ref} term is usually assumed to be the characteristic cross-sectional area of the rocket. This term scales with the square of the diameter. In the denominator, m, the mass of the vehicle, depends on the volume of the vehicle, which can be roughly expressed as $A_{ref}*L$, where L is the length of the vehicle. therefore, the integral for drag loss on the vehicle scales with 1/L.

For large boosters the size of an Atlas IIAS or a Proton, this drag loss is on the order of 1% of the ΔV delivered to the vehicle from the propulsion system.[59] However, as the vehicle size decreases, this term becomes more significant. Figure 1.2 illustrates this effect for various vehicle sizes. (The method and assumptions made in creating vehicles and the software used to determine performance are explained in depth in Chapter 2. The vehicles used to generate Figure 1.2 are based on the baseline design outlined in Chapters 2 and 3.) Figure 1.2 plots two parameters vs. vehicle size. First, the relative size of the drag loss integral (ΔV_{drag}) as a percentage of the total ΔV provided by the propulsion system is plotted. Also, the payload fraction is plotted as a percentage for each vehicle. Each vehicle was calculated for a ground-launched trajectory to a 770 km reference orbit with 90.0° inclination.
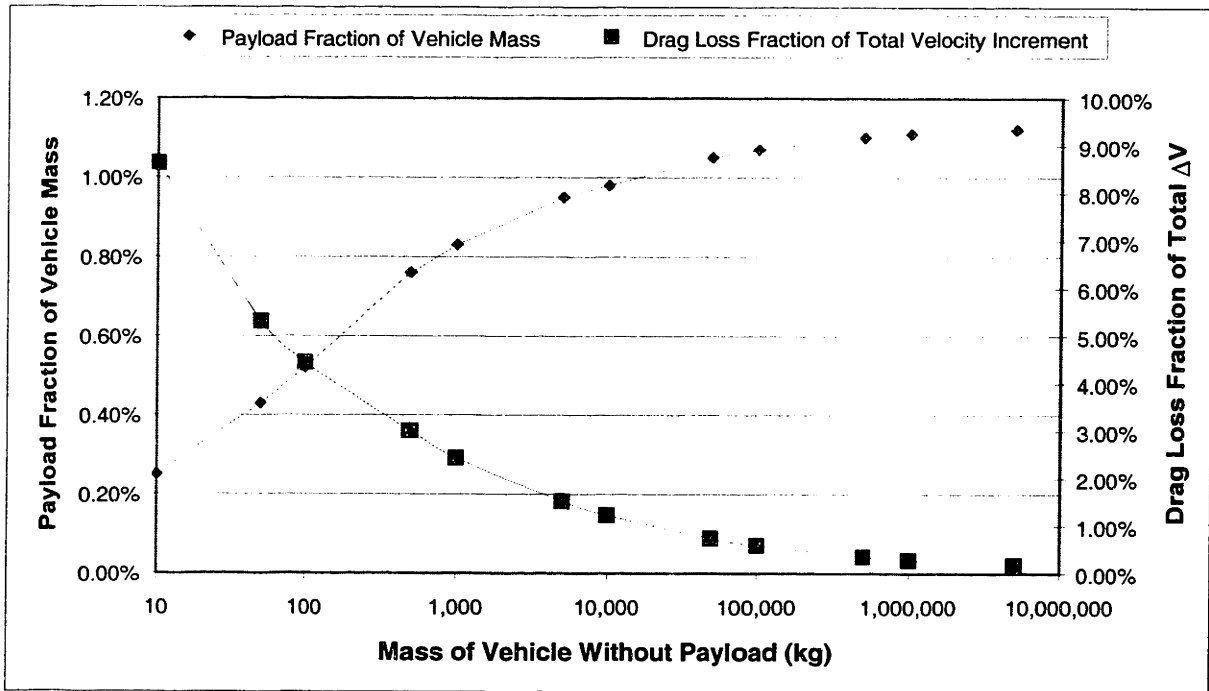
**Figure 1.2 – Effect of Air Drag on Launch Vehicle Performance
(770 km Orbit / 90.0° Inclination / Ground Launched)**

Figure 1.2 shows that the drag force becomes increasingly significant as geometrically similar vehicles get smaller. The effect becomes increasingly significant with tangible impacts on performance to orbit for vehicles smaller than 10,000 kg. The vehicle will not be able to make orbit at all somewhere below 10 kg. However, even a 15 kg vehicle can make orbit, which suggests that aerodynamic drag will not physically prevent the launch of 0.1 kg to 100 kg satellites to orbit, although it will have a significant negative impact on the payload fraction. These trajectory numbers are idealized as will be explained in Chapter 2 and do not take into account specialized maneuvers such as adjustment to transient side loads, etc. Actual performance numbers would be somewhat lower, but this gives a good feel for the trend of drag on vehicle performance as size is varied.

Scaling down a component can introduce manufacturing and design complexity at very small sizes. Standard bolts, mechanical interfaces, and fittings might not be available in the desired size, thus new components and/or system integration approaches may be needed. Very small components for launch vehicles do not now exist, and would have to be either develr ped or adapted from other types of systems.

Another challenge to scaling down a vehicle is that cost tends not to scale down with size. Fixed costs such as range operations do not now decrease linearly with vehicle size. Since all launch vehicles are low production items, their components are very specialized items and usually have to absorb a great deal of variable overhead cost such as for design and tooling. This will scale slightly with size, but not linearly. These costs could raise the net cost per kilogram to orbit as the vehicle gets smaller unless different manufacturing methods are implemented.

1.4 ENABLING TECHNOLOGIES

New design, manufacturing, and operations technologies for making small systems may be able to address some of the difficulties above. Developments in recent years have already brought smaller electrical and mechanical systems. Some of these technologies could come in useful in the design of a small launch vehicle.

1.4.1 MINIATURIZED ELECTRONICS

In 1965, former Intel chairman Gordon Moore stated, that the number of transistors the computer industry would fit on a silicon microprocessor would double every 18 months[40,41]. As
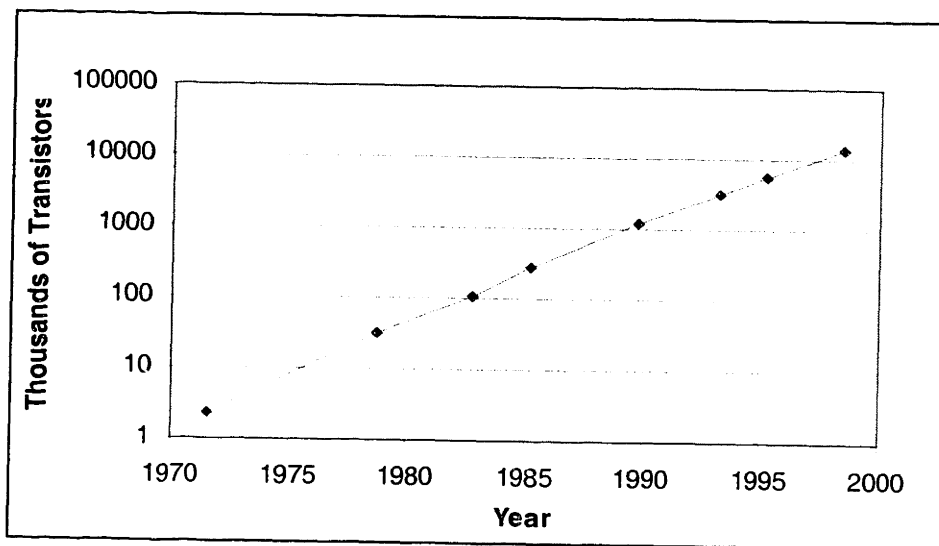
Figure 1.3 – Moore's Law for Microprocessors[40,41]

seen in Figure 1.3, this theory has held up pretty well over the years, and Mr. Moore himself postulates that this will most likely be valid for another "five generations" of chips until the finite size of atomic particles becomes a natural limit to the expansion of processing power. He speculates that this might occur in about 2017.[41]

This process of miniaturization of electronics has enabled huge increases in computing and processing power. This results in lighter and more capable systems for avionics and communication, systems required for small launch vehicles or satellites. For example, the communication system on an Iridium mobile phone handset weighs around 400 grams when stripped of its case and other components. Current research efforts involve creating a "GPS on a chip", which would weigh only 6 grams and enable a vehicle to read satellite GPS signals.[63]

1.4.2 MEMS

Microelectrical and mechanical systems (MEMS) is a technology with the potential to do the same for power, and energy production that the silicon chip did for computing power. Starting from the technological and industrial base in microfabrication of silicon for electronics, MEMS researchers aim to create miniaturized power generators, mechanisms, and even propulsion sources on the order of $\sim cm^2$ in large quantities at very low cost.

For some applications, it is envisioned to use silicon directly as the structural material to maximize the compatibility with current silicon chip fabrication techniques. However, its mechanical properties significantly degrade above 1100°K. Therefore, for high temperature applications, silicon carbide could be used to increase the device's thermal strength.

Current micromachining technology primarily uses lithography to define planar geometries which are then formed into prismatic structures by etching or vapor deposition.[37] Multiple layers / wafers are combined together to form 3-D geometries. Current technology has the capability of combining less than ten wafers. One of the primary advantages of this manufacturing technique is that in-plane geometric complexity is relatively inexpensive to add and that many units can be produced simultaneously. Therefore, there is potential of ending up with extremely complex electromechanical systems at very low cost.

Some example of applications of this technology include valves and fluid flow components, small mechanical locks for nuclear weapons, small transmissions, etc.[37] Some

21

potential uses of MEMS in the design of a small launch vehicle are: microrocket engines and inertial instruments (accelerometers and gyros) needed for navigation.

1.4.3 MICRO-PROPULSION TECHNOLOGY

Much in the same way that the first computer took up a room, current power and propulsion devices are large. Power is produced in large quantities to take advantage of economies of scale, and propulsion is carried out by as few engines as possible in aircraft and spacecraft. However, producing power and/or propulsion in small quantities is an attractive option for mobile power sources, propulsion engines, boundary layer and circulation control, and coolers for both electronics and people.[37]

One example of this miniaturizing of electromechanical systems is a micro-gas turbine engine. Figure 1.4 shows the micro-gas turbine engine as conceived by the Gas Turbine Laboratory at the Massachusetts Institute of Technology (MIT). The micro-gas turbine is a 2 cm
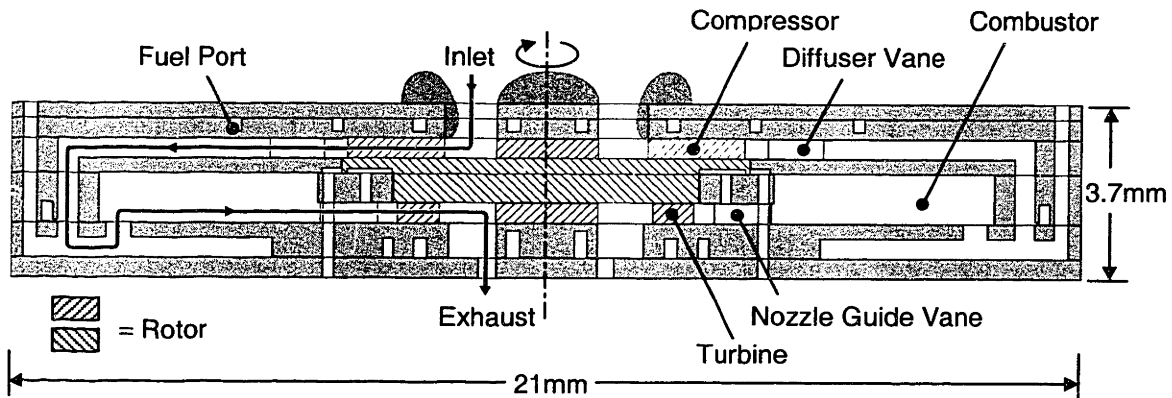
Figure 1.4 – Cross-Sectional Diagram of MIT Micro-Gas Turbine Demonstration Engine.[39,44,45] (Courtesy Jon Protz)

diameter by 4 mm thick silicon heat engine designed to produce 10-20 W of electric power or 0.05 – 0.10 N of thrust while consuming under 10 grams / hour of hydrogen gas as the fuel.[37] Air is the oxidizer. Improvements on the initial design could see a power output of 50 W. The thrust to weight ratio of this device tends to be 5-10 times greater than that of current aircraft engines. This is primarily due to a phenomenon alluded to before in the discussion on drag

called the cube-square "law." As the engine size decreases, the power / thrust decreases by the intake area ($\sim L^2$). The weight of the engine, however, decreases by the volume ($\sim L^3$). Therefore, the thrust-to-weight ratio scales as 1/L.

This scaling principle is one advantage of micro-scale power and propulsion systems. For power systems, the energy density of micro-gas turbine generator could be 20-30 times that of the best battery technology, due to the energy density of the propellants. These generators could be used as distributed, compact, highly redundant auxiliary power units in air and land vehicles.[37]

A micro-gas turbine has propulsion application for small micro aircraft or unmanned aerial vehicles (UAV's). A research project is also currently underway at MIT to design a Micro-Air Vehicle (MAV) using the micro-gas turbine engine as propulsion (Figure 1.5).
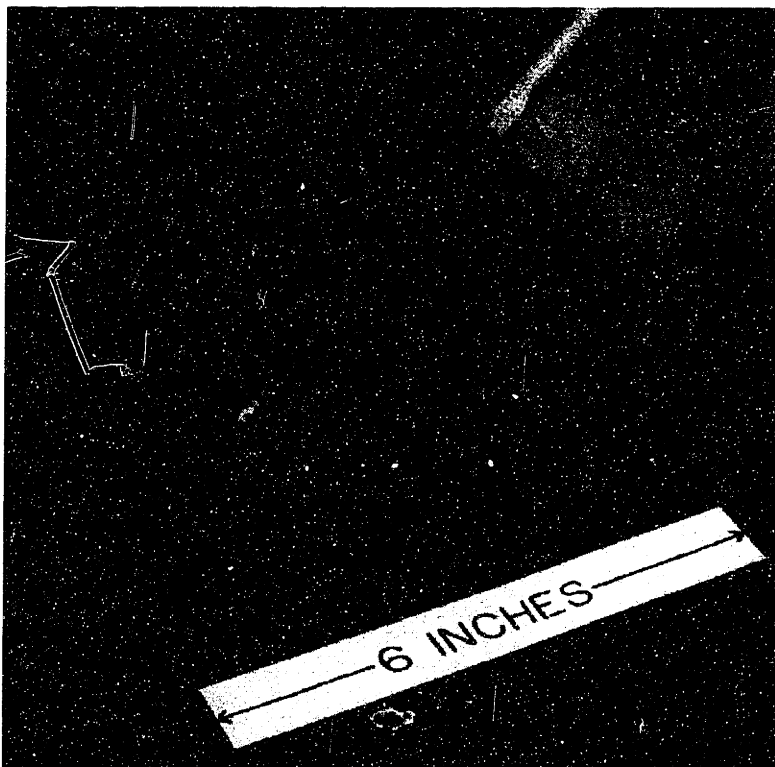
Figure 1.5 – Micro Air Vehicle Mock Up[45]

(Courtesy Mark Drela and Patrick Yip)

The most relevant application of MEMS technology is a micro-bipropellant rocket engine. The micro-gas turbine engine turbomachinery can be adapted to serve as a liquid high pressure turbopump. Combined with a regeneratively cooled combustion chamber and exhaust nozzle, valves and controls, and plumbing, these components form a complete microrocket engine.[37]

An engine of this size would have similar performance advantages due to scaling as the micro-gas turbine. Despite the structural inefficiency of the planar geometry of such an engine, the high strength of the silicon (1 GPa) combined with the cube-square "law" leads to high thrust to weight ratios.[37] Estimated thrust-to-weight ratios for such a device are on the order of 750:1. Table 1.5 shows a sampling of current and historical rocket engines. From Table 1.5 it is apparent that MEMS-based rocket engines offer large potential performance payoff. Also, they can be combined for greater thrust.

Table 1.5 – Thrust-to-Weight Ratios of Various Rocket Engines[32,33,67]

Engine	Launch Vehicle(s)	Propellants	Thrust (vac.) (N)	Mass (kg)	Thrust to Weight Ratio
Microrocket Engine	Very Small Launch Vehicle	Various	15	0.002	765
RD-253	Proton	N_2O_4 / UDMH	1,635,000	1,280	130
RD-210	Proton	N_2O_4 / UDMH	582,100	566	105
RS-27A	Delta 3	LO_2 / Kerosene	1,054,200	1,091	99
F-1	Saturn V	LO_2 / Kerosene	7,740,500	8,391	94
RS-56-OSA	Atlas IIAS	LO_2 / Kerosene	386,400	460	86
Vulcain	Ariane V	LO_2 / LH_2	1,075,000	1,300	84
LR 91-7	Titan II	N_2O_4 / Aerozine-50	444,800	565	80
RD-180	Atlas III	LO_2 / Kerosene	4,152,000	5,393	79
J-2	Saturn V	LO_2 / LH_2	1,033,100	1,438	73
SSME	Space Shuttle	LO_2 / LH_2	2,278,000	3,177	73
RL-10A-4	Atlas IIAS	LO_2 / LH_2	73,400	141	53
RL-10	Saturn IV	LO_2 / LH_2	66,700	131	52
L7	Ariane V	N_2O_4 / MMH	27,400	110	25

MIT is embarked on a research program to develop a microrocket engine using liquid oxygen and methanol as propellants. It is sized to produce 15 N of thrust in a package about the size of a dime (Figure 1.6) weighing about 2 grams. The current configuration is pressure-fed, but subsequent generations are planned to be pump-fed devices, using the micro-gas turbine

Figure 1.6 – Dime-Sized Micro-Rocket
(Courtesy Adam London)

technology for the turbopumps. A schematic of the MIT Micro-Rocket complete with propellant pumps is shown as Figure 1.7.

Integrating the microrocket engine's systems on one chip has many advantages. Since only one manufacturing process is needed to produce the entire engine, the cost of interfaces and related integration activities is eliminated. As well, reliability will be increased with the lack of separate, connected components. It is also possible to combine the valves and control for the engine on the same chip, which would even further lower costs and increase reliability.
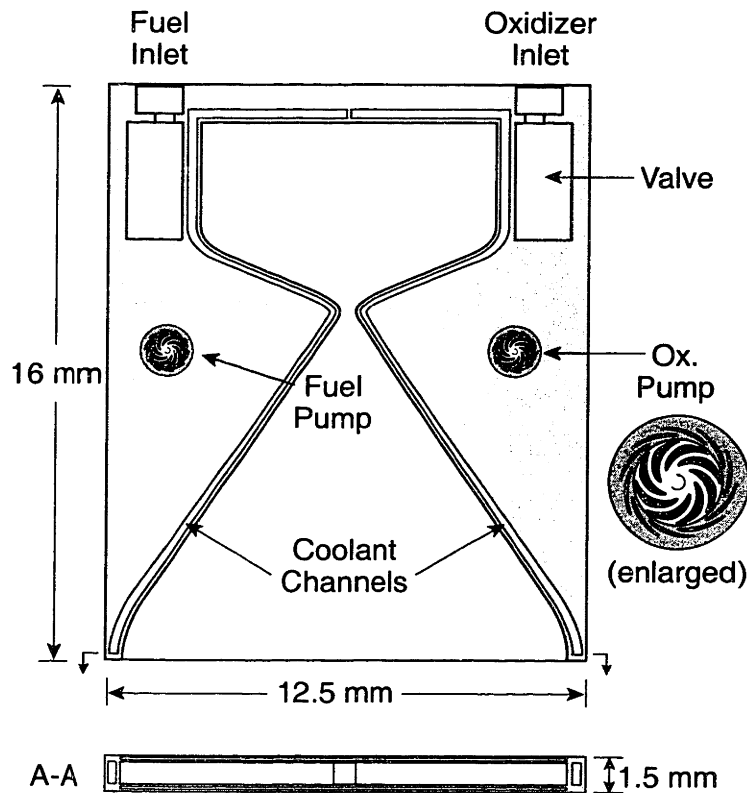
Figure 1.7 – Schematic of MIT / NASA Microrocket Engine Including Pumps
(Courtesy Adam London)

25

A study is currently being conducted to adapt the MIT Microrocket Engine to use storable propellants instead of cryogenic ones like LO_2. This would suit a vehicle that would be transportable and could be preloaded in the factory. They eliminate the need for thermal conditioning devices for cryogenic propellants, which is an advantage of storable propellants over cryogenic ones. Storable propellants are also easier to handle. However, the performance of storable propellants is usually inferior to LO_2 combinations. The system designs are being developed for nitrogen tetroxide (N_2O_4) and hydrazine (N_2H_4), and for hydrogen peroxide (H_2O_2) and ethanol.[42] Section 2.1 explains the propellant choices and the baseline microrocket engine used in the vehicle systems design in greater detail.

1.5 MISSION REQUIREMENTS

Chapters 2 and 3 develop a preliminary design and layout for a small launch vehicle to service a small payload. Keeping in mind the potential missions for small (nano or microsatellite sized payloads) outlined in Section 1.2, some goals for the vehicle design need to be laid out in advance.

One advantage of using a microrocket engine as the main propulsion system for a small launch vehicle lay in the modularity of the engines. If the engines can be efficiently arrayed together and controlled, a "building block" approach can be taken to the thrust of the engines. In this way, propulsion can be configured to loft any payload into orbit. Considering this, the vehicle will use an array of microrocket engines for main propulsion. Attitude control can be accomplished by differentially throttling engines.

There is a wide range of payload types and sizes that may be carried by a small launch vehicle. Due to the size and weight of current electronics components and projected nanosatellites, a vehicle should be designed to lift 100 grams or greater into orbit. However, the exact selection of a target payload is arbitrary. With that in mind, the design will focus on a default size, to be explained in Chapter 2. With this configuration, the final stage of the launch vehicle must have at least one engine, although three are needed if attitude control is done by thrust vectoring.

Two delivery orbits will be considered for the vehicle. First, a standard 200 km (108 n.mi.) circular orbit at 28.5° inclination will be used. This represents a standard low earth orbit mission launched from Cape Canaveral Air Force Station in Florida. The second mission is a 770 km (416 n.mi.) circular polar orbit at 90.0° inclination. This orbit is the most difficult to reach since the launch vehicle does not use the initial velocity generated by the spinning of the earth to its advantage. Therefore the two orbits define a performance envelope encompassing a large portion of the missions outlined in Section 1.2.

In meeting these requirements, both air and ground launched configurations will be looked at. Air launched configurations offer benefits with reduced aerodynamic drag, flexible launch location, and the possible avoidance of range costs discussed in Section 1.3.

In summary, the guidelines for the subsequent launch vehicle design are outlined below. The advantage of the resulting design is that it can be reconfigured for different thrust levels.

- Microrocket engines used for main propulsion and attitude control.
- Capable of delivering at least 100 g to orbit.
- Capable of 200 km circular orbit at 28.5° inclination.
- Capable of 770 km circular orbit at 90.0° inclination.
- Lowest cost design possible without sacrificing mission capability.

CHAPTER 2
VEHICLE DEFINITION

Before launching into the detailed design of the launch vehicle's systems, the overall vehicle size and performance must be determined. Using set values for the performance of the microrocket engine and assumptions for certain vehicle parameters for the overall vehicle such as inert mass fraction, it is possible to parametrically vary several design variables to obtain a preliminary configuration for the vehicle. After completing this, the systems for the vehicle can be determined. The results of the system design are then compared with the assumptions made during the initial vehicle definition phase.

2.1 MICROROCKET PROPULSION SYSTEM

As was mentioned in Section 1.5, the MIT microrocket engine will be used as the baseline for performance calculations for the launch vehicle. The current version being fabricated and tested is a pressure-fed configuration using methanol and liquid oxygen as propellants. The next generation of the microrocket is envisaged as using micro-turbopumps.

For small launch vehicle applications, there is considerable advantage to using storable propellants instead of cryogenic ones. Storable propellants are liquid at room temperature and can be stored for long periods in sealed tanks. This provides flexibility and simplicity in the design, making it easier for the launch vehicle to be mounted to an airplane and air-launched, if desired. Even with heavy insulation and low conductivity structural tank supports, it is not possible to prevent the continuous evaporation of cryogenic fluids.[27] Hydrazine (N_2H_4) and nitrogen tetroxide (N_2O_4), one of the most popular storable propellant combinations, has the added advantage of being hypergolic. This eliminates the need for an ignition system.

When examining candidate propellant combinations, two of the most important considerations are specific impulse and propellant density. Specific impulse, the ratio of thrust over mass flow rate of propellants, is the most important indicator of performance. Density of

propellants is important, as that dictates the overall size and mass of propellant tanks and propellant fluid management systems.

Most storable propellants have disadvantages. They have lower specific impulse values than cryogenic combinations with liquid hydrogen. However, those cryogenic propellant combinations experience a penalty in fluid density. The density of liquid hydrogen is 7% that of water, where most other propellants are 60% - 140% the density of water.[27]

In deciding which propellant combination to use in the vehicle, there are many considerations. The foremost are performance (i.e. the specific impulse), maximum operating temperature, density, compatibility, cost, and usability as coolant for the overall engine cycle. Table 2.1 shows a few rocket propellant combinations, their maximum performance values, cost per kilogram and Newton of thrust[33] (where available),average density, and adiabatic flame temperature (chamber temperature).

Table 2.1 - Performance and Cost Data for Propellant Combinations[33,68,69]

| Oxidizer | | | | Fuel | | | | MR | | | | |
Name	Type	ρ (kg/m³)	Cost per kg ($/kg)	Name	Type	ρ (kg/m³)	Cost per kg ($/kg)	MR	ρ (kg/m³)	Isp (s)	Cost per N thrust ($/N)	Tc (K)
Nitrogen Tetroxide	Storable	1440	$6.00	Hydrazine	Storable	1010	$17.00	1.10	1197	318	$0.035	3183
Nitrogen Tetroxide	Storable	1440	$6.00	MMH	Storable	880	$17.00	1.80	1173	312	$0.032	3332
Nitrogen Tetroxide	Storable	1440	$6.00	UDMH	Storable	790	$24.00	2.20	1145	309	$0.038	3390
Hydrogen Peroxide (70%)	Storable	1308	$4.04	Ethanol	Storable	870	$0.52	6.25	1223	258	$0.014	2155
Hydrogen Peroxide (95%)	Storable	1418	$5.48	Ethanol	Storable	870	$0.52	4.25	1267	294	$0.015	2810
Hydrogen Peroxide (98%)	Storable	1431	$5.66	Ethanol	Storable	870	$0.52	4.00	1268	297	$0.016	2862
Liquid Oxygen	Cryogenic	1140	$0.08	Liquid Hydrogen	Cryogenic	70	$3.60	3.70	268	431	$0.002	2835
Liquid Oxygen	Cryogenic	1140	$0.08	Ethanol	Storable	870	$0.52	1.60	1018	312	$0.001	3440
*Frozen / non-shifting equilibrium condition used for performance data. *MR is mass mixture ratio of oxygen to fuel.												
*Cost data for H₂O₂ and Ethanol from current sources. N₂O₄, N₂H₄, MMH, UDMH from 1990. LO₂, LH₂ from ~1985.												

Performance values were calculated using NASA's Chemical Equilibrium Code[46], which calculates the combustion of propellants and their subsequent inviscid, adiabatic expansion through a specified converging-diverging nozzle. Input parameters specified were the same as that for the current LO$_2$-methanol microrocket engine. That is, a supersonic expansion ratio (exit

area divided by throat area) of 15 and a chamber pressure of 125 atm (1837 psia). Frozen, non-shifting equilibrium results are selected over shifting equilibrium data due to the short residence time of the propellants in the microrocket engine chamber. These result in lower values for specific impulse (I_{sp}) than the equilibrium case, and are used in Table 2.1.

Nitrogen tetroxide and hydrazine derivatives (MMH, UDMH) have been used extensively for main propulsion for launch vehicles, attitude control, and satellite propulsion applications. These combinations are probably the most utilized storable propellant combination.

Hydrazine (N_2H_4) is a clear organic liquid compound that is spontaneously ignitable with nitric acid and nitrogen tetroxide. Its vapors can form explosive mixtures with air. Hydrazine has a positive heat of formation, which gives it good performance. Pure anhydrous hydrazine is stable up to at least 530°K (493°F), however, it is extremely shock sensitive. If shocked by a pressure wave, it can decompose or combust at temperatures as low as 367°K (209°F). It is extremely toxic and is a known carcinogen. This fact accounts for the high cost per kilogram of hydrazine derivatives. Environmental regulations have made it complicated and expensive to use the compound, which has driven aerospace designers to look for alternative propellants. Unsymmetrical dimethyl hydrazine [$(CH_3)_2NNH_2$], or UDMH has replaced hydrazine in most main propulsion applications due to its lower shock sensitivity, lower freezing point, and higher boiling point. Monomethyl hydrazine (CH_3NHNH_2), or MMH is used more often in satellite applications due to its slightly higher density and performance when compared to UDMH.[27] As can be seen in Table 2.1, UDMH and MMH have slightly lower performance than N_2H_4, which is the main penalty for the increased stability and liquid temperature range.

Nitrogen tetroxide is a reddish-brown mildly corrosive liquid when pure, which forms strong acids (HNO_3) with water. While not shock sensitive, it is highly toxic and environmental regulations account for its high cost per kilogram, much the same as with hydrazine derivatives.[27]

Hydrogen peroxide has been proposed in recent years as a "non-toxic" alternative oxidizer to nitrogen tetroxide. Its theoretical performance in combination with ethanol, as noted in Table 2.1, is less than NTO – hydrazine combinations. While not a carcinogen nor toxic, it still has significant issues that need to be considered when determining its suitability as a propellant. Hydrogen peroxide is stable and safe in concentrations at 70% or below. In those concentrations it can be shipped cross-country with little regulation.[69] However, 70% hydrogen peroxide with

ethanol has very poor performance when compared to NTO-hydrazine. To be a useful propellant, it needs to be used in 95% or 98% concentrations, commonly called high test peroxide (HTP). At these concentrations, H_2O_2 is extremely sensitive to impurities which act as catalysts for the exothermic decomposition of H_2O_2 into oxygen and superheated steam. Contaminated liquid peroxide may explode at temperatures above 448°K (346°F). H_2O_2 is also not by itself hypergolic with other propellants. The H_2O_2 must be decomposed and then the heat generated can be used to begin the combustion process.[12] Research has been recently conducted into a methanol-based catalytic fuel called NHMF which uses the catalyst suspended in the fuel to lower the ignition delay sufficiently to make the combination effectively hypergolic.[60]

Propellant selection is a major design issue for this small launch vehicle. If a hydrazine-nitrogen tetroxide combination is chosen, the vehicle will have high performance with hypergolic propellants. Hypergolic propellants will eliminate the need for a separate ignition system. However, the system will have to be designed to avoid any accidental propellant contact, and encounter increased handling difficulty and eventually cost due to the hazards of using NTO and hydrazine. If a hydrogen peroxide and ethanol combination is chosen, it will either have to add an ignition system or operationally prove a catalytic fuel like NHMF.

Engine cooling requirements stemming from of the relatively low melting temperature of the silicon structural material limits the engine chamber temperature. Preliminary concerns with the cooling capacity of the engine led to setting the adiabatic flame temperature to 3000°K.[47] Hydrogen peroxide – ethanol has a chamber temperature below 3000°K (2862°K for 98% H_2O_2) at the mixture ratio of maximum performance. However, as can be seen in Table 2.1, nitrogen tetroxide – hydrazine has a chamber temperature of 3183°K at the mixture ratio of maximum performance. In Figure 2.1, the variation of vacuum specific impulse with mixture ratio can be seen for frozen / non-shifting equilibrium of nitrogen tetroxide – hydrazine. The chamber temperature roughly follows the I_{sp} curve. To achieve a chamber temperature of no more than 3000°K, the mixture must either be oxidizer or fuel rich. In order to meet cooling requirements, a fuel rich configuration was considered with a mixture ratio of 0.9 instead of the optimum of 1.1. This gives a theoretical vacuum specific impulse value of 315 seconds with a chamber temperature of 2952°K. In practice, specific impulse values in actual rocket engines are 3% to 12% lower than the theoretical[27], due to nozzle and combustion inefficiencies. For this reason, the vacuum specific impulse has been derated to 290 seconds, 8% less than the theoretical value.

31

This is the value considered for performance of the nitrogen tetroxide – hydrazine system. Since then, calculations have indicated that the optimum mixture can be used and that there is enough cooling capacity in the propellants to keep the material temperature within limits even with a
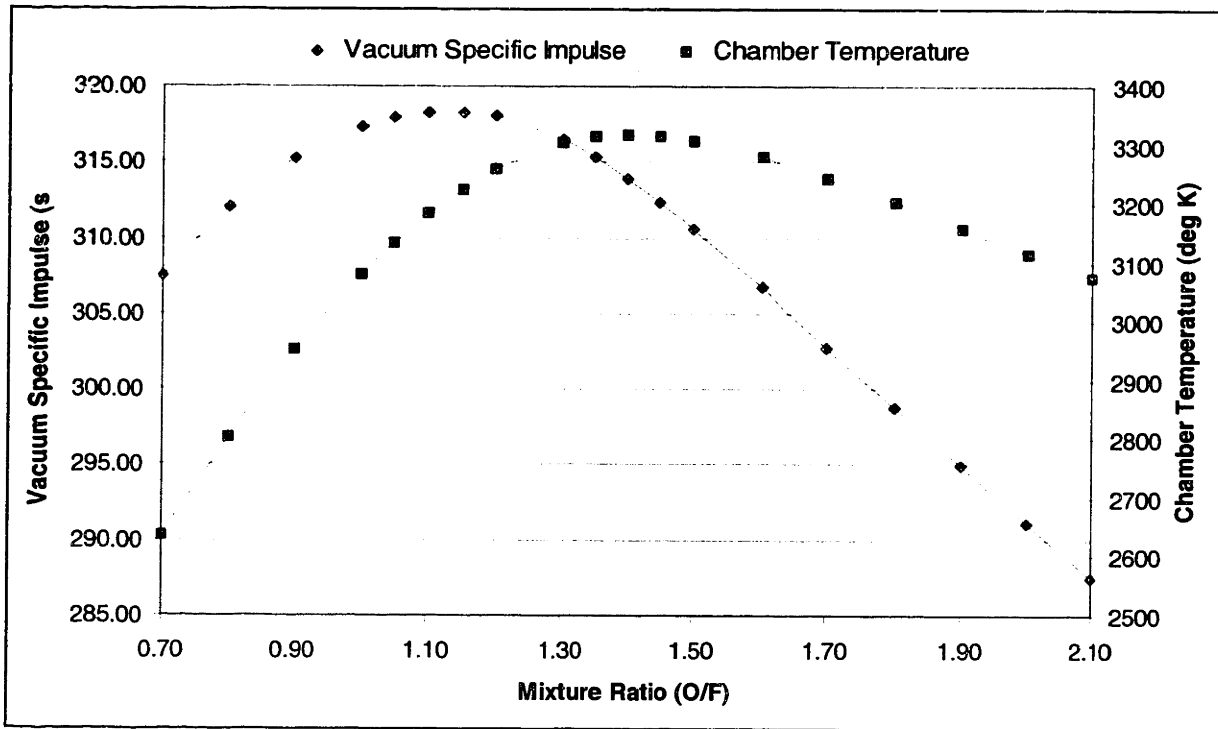
Figure 2.1 – Performance of a Nitrogen Tetroxide – Hydrazine Microrocket Engine (Non-shifting Equilbrium)

chamber temperature of 3183°K.[47] Therefore, the I_{sp} used in the subsequent calculations is conservative, but should serve to set a margin of error on all of the performance numbers. Of course, future experimental verification of the microrocket engines thermal integrity is planned and required.[63]

For such a temperature limited design, the hydrogen peroxide - ethanol and nitrogen tetroxide – hydrazine combinations have roughly equivalent performance. Cycle analysis is currently being conducted on both propellant combinations to look extensively into cooling issues, power generation for turbopumps, etc.[42] Considering the uncertainties with creating a micro-catalyst for the hydrogen peroxide and the relatively large experience base with nitrogen tetroxide and hydrazine, it was decided to carry both combinations forward. Hydrazine was also

chosen above UDMH or MMH due to its slightly higher performance and the fact that it can be catalytically decomposed, where UDMH and MMH can not be. The design team is still considering decomposing the hydrazine to power the turbopumps. Specifications for the nitrogen tetroxide – hydrazine microrocket for the small launch vehicle appear in Table 2.2.

Table 2.2 – Specifications for Nitrogen Tetroxide – Hydrazine Microrocket Engine

Performance	
Thrust	15 N
Isp-vac	290 s
Pchamber	125 atm
Dimensions	
Length	18.0 mm
Width	13.5 mm
Height	2.8 mm
Mass	0.002 kg
Exit Area	11.5 mm^2
Exit Area / Nozzle Area	15

2.2 VEHICLE PERFORMANCE MODELING

With engine specifications determined, the next step is to determine a series of vehicles for which trajectories will be calculated to define capabilities to meet the targeted missions. The baseline for propulsion will be the nitrogen tetroxide – hydrazine fueled microrocket described in Section 2.1. The total propulsion system will be configured in a building block approach by combining together as many base propulsion units (microrocket engines) as necessary to meet a desired thrust level.

Various other parameters are specified and performance is calculated using a commercial, 3 degree of freedom trajectory code called DAB Ascent 2.0. Assumptions about vehicle inert mass, drag, etc. made in this phase of the study will serve as design targets for the next phase (Chapter 3). This systems design phase will validate the parameters set in this phase, closing out the preliminary design.

DAB Ascent 2.0 is a three degree of freedom trajectory code which tracks vehicle orientation in all three axes as dictated by control logic, and does not reflect moments of inertia

nor torques. Values and tables for the atmosphere, gravitational conditions, and aerodynamic effects (drag and lift coefficients) can be specified in the program to allow customization of the problem.

Ascent 2.0 uses a standard fourth-order Runge-Kutta integrator with a step size controlled by either the user or the program. Finite differencing determines the sensitivities of specified target sensitivities to controls. This general method allows the user to meet targets by specifing controls.[48]

The program is quite flexible in allowing a wide variety of vehicles to be simulated. It is an event driven code, so times for ignition and burnout of stages must be specified along with thrust profile for each stage. Any number of stages may be specified, along with any thrust history that can be tabularly expressed. The mass flow rate to produce the specified thrust must be specified, which in turn fixes the vacuum specific impulse. These values are input in a tabular format indexed with time, and the code linearly interpolates between consecutive entries. Values may be input for aerodynamic coefficients (i.e. lift and drag), which allow flexibility in specifing the vehicle's geometrical configuration. For example, by entering in the appropriate lift and drag coefficients, a winged air-launched vehicle like the Pegasus XL may be modeled as easy as a simple cylindrical vehicle like a Titan II.

One of Ascent 2.0's most useful features are its controls and targets. The user can link desired output conditions, such as orbital altitude, to steering rates and other variable inputs in order to position the vehicle. Table 2.3 shows a list of the controls and targets that Ascent 2.0 features.

Table 2.3 – Controls and Targets in Ascent 2.0

Controls	Targets
• Ignition Time	• Orbit Radius
• Ballast	• Orbital Velocity
• Pitch Rate	• Flight Path Angle
• Yaw Rate	• Inclination
• Roll Rate	• Right Ascension of Ascending Node
• Launch Aziamuth	• Argument of Periapsis
• Launch Elevation	• Specific Energy
	• Periapsis Radius
	• Apoapsis Radius
	• Latitude and Longitude

The ballast feature was key to determining payload performance to orbit in simulations for the launch vehicle design. This control allows the user to specify a vehicle configuration and add "dead" weight to the configuration until the vehicle is just heavy enough to make it to a stable orbit. This defines the payload the configuration can loft into that desired orbit. It should be noted that this mass includes all orbitally inserted elements such as the payload housing or shroud.

2.3 DEFINITION OF VEHICLE PARAMETERS

The objective of this phase of design is to determine the overall configuration of the launch vehicle and determine its performance to orbit. However, knowing the thrust and vacuum specific impulse of each engine is not sufficient to directly calculate how much payload can be delivered to orbit using the trajectory software. The following information must be determined (or estimated) in order to determine necessary input parameters so as to obtain useful results using Ascent 2.0:

- Number of stages
- Volume of each stage
- Diameter of each stage
- Thrust in each stage
- Mass fraction of propellant of each stage (propellant mass fraction)
- Relative sizes of each stage (stack fraction)

2.3.1 MULTI-STAGE VEHICLES

The principle challenge to the rocket designer is to have as little unnecessary mass in the vehicle as possible. Equations 1.1 and 1.2 show that the propulsive input to the system is dependent on the ratio of initial to final mass over the period of time the engines are firing. This is expressed as $\Delta V_{delivered}$ in Equation 2.1 below. One way to increase vehicle performance is to section the launch vehicle into multiple stages, and eject the used stages during flight. Most

launch vehicles consist of 2 to 4 stages.[32] There is much interest thoroughout industry in creating single stage to orbit or SSTO vehicle, but to date, no one has succeeded in building one.

$$\Delta V_{delivered} = gI_{SP} \ln \frac{m_{initial}}{m_{final}}$$ **Equation 2.1**

To show the advantages of staging and the penalties of a SSTO vehicle, a simple mathematical model is presented to help determine an appropriate number of stages for the launch vehicle being designed. A notional rocket is divided into N stages, all with a average specific impulse of 290 seconds. Each stage has a ratio of propellant mass to the overall vehicle mass (propellant mass fraction, or ζ) of 0.90. A velocity increment (ΔV) for the mission is selected to range from 7,000 to 11,800 m/s. This ΔV is approximately the change in velocity required to reach most LEO orbits. These numbers come from existing vehicles[27], and the results of trajectory runs made for the baseline launch vehicle (Section 2.7). Of course, exact ΔV amounts for gravity, drag, and steering are going to be highly dependent on the particular mission in question, but this analysis serves to give an idea of how useful multistage rockets can be. Finally, the initial launch mass of the vehicle (w/o gross payload) is assumed to be 77 kg.

The mass ratio of the vehicle is defined as the initial mass at launch over the mass of the vehicle after last stage burnout. Likewise, the mass ratio of each stage is defined as the initial mass of each stage divided by the mass of each stage after engine burnout. It can be proven that the optimal configuration of a multistage rocket occurs when the mass ratio of each stage is the same.[27] Table 2.4 summarizes the variables and Equations 2.2 through 2.6 outline the equations to complete the simple model.

Table 2.4 – Variables Used in Multistage Rocket Calculations

m_0	= Initial mass of vehicle at launch
$m_{initial-i}$	= Initial mass of stage i (including everything above it)
$m_{final-i}$	= Final mass of stage i (including everything above it)
MR_i	= Mass Ratio, the ratio of initial over final mass of a stage
m_{pl}	= Payload mass
$m_{stage-i}$	= Mass of stage i
m_{prop-i}	= Propellant mass of stage i
$m_{inert-i}$	= Inert mass of stage i
I_{sp}	= Specific impulse
ΔV_i	= Velocity Increment delivered by stage i
ζ_i	= Propellant mass fraction of stage i (m_{prop-i}/m_{st-i})

$$\Delta V_i = gI_{SP-i} \ln\frac{m_{initial-i}}{m_{final-i}}$$

Equation 2.2

$$m_o = \sum_1^N m_{stage-i} + m_{pl}$$

Equation 2.3

$$m_{stage-i} = m_{prop-i} + m_{inert-i}$$

Equation 2.4

$$m_{prop-i} = \zeta_i * m_{stage-i}$$

Equation 2.5

$$m_{inert-i} = (1-\zeta_i) m_{stage-i}$$

Equation 2.6

Figure 2.2 shows the payload performance to orbit of 2, 3 and 4 stage rockets vs. ΔV requirements between 7,000 m/s and 11,800 m/s for the vehicle specified. A SSTO at Isp = 290 seconds and $\zeta = 0.90$ is unable to deliver any payload for a ΔV requirement above 6400 m/s, so it is not plotted on the graph. Equations 2.2 through 2.6 were solved using TK Solver, a commercial equation solving program.[49]
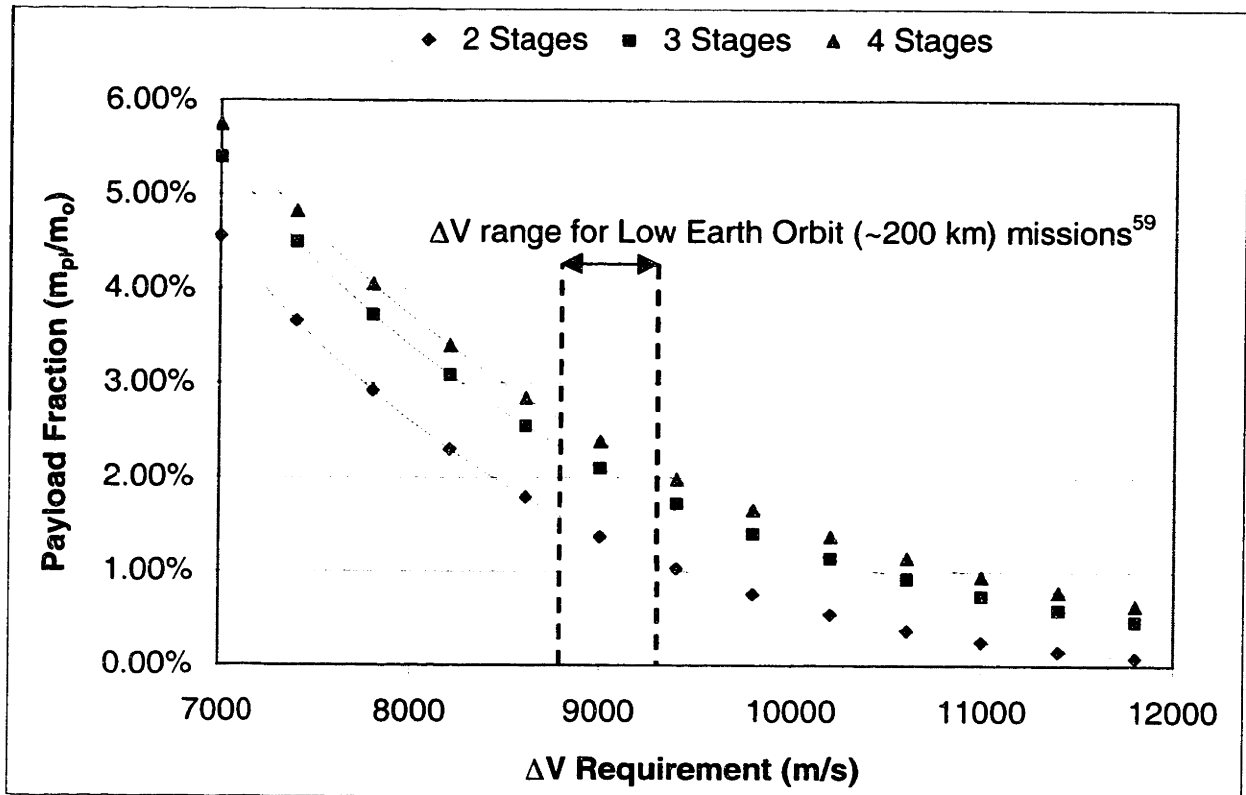
Figure 2.2 – Idealized Performance of Multistage Rockets
(Average I_{sp} = 290 sec ; ζ = 0.90)

Figure 2.2 shows that two, three and four-stage vehicles with the I_{sp} and ζ specified should be able to make all of the ΔV requirements for most LEO missions. However, the advantage of increasing the number of stages is apparent. The advantage of increasing stages diminishes rapidly as you add more and more stages. For example, for a 9000 m/s ΔV mission, the two-stage vehicle lofts 1.37% of its liftoff mass into orbit. Adding an extra stage will get you 2.10% to orbit, a 53% improvement. However, going to a fourth stage gives you 2.38% to orbit. This is only a 13% improvement over the three-stage performance and a 74% improvement over the two-stage design.

The performance increase of adding stages must be traded off against the increased system complexity of multiple stage systems. Each stage added on requires a separate interstage structure, stage separation mechanism, and couplings in all pipes and cables. This added complexity will tend to reduce the overall system reliability. For these reasons, the vehicle with the minimum number of stages that meets the payload and ΔV requirements is usually selected.[27]

For the small launch vehicle being designed, it is likely that a two-stage vehicle will meet the ΔV requirements. One complication with multiple stage vehicles is specific to the size vehicle being considered. Each consecutive stage is considerably smaller than the one before it. This design is constrained by the thrust of the microrocket for the smallest stage. For that reason, a two-stage vehicle will allow the smallest possible vehicle to be designed. For both these reasons, and in order to maximize simplicity in the design, a two-stage design will be carried forward for further consideration.

2.3.2 SCALING OF PHYSICAL PARAMETERS

The process of defining many of the parameters for the micro launch vehicle is an iterative one. A reasonable starting point for this process is to start with the parameters for a current launch vehicle, and use those values as a starting point. Table 2.5 shows various current launch vehicles and their design parameters that are needed by the Ascent 2.0 program to calculate trajectories.

Table 2.5 – Physical Specifications of Current Launch Vehicles[32,33]

Vehicle	Vehicle Mass (kg)	Thrust to Weight Ratio	L/D	Propellant Mass Fractions (λ)				Stack Fractions (f)			
				Stg 1	Stg 2	Stg 3	Stg 4	Stg 1	Stg 2	Stg 3	Stg 4
Energia	2,524,600	1.48	7.54	0.901	0.906			0.611	0.389		
Ariane V	737,000	1.73	10.00	0.874	0.912	0.768		0.750	0.237	0.013	
Proton D-1	712,460	1.27	7.97	0.931	0.930	0.918	0.858	0.657	0.245	0.073	0.025
Ariane IV (44L)	470,000	1.17	15.37	0.897	0.928	0.902	0.872	0.374	0.520	0.079	0.026
Soyuz	297,400	1.38	11.50	0.917	0.936	0.906		0.575	0.340	0.085	
Delta II (7925)	230,000	1.56	15.88	0.896	0.942	0.883	0.883	0.511	0.443	0.030	0.016
Titan II	150,530	1.28	11.61	0.943	0.917			0.803	0.197		
Kosmos	107,500	1.40	10.96	0.939	0.931			0.810	0.190		
Rokot	97,170	1.63	8.80	0.926	0.878			0.863	0.136		
Conestoga	87,407	1.99	12.67	0.882	0.877	0.877	0.892	0.556	0.278	0.139	0.026
Taurus	73,030	1.80	11.25	0.913	0.867	0.898	0.794	0.743	0.196	0.047	0.014
Athena	64,820	2.02	6.25	0.921	0.895			0.830	0.170		
Pegasus XL	24,000	2.07	13.54	0.839	0.904	0.794		0.771	0.186	0.042	
Shavit	23,400	1.80	11.54	0.892	0.839	0.917		0.440	0.472	0.088	
Notes:											

Notes:
 -Many vehicles have strap-on stages that burn in parallel with a core stage. Since these stages burn
 out before the core stage, they were called stage 1 in these cases.
 -Stack Fraction is the ratio of the stage mass to the overall vehicle mass without payload (stack mass).

It is interesting to observe a few trends in Table 2.5. First, the propellant mass fraction (ζ) tends to be higher in the upper stages than the lower. Some of this might be due to the inability of components to scale down relatively in size, as mentioned in Section 1.3. Another cause of this might be that much of the avionics mass in usually contained in the upper stages since they are not discarded until the end of flight. The initial thrust to weight ratio also seems to be a bit higher for smaller vehicles. It is likely that the smaller vehicles, concerned more with drag effects on the vehicle's performance, want to accelerate out of the atmosphere more quickly and not accumulate drag losses.

As a first cut at defining the vehicle size, it is useful to look at vehicles that have similarities with the vehicle being designed. For example, the Titan II is a two-stage launch vehicle that has much in common with the small launch vehicle. It uses N_2O_4 and Aerozine-50, a 50/50 blend of UDMH and hydrazine, as propellants. Although it is several orders of magnitude larger than the vehicle being designed here, it will serve as a reasonable departure point for subsequent analysis.

For determining the diameter and volume of each stage, a "scale model" of the Titan II will be used. Based on a specified mass, and assuming the same L/D (10.00) and average density as the Titan II (475 kg/m^3)[32], scale model vehicles will be specified. For the thrust of each stage, a set initial thrust to weight ratio of 2.00 will be used. This is assumed since it is in line with the thrust to weight ratios of the smallest launch vehicles in service today (Table 2.5). Equations 2.7 through 2.10 show the equations that are used to scale the vehicles. F_T is the thrust of the vehicle, and TTW is the initial thrust to weight ratio, which is assumed to be constant for both stages. L/D is the ratio of the vehicle's overall length to its core diameter.

$$V_{new} = \frac{m_{new}}{m_{old}} V_{old} \qquad\qquad \textbf{Equation 2.7}$$

$$D_{new} = \sqrt[3]{\frac{m_{new}}{m_{Ti\,tan}}} D_{Ti\,tan} \qquad\qquad \textbf{Equation 2.8}$$

$$L_{new} = \frac{L}{D} D_{new} \qquad\qquad \textbf{Equation 2.9}$$

$$F_T = TTW * m_o \hspace{4cm} \textbf{Equation 2.10}$$

These equations are useful in obtaining starting values for the initial series of Ascent 2.0 trajectory runs. The systems specification in Chapter 3 will refine these values and lead to more refined performance numbers.

For the type of vehicle we are considering, we are between the world of missiles and the world of launch vehicles. Missiles tend to have longer L/D's than launch vehicles and lower values of ζ, due to aircraft drag considerations and the fact that they do not have to make orbit. We will consider longer L/D's in this design, provided attitude control and structural integrity is not compromised. However, the high ζ values are unavoidable and this value must be kept in the range of those for current launch vehicles.

Naturally, it is desirable to have the largest ζ possible, which will directly improve performance to orbit. However, at this point a reasonable value of ζ will be chosen, which will set the amount of inert (non-propellant) mass in each stage. The systems design in Chapter 3 will determine the reasonableness of these assumptions. To determine a reasonable value for ζ, it is informative to once again look at Table 2.. Values of ζ for the first and second stages range from 0.839 to 0.943. The Titan II has a first stage ζ value of 0.943 and a second stage ζ value of 0.917. This is among the best values. We anticipate some problems with scaling down the vehicle and its associated subsystems, especially in the smaller second stage. However, the thrust to weight advantages of the microrocket should reduce engine weight. The effect of each is uncertain, so values of 0.940 for the first stage and 0.920 for the second stage will be used in the current design, in line with the Titan II values.

2.3.3 STACK FRACTION OPTIMIZATION

As explained in Section 2.3.1, it is straightforward to determine the optimum configuration of a multistage vehicle with equivalent propellant mass fractions and specifc impulse values. In that case the optimum configuration occurs when the mass ratios of each stage are the same.[27] In the case where one stage might have a different value for ζ or I_{sp} (as in this case), a different method for determining the optimum mass split of the stages must be carried out.

To conduct this analysis, we return to the model presented by Equations 2.2 through 2.6 in Section 2.3.1. Adding Equations 2.11 through 2.13 below, a model can be made for optimizing the stack fractions, denoted by f_i. By assuming a value of ΔV, and parametrically varying f_1 and f_2, it is possible to solve for the combination of f_1 and f_2 that provides the greatest payload performance to orbit for the ΔV requirement.

$$m_{stack} = m_o - m_{pl} \qquad\qquad\qquad \textbf{Equation 2.11}$$

$$f_i = \frac{m_{stage-i}}{m_{stack}} \qquad\qquad\qquad \textbf{Equation 2.12}$$

$$f_1 + f_2 = 1 \qquad\qquad\qquad \textbf{Equation 2.13}$$

A simple iterative procedure was written in Visual Basic interfacing with Microsoft Excel 97 to try the various combinations of f_1 and f_2 for different ΔV requirements between 7,000 m/s and 12,000 m/s. All cases assumed a two stage vehicle with $\zeta = 0.94$ in the first stage and $\zeta = 0.92$ in the second stage. The average I_{sp} for the mission was assumed to be 290 seconds (real value will be slightly lower). Figure 2.3 shows the optimal value of f_1 for a range of ΔV requirements ranging from 7,000 m/s to 12,000 m/s. Figure 2.4 provides a picture of how a non-optimal first stage stack fraction will affect the payload performance to orbit. It shows the effect of varying f_1 on payload fraction for every 1000 m/s increment of ΔV between 7,000 and 12,000 m/s.
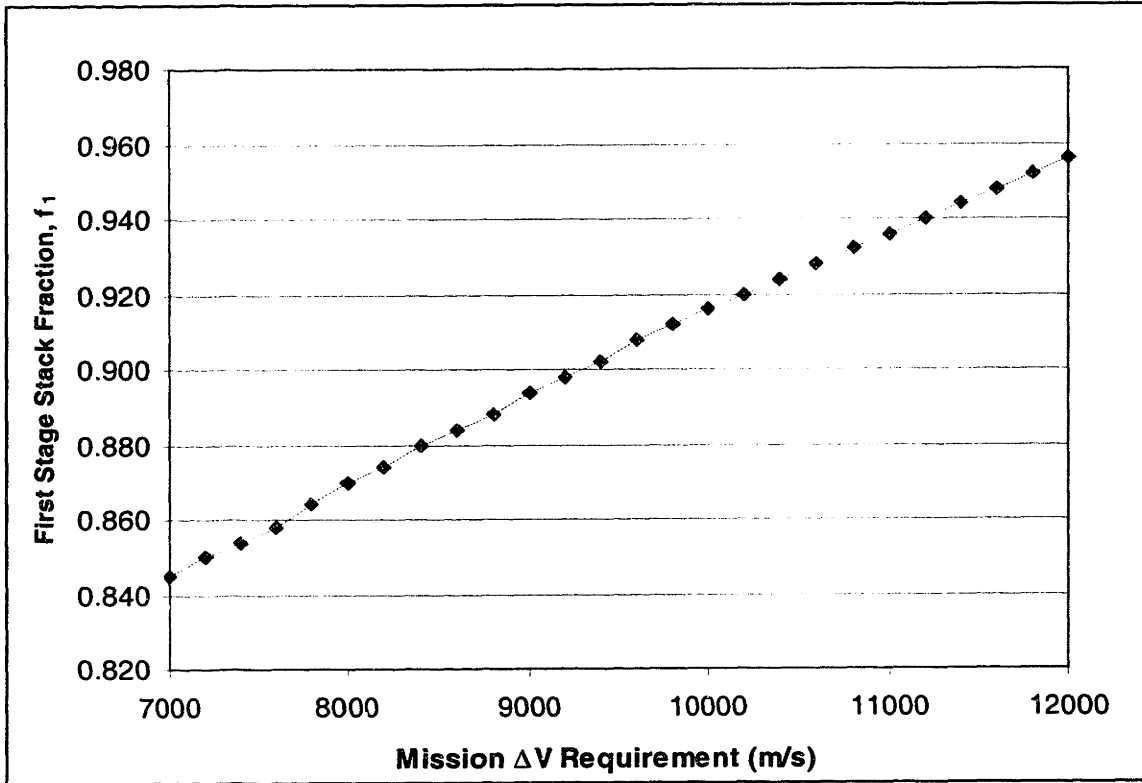
Figure 2.3 – Optimum First Stage Stack Fraction vs. ΔV Requirement
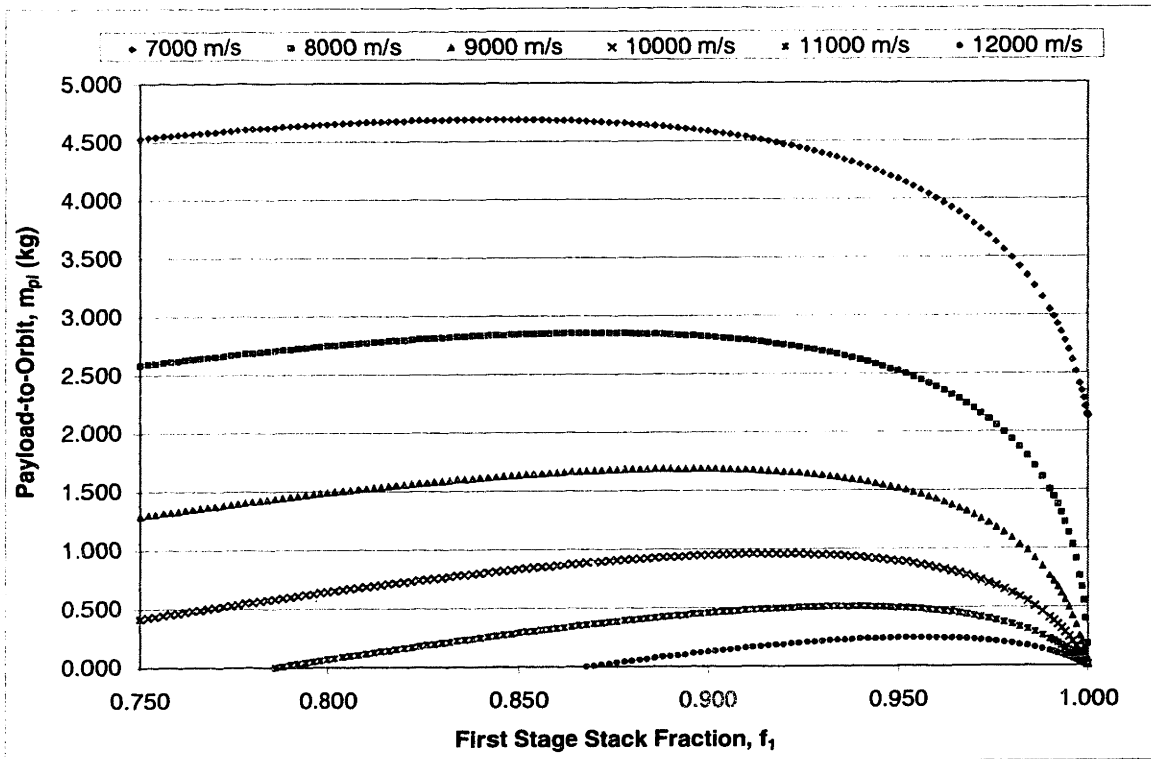
Figure 2.4 – Payload Performance vs. Stack Fraction

As can be seen in Figures 2.3 and 2.4, the optimal mass distribution between stages shifts in response to different ΔV requirements. As expected, the payload to orbit drops sharply towards zero as the first stage stack fraction converges to one, since this would be a SSTO, and it was shown earlier that an SSTO witn $\zeta = 0.90$ and $I_{sp} = 290$ cannot deliver any payload to orbit for a ΔV greater than 6400 m/s. Note however that the optimums are quite broad for ΔV requirements below 10,000 m/s. For example, at a ΔV of 9,000 m/s, the payload varies from the maximum by only 11% between f_1 values of 0.85 and 0.95.

These results suggest that a particular ΔV needs to be selected for the vehicle as an optimization point. With that in mind, the vehicle could perform other missions, but at a non-optimal performance. This is analogous to the design of a commercial aircraft, which is usually optimized for one speed and altitude. The vehicle being designed has four potential missions, which will be discussed in greater detail in subsequent sections. As defined in Section 1.5, the vehicle is being designed for a 200 km circular orbit at 28.5° inclination as well as a 770 km circular orbit at 90.0° inclination. For each of these orbits, both air launching and ground launching will be considered.

Table 2.6 shows the actual ΔV results for the four cases listed above for the final baseline vehicle design. Considering performance results that will be explained later in this chapter, it was decided to choose the 770 km, 90.0° inclination air-launched trajectory as the baseline for design. As a result, a first stage stack fraction of 0.914 exists for the baseline, which is approximately the optimum for the 770 km, 90.0° inclination air-launched mission.

Table 2.6 – ΔV Results For Baseline Vehicle Configuration

Mission			$\Delta V_{required}$
Orbit	Inclination	Launched	(m/s)
200 km	28.5 degrees	Air	8,077
200 km	28.5 degrees	Ground	9,583
770 km	90.0 degrees	Air	9,841
770 km	90.0 degrees	Ground	11,630

2.3.4 VEHICLE PARAMETER SUMMARY

Parameters are now defined for Ascent 2.0. Equations 2.2 through 2.15 and values specified and/or bounded in Table 2.7 are solved for the input parameters in Table 2.8.

Solving for the input parameters usually gives a value of thrust that is not an even multiple of 15 N. That is to say that the vehicle is being designed for a fractional number of microrockets. In this case, the thrust value is rounded off to the nearest multiple of 15 N, which would require an whole number of engines.

$$I_{sp} = \frac{F_T}{\dot{m}g}$$

Equation 2.14

$$t_b = \frac{m_{prop-i}}{\dot{m}}$$

Equation 2.15

Table 2.7 - Vehicle Parameter Summary

Vehicle Definition	
Vehicle Mass	Variable
Number of Stages	2
Propellant Mass Fractions (ζ)	
Stage 1	0.94
Stage 2	0.92
Stack Fractions (f)	0.85 < f < 0.95
Volume, Length, Diameter	Ratioed to Titan II Data
L/D Ratio	6 < L/D < 20
Propulsion	
Number of Engines	Variable (At least 3 in 2nd Stage)
Thrust per Engine	15 Newtons
Engine Exit Area	11.25 mm^2
Thrust To Weight Ratio	2.00
Propellants	
Oxidizer	Nitrogen Tetroxide (N_2O_4)
Fuel	Hydrazine (N_2H_4)
Vacuum Specific Impulse	290 seconds
Initial Conditions	
Launch Height	0 < h < 25,000 m
Launch Inclination	65 deg to 90 deg
Initial Launch Velocity	M = 0.0 to 2.0

Table 2.8 - Ascent 2.0 Required Input Variables

Stage Information	Source
Thrust	User Input
Mass Flow Rate	User Input
Volume	User Input
Mass	User Input
Exit Area	User Input
Ignition Time	User Input
Burn Time	User Input
Aerodynamic Information	**Source**
Cross Sectional Area	User Input
Drag Coefficients	Table Input by User
Atmospheric Conditions	Table in Ascent

2.3.5 TABLE INPUT TO ASCENT 2.0

Ascent 2.0 is flexibile in that you can specify a series of tabular inputs from which the program will linearly interpolate data. This allows the user to specify wind conditions, atmospheric conditions, aerodynamic coefficients (lift, drag), and other parameters.

The default atmosphere table that is used in Ascent 2.0 is based on the 1976 NASA Standard Atmosphere.[51] It indexes pressure, density, temperature, and the speed of sound vs. the altitude above the earth's surface. The program linearly interpolates between data points.

The user is allowed to specify values of aerodynamic coefficients such as lift and drag against the vehicle Mach number. The most accurate way to determine these variables vs. Mach number is by wind tunnel or flight tests. However, since the final vehicle design shape is still undecided, a correlation for the drag coefficient (C_D) vs. Mach number of bodies of revolution was developed in 1959 by Hoerner.[50] The correlation appears in Figure 2.5 below.

For M < 1.3 $\qquad$ For M > 1.3

$C_D = 0.25 * (1 + M^2)$ $\qquad$ $C_D = 0.765 / M^{1/2}$

*Reference area used is the area of frontal projection.

*$C_{D\text{-}MAX} = 0.67$ at M = 1.3.

Figure 2.5 – Correlation for Aerodynamic Drag Coefficient

2.4 PAYLOAD TO ORBIT

A straightforward approach is used to determine the gross payload to orbit. Ascent's targeting features are used to calculate an orbit for a specified altitude, circular orbit, and orbital velocity.

When specifying the burnout altitude (200 or 770 km for our vehicle), a burnout radius is specified. The altitude of the vehicle is the position vector of the vehicle minus the local radius. Due to oblateness of the earth, the local radius can vary slightly, depending on the location. Assuming an average Earth radius of 6378 km, targets were specified as 6578 km for the 200 km orbit and 7148 for the 770 km orbit.

To obtain a circular orbit, the vehicle inertial velocity vector must be in line with the horizon vector. The horizon vector is perpendicular to the position or radius vector, which is measured from an inertial coordinate system centered in the Earth. This calls for an inertial flight path angle of zero degrees. This condition is imposed on the solution to obtain a circular orbit. An illustration of these relationships appears in Figure 2.6.
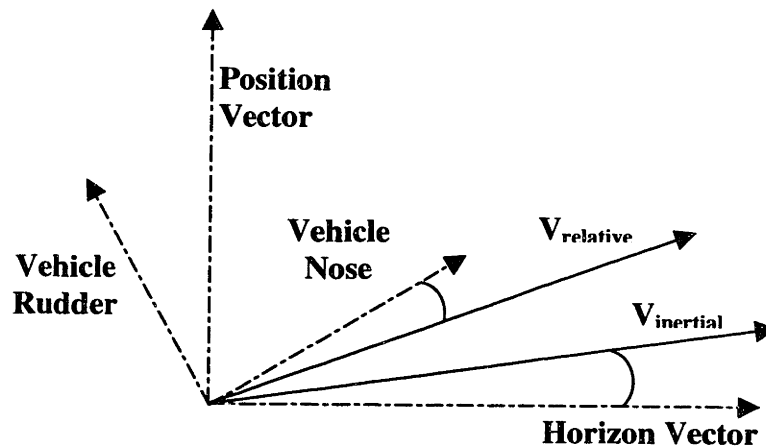
Figure 2.6 - Velocity and Flight Path Angle in Both Coordinate Systems in Ascent 2.0

Orbital velocity required to maintain orbit varies with the altitude / radius of the orbit. Equation 2.16 is used to calculate the required velocity (V_c) to maintain a specified orbit, where r

is the radius of the orbit, and Gm_e is equal to the Earth's gravitational constant of 3.986 x 10^5 km^3/s^2. For the 200 km and 770 km orbit cases, target velocities of 7784.3 and 7467.5 m/s were used, respectively.

$$V_c = \sqrt{\frac{Gm_e}{r}}$$ **Equation 2.16**

In order to determine the amount of payload that could be lofted to the target orbit, the ballast control was used. This varies a fixed mass that is carried with the vehicle throughout flight, much like a payload. However, one point must be made about this. In all of the calculations, the mass of a payload shroud, that would be needed to protect the payload, has not been subtracted from the payload itself. Therefore, unless noted, all of the payload mass to orbit results include a yet to be designed payload shroud.

2.5 BALLISTIC DELIVERY

Two possible roles for a small launch vehicle discussed in Section 1.2 were fast package and micro-air vehicle (MAV) delivery. To accomplish these objectives, the payload that can be delivered by the vehicle on a ballistic trajectory needs to be determined.

A simple ballistic trajectory involves taking off from the launch pad and following a gravity turn trajectory. A gravity turn trajectory is a semi-parabolic trajectory where the vehicle is only turned slowly by the gravity force component acting in a direction normal to the vehicle's flight path. This is the minimum energy required for a given payload and distance.

The first and second stage burns used in the orbital insertion cases (Section 2.4) are still burned in series, but there is no coast phase in between stage burns. Instead of using the orbital conditions as a target, the impact longitude is used to define the vehicle range. By setting the launch site longitude at 0°, and targeting the impact longitude, it is possible to solve for the downrange distance. The launch site latitude is also set at 0° to be conservative, since the Earth's circumference is widest at the equator. Since the spin of the earth can either help (posigrade trajectory) or hinder (retrograde trajectory) the vehicle's performance, the ballistic

48

delivery cases were simulated on a non-rotating earth, which was approximated by increasing the Earth's orbital period by 10 orders of magnitude. This, in effect, will "turn off" the rotation of the Earth. The control for this target is the inclination of the launch pad.

Two ranges were analyzed when looking at ballistic delivery performance. A short range, 1000 nautical mile (7241 km / 65.03° longitude change) trajectory was examined as well as a long range, 4500 n.mi. (1855 km / 16.66° longitude change) trajectory. Payload masses were determined using the ballast control, same as for the orbital cases.

2.6 LAUNCH VEHICLES EXAMINED

With a basic design envelope to work within, a series of launch vehicle designs and configurations were looked at and their performances determined. This information was then used to select a baseline design to be carried forward for systems design and analysis. The masses cited as sizes for the following vehicles are the stack mass. This is the liftoff weight of the vehicle minus the payload mass.

2.6.1 2000 KG LAUNCH VEHICLE

One way to reduce the drag effects of the atmosphere is to launch the vehicle from an airplane. Orbital Sciences Corporation's Pegasus XL launch vehicle is released at approximately 38,000 feet (11,582 m) from the underside of a L-1011 aircraft.[53] At this altitude, the atmospheric density is about 27% of its sea level value[52]. In order to increase the flexibility of the launching platform, the 2000 kg vehicle concept was designed to be able to be air-launched from a US fighter aircraft or smaller commercial jet than the L-1011. Table 2.9 shows the payload carrying capacity of some aircraft. A 2000 kg launch vehicle could be carried by an F-16. This is the

Table 2.9 – Payload Carrying Capacity of Selected Aircraft

Launch Aircraft	Maximum LV Mass	
	(kg)	(lb.)
F-16 C/D	2041	4500
B-1B	1814	4000
B-2	1814	4000
F-22	1361	3000
F-18 E/F	1361	3000

largest vehicle considered in this study. Tables 2.11, 2.12, and 2.13 summarize the vehicle's key design and performance parameters.

2.6.2 MISSILE – LAUNCH VEHICLE COMBINATIONS

Another possibility to lower cost of the overall system would be to use an existing missile as a first stage for the launch vehicle and then, with microrocket engine powered second and third stages, complete the vehicle. This would provide a vehicle in the same size class as the 2000 kg air-launched one without having to worry about the complexity and cost of designing the first stage. If not a primary launch vehicle, this could be a useful testbed for testing microrocket engine powered stages.

Table 2.10 lists the specifications of a representative missile first stage that was considered as a potential first stage for this type of launch vehicle. The propellant mass fraction is well below that of a launch vehicle, which will result in lower performance than for a standard launch vehicle of similar mass. The missile has a stepped thrust profile, burning 40% of its propellant in the first 5 seconds, and 60% of its propellant over the remaining 15 seconds.

Table 2.10 – Missile 1st Stage Parameters

Mass	612 kilograms
$I_{sp\text{-}sea\ level}$	275 seconds
ς	0.78
Thrust	40% m_{prop} during 5 seconds
	60% m_{prop} during 15 seconds
Diameter	0.340 meters
Length	1.727 meters

The remaining stages were sized according to the equations and guidelines given in Sections 2.3.2 through 2.3.4 with one minor variation. The overall vehicle stack mass is constrained at 800 kg, and the first stage mass is assumed constant at the missile mass of 612 kg. This essentially reduces the problem to optimizing the second and third stages within a size envelope of 188 kg.

It should be noted that the above optimization is not actually representative of the optimal stage split for the vehicle. A calculation was performed where the vehicle mass was allowed to fluctuate with the fixed first stage mass. In this case, the optimal vehicle configuration's stack mass was about 1500 kg. When more detailed design was carried out later, the vehicle had a L/D ratio that was considered to be too great. For that reason, the total size of the vehicle was constrained and the 800 kg case was eventually chosen.

The top two stages were analyzed as a stand-alone launch vehicle with a stack mass of 188 kg. This amounts to merely removing the missile 1st stage. Tables 2.11, 2.12, and 2.13 summarize both vehicles' key design and performance parameters.

2.6.3 77 KG LAUNCH VEHICLE W/ AIM-7 LAUNCH TUBE

To complement the larger vehicles determined earlier, a series of smaller launch vehicles was specified. Although performance for ground and air launch was calculated, these vehicles are envisioned to be air launched. This vehicle has a 77 kg stack mass and a 7.5" (0.190 m) diameter.

One of the potential cost drivers for developing a vehicle of this size that will be launched from an aircraft is testing and verification for safety assurance purposes. The aircraft operators (for example, the US Air Force) need to be assured that the vehicle will not impact or damage the plane due to some unforseen effects. Frequently, new vehicles are tested on a rocket sled. The data from these experiments will serve to verify the vehicle's behavior. While not complicated, the process is expensive and will affect the per unit cost of the vehicle. A different approach is to use a known aerodynamic shape, such as a missile, as a launch tube. The launch vehicle, which would be slightly smaller than the missile, could fit inside it. This philosophy was adopted here.

AIM-7 Sparrow
- Length = 144 in. (3.66 m)
- Diameter = 8 in. (0.203 m)
- Mass = 227 kg (501 lb$_m$)
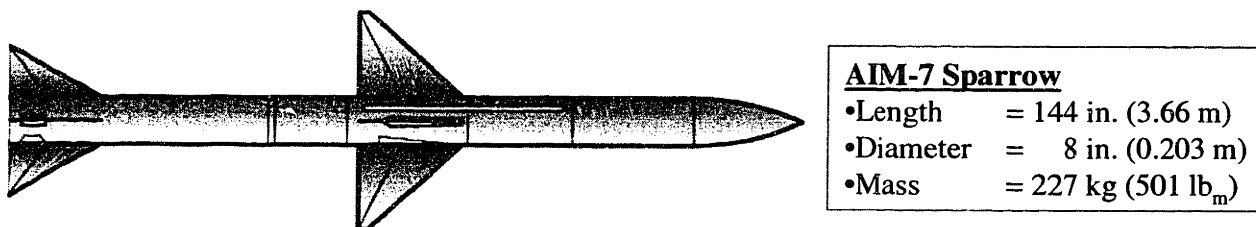
Figure 2.7 – AIM-7 Sparrow Air-to-Air Missile

Figure 2.7 shows an AIM-7 Sparrow air-to-air missile. The 77 kg launch vehicle is designed to fit inside the Sparrow. The Sparrow's outer diameter is 8.0 inches (0.203 meters). The 77 kg launch vehicle is designed at a 7.5 inch (0.190 meter) diameter, leaving 0.5 inches

(.013 meters) for the launch tube housing. Tables 2.11, 2.12, and 2.13 summarize the vehicle's design and performance parameters.

2.6.4 55 KG LAUNCH VEHICLE

A range of still smaller vehicles was also defined and analyzed. The 55 kg launch vehicle was designed to utilize 72 engines in the first stage and 6 engines in the second stage. Tables 2.11, 2.12, and 2.13 summarize the vehicle's design and performance parameters.

2.6.5 27 KG LAUNCH VEHICLE

This vehicle represents the smallest two stage vehicle consistent with second stage steering by differential throttling. The 27 kg launch vehicle utilizes 36 engines in the first stage and 3 engines in the second stage. Tables 2.11, 2.12, and 2.13 summarize the vehicle's design and performance parameters.

2.6.6 PERFORMANCE SUMMARY

Table 2.11 lists the six vehicles described in the previous section by a vehicle designator, VSLV-X (Very Small Launch Vehicle). The design parameters specified for each vehicle appear in Table 2.12. Finally, the vehicles' performance to each of the four orbital and four ballistic delivery missions is summarized in Table 2.13.

Table 2.11 – Very Small Launch Vehicles and Descriptions

Vehicle Designator	Stack Mass	Description
VSLV-1	2000 kg	Launch Vehicle
VSLV-2	800 kg	Missile and Launch Vehicle Combination
VSLV-3	188 kg	Upper Stages Only of VSLV-2
VSLV-4	77 kg	Launch Vehicle w/ AIM-7 Launch Tube
VSLV-5	55 kg	Launch Vehicle
VSLV-6	27 kg	Launch Vehicle

Table 2.12 – Very Small Launch Vehicle (VSLV) Design Parameters

Vehicle Designator	Stack Mass (kg)	Stage Mass 1 (kg)	2 (kg)	3 (kg)	Prop. Mass Fract. (ζ) 1 (kg)	2 (kg)	3 (kg)	Stack Fraction (f) 1 (kg)	2 (kg)	3 (kg)	Length (m)	(in)	Diameter (m)	(in)
VSLV-1	2000.0	1842.0	158.0		0.94	0.92		0.921	0.079		6.360	250.4	0.636	25.0
VSLV-2	799.9	612.2	169.0	18.7	0.78	0.94	0.92	0.765	0.211	0.023	4.558	179.5	0.340	13.4
VSLV-3	187.7	169.0	18.7		0.94	0.92		0.901	0.099		2.831	111.5	0.340	13.4
VSLV-4	77.1	70.4	6.7		0.94	0.92		0.914	0.086		3.230	127.2	0.190	7.5
VSLV-5	55.1	50.5	4.6		0.94	0.92		0.917	0.083		2.889	113.7	0.170	6.7
VSLV-6	27.5	25.2	2.3		0.94	0.92		0.917	0.083		2.293	90.3	0.135	5.3

Notes:
-All stages have a vacuum Isp of 290 s except for first stage of VSLV-2.

Table 2.13 – Very Small Launch Vehicle (VSLV) Gross Payload Performance

Vehicle Designator	Orbital Performance 770 km / 90.0 deg Ground (kg)	(%)	Air (kg)	(%)	200 km / 28.5 deg Ground (kg)	(%)	Air (kg)	(%)	Ballistic Delivery 4500 n.mi. (7241 km) Ground (kg)	Air (kg)	1000 n.mi. (1855 km) Ground (kg)	Air (kg)
VSLV-1	17.550	0.87%	32.070	1.58%	34.760	1.71%	55.990	2.72%	73.29	104.83	269.65	377.88
VSLV-2	5.350	0.66%	9.220	1.14%	10.100	1.25%	16.930	2.07%	17.64	27.07	67.36	102.00
VSLV-3	0.300	0.16%	2.120	1.12%	2.630	1.38%	6.210	3.20%	5.39	10.02	21.24	36.09
VSLV-4	0.389	0.50%	1.140	1.46%	1.260	1.61%	2.580	3.24%	2.35	3.94	8.98	14.24
VSLV-5	0.194	0.35%	0.781	1.40%	0.719	1.29%	1.753	3.09%	1.33	2.55	5.57	9.71
VSLV-6	0.053	0.19%	0.375	1.34%	0.303	1.10%	0.845	2.98%	0.63	1.28	2.58	4.80

Notes:
-Percentage values represent the ratio of payload mass to vehicle liftoff mass.

As can be seen above, performance varies across the vehicles due to differing propellant mass fractions in the case of the largest vehicle, drag in the smallest vehicle, and slightly different stack fractions in other vehicles. Depending on the mission, payload performance ranges up to 3% of the gross liftoff weight of the vehicle. Ballistic payloads are considerably larger in all cases due to the reduced ΔV need for a ballistic trajectory than an orbital one. These very small launch vehicles provide several options for meeting a wide variety of payload objectives. Although only one design (VSLV-4) is carried forward through a preliminary design, much of the discussion of Chapter 3 is applicable to any of these vehicles.

2.7 VEHICLE DOWNSELECT

One important consideration is keeping the final unit cost reasonable. One cost driver is the development cost of the first vehicle, which will then be distributed over the entire production

run. Most of the vehicles described in Section 2.6 are of arbitrary size. The 77 kg launch vehicle with an AIM-7 launch tube described in Section 2.6.3 is a design approach which aims to eliminate a portion of the vehicle demonstration cost. This effort imposes a size constraint on the vehicle. This vehicle was chosen for further study as it seemed to be the concept with a lower development cost coupled to a payload capability realizable in the near term. Even if the AIM-7 launch tube is not adopted, this vehicle will be able to loft a reasonable payload to orbit and be launched from a wide variety of aircraft.

2.7.1 STANDARD MISSION PERFORMANCE

Table 2.1 reiterates the vehicle performance data of VSLV-4, now that its design will be carried through for further analysis. Vehicle sizing parameters have been refined with the sizing numbers obtained from the systems analysis of Chapter 3. Thus, these parameters are not ratioed from Titan II data as described in Section 2.3.2. The baseline design is air launched to a 770 km circular orbit at 90.0° inclination. An air launch was chosen over a ground launch due to the performance advantages from lowered drag losses experienced by avoiding the denser portions of the atmosphere. This additional performance could help if any of the other design targets are not met or if engine performance is lower than predicted. The 770 km mision is chosen as baseline since it required more ΔV. If it is possible to meet the 770 km mission, the 200 km mission will be met as well. Other non-optimal missions can be accomplished and are listed in Table 2.14.

Table 2.14 – Baseline Vehicle Performance Data

Orbital Performance	Gross Payload (kg)	(%)
770 km / 90.0 degrees		
Ground-Launched	0.39	0.50%
Air-Launched	1.14	1.46%
200 km / 28.5 degrees		
Ground-Launched	1.26	1.61%
Air-Launched	2.58	3.24%
Ballistic Performance	(kg)	(%)
4500 n.mi. (7241 km)		
Ground-Launched	2.35	2.96%
Air-Launched	3.94	4.86%
1000 n.mi. (1855 km)		
Ground-Launched	8.98	10.43%
Air-Launched	14.24	15.59%

The effects of varying input parameters on the vehicle's performance are examined in the next few sections. This allows a look at the sensitivity of design assumptions.

2.7.2 DESIGN VARIATIONS

Assumptions have been made regarding launch conditions, engine efficiency (specific impulse), and the inert weight in each stage (propellant mass fraction).

2.7.2.1 LAUNCH VELOCITY

The baseline design is launched from an airplane at 40,000 ft (12,192 m) at a Mach number of 0.88. This is intended as a representative number and will be revised depending on the launch aircraft. Figure 2.8 shows the payload performance for other initial launch velocities at the same launch altitude (40,000 ft / 12,192 m). The Mach number is calculated from the velocity and speed of sound, a, using Equations 2.17 and 2.18 along with data from the 1976 NASA Standard Atmosphere.[52]

$$M = \frac{V}{a}$$

Equation 2.17

$$a = \sqrt{\gamma RT}$$

Equation 2.18
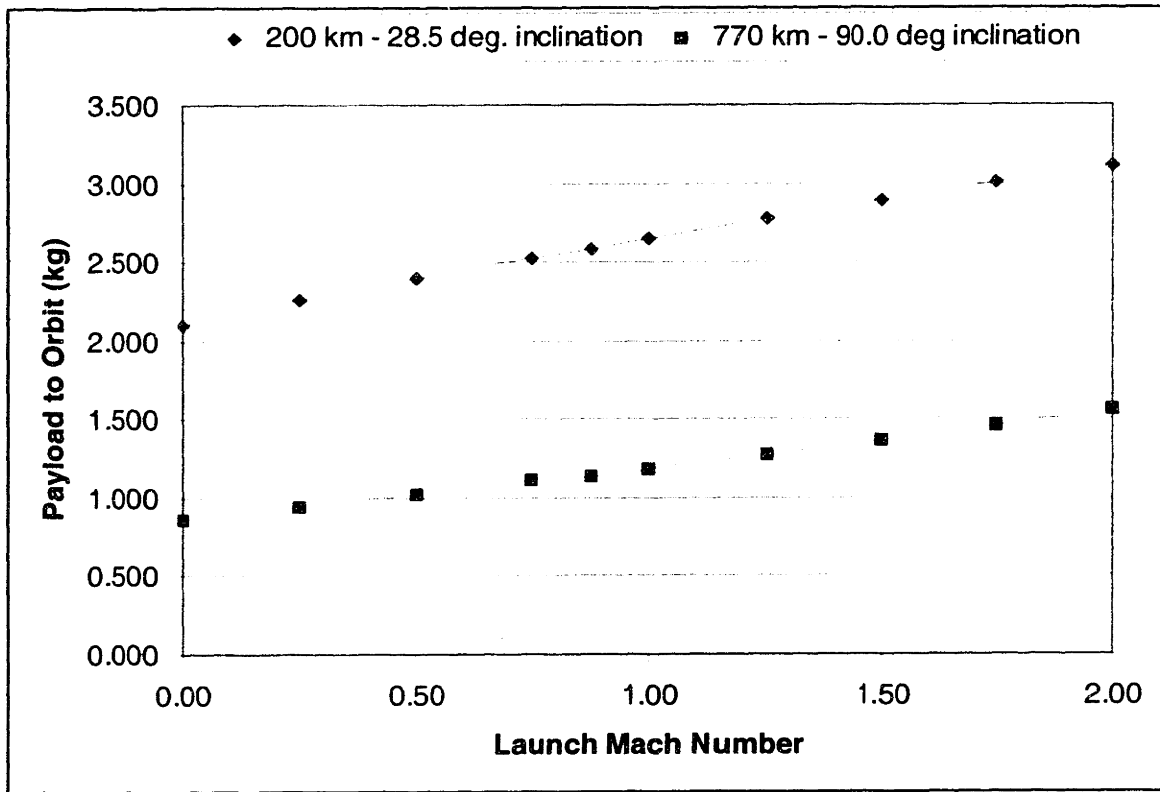
Figure 2.8 – Payload Performance for Varying Initial Launch Velocities

2.7.2.2 LAUNCH ALTITUDE

The initial altitude from which the vehicle is released might vary as well. Figure 2.9 shows the effect of varying the launch altitude on payload performance.
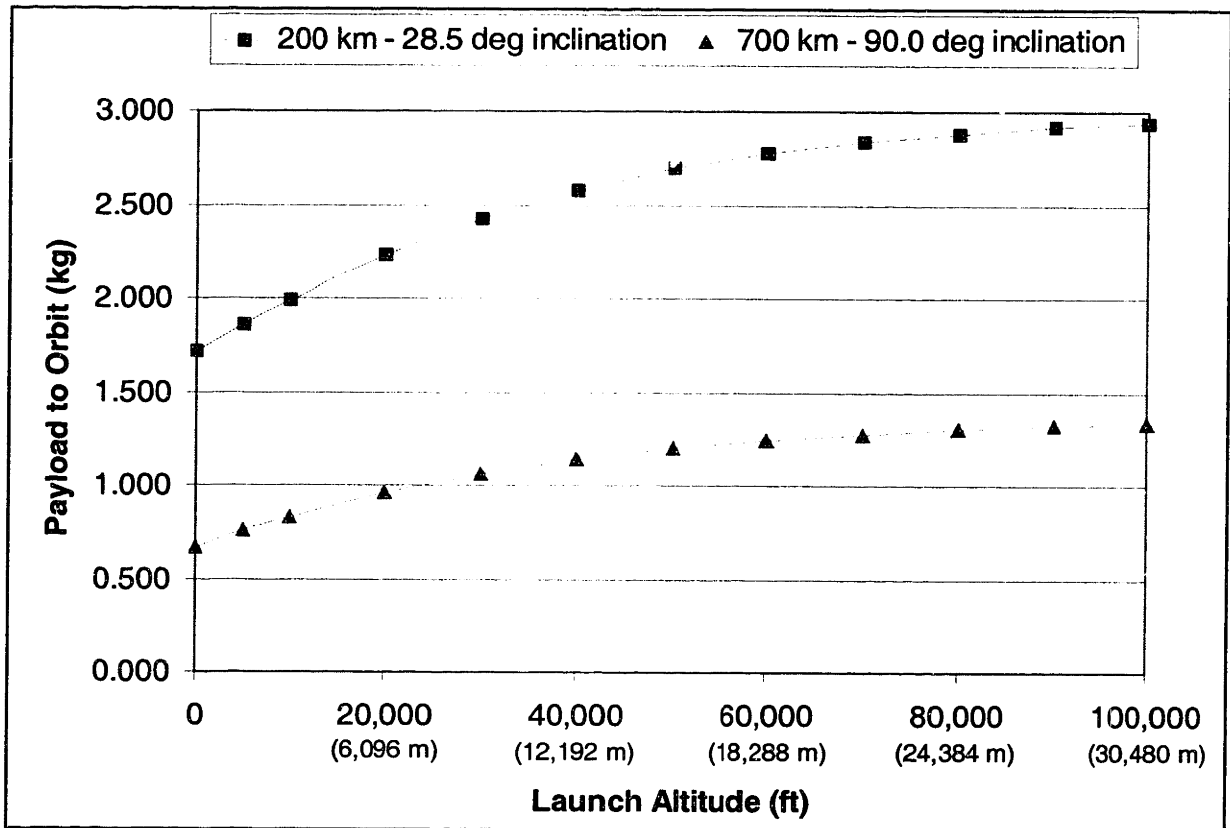
Figure 2.9 – Payload Performance for Varying Initial Launch Altitudes (M=0.88)

The effect of drag losses on the vehicle's performance is visible in Figure 2.9. At 40,000 ft (12,192 m), the density of the atmosphere is about 27% of its sea level value.[52] This altitude achieves most of the performance benefit from air launch.

2.7.2.3 SPECIFIC IMPULSE

As discussed in Section 2.1, the assumed vacuum specific impulse value of 290 seconds may be improved by 5 to 25 seconds in subsequent engines. This implies that the current design is conservative, and changes are likely to improve performance. The effect of varying the vacuum I_{sp} on performance is illustrated in Figure 2.10.
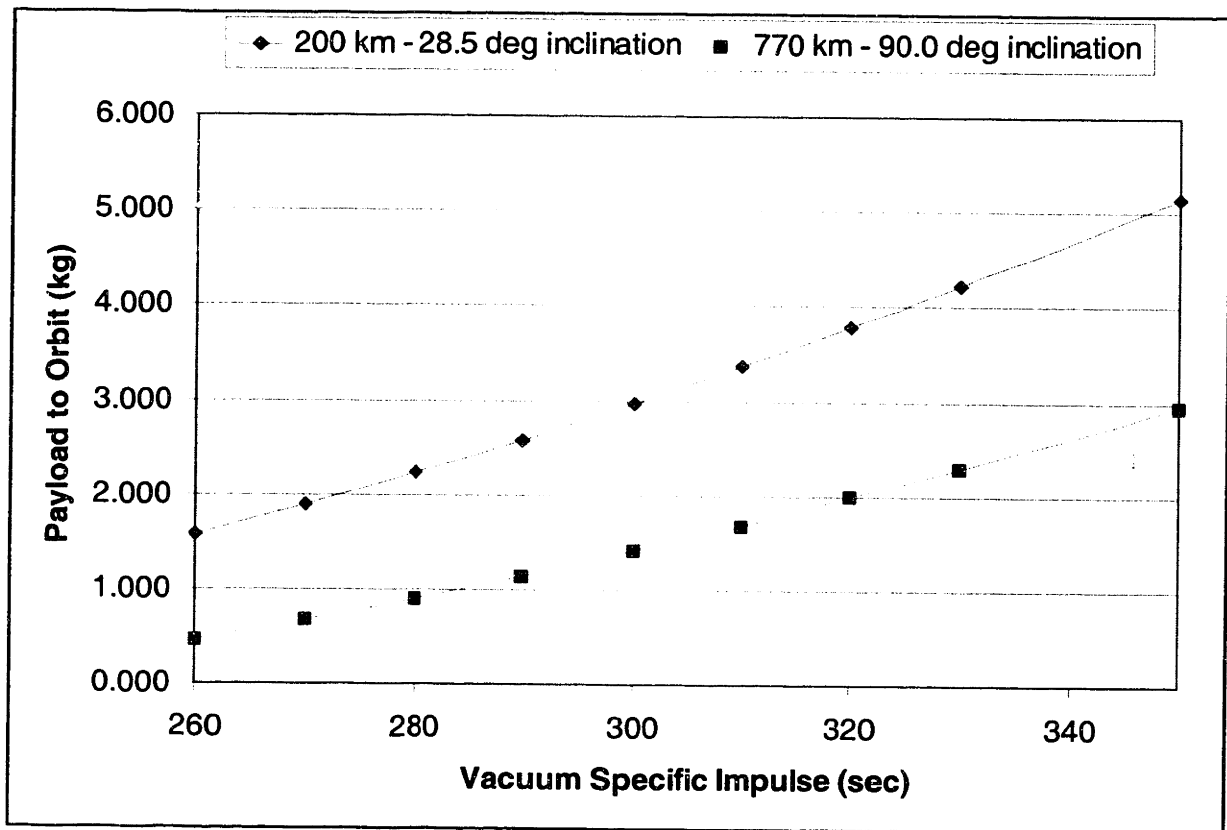
Figure 2.10 – Payload Performance for Varying Vacuum Specific Impulse (I_{sp})

Figure 2.10 is interesting in the fact that it shows that payload performance to orbit can be maintained with a lower specific impulse. However, if the vacuum I_{sp} increases to the theoretical maximum of 318 seconds for these propellants discussed in Section 2.1, the payload of the baseline case (770 km / 90.0° inclination) could improve more than 18% from 1.14 kg to 1.35 kg.

2.7.2.4 MASS FRACTIONS

The mass fraction is one of the more uncertain assumptions made in this initial phase of design. It is better looked at as a target, which the systems design of Chapter 3 will attempt to meet. Keeping the inert mass as low as possible, and, as a result, the propellant mass fraction as high as possible, is one significant challenge of designing any launch vehicle. It is here where scaling concerns discussed in Section 1.3 will come into play, particularly with the second stage of the vehicle.

The baseline design has a propellant mass fraction (ζ) of 0.94 in the first stage and 0.92 in the second. This was roughly the same as the Titan II, which is a geometrically similar two-stage vehicle using the same propellants. Figures 2.11 and 2.12 show the effect on payload performance of different ζ values for both the first and second stages. Figure 2.11 shows results for the 770 km / 90.0° baseline case, and Figure 2.12 shows results for the 200 km / 28.5° case, air-launched from 40,000 ft (12,192 m) at a Mach number of 0.88.
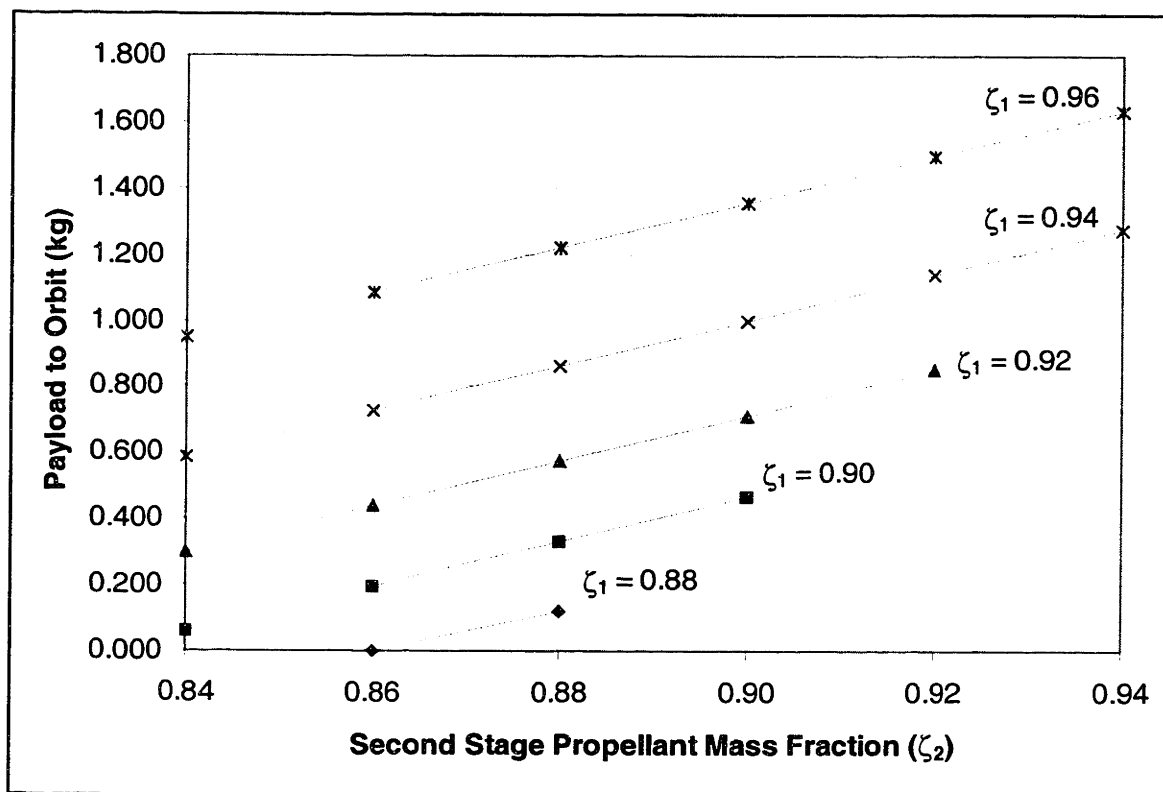
Figure 2.11 - Payload Performance for Varying ζ to 770 km / 90.0 degree orbit (Baseline)
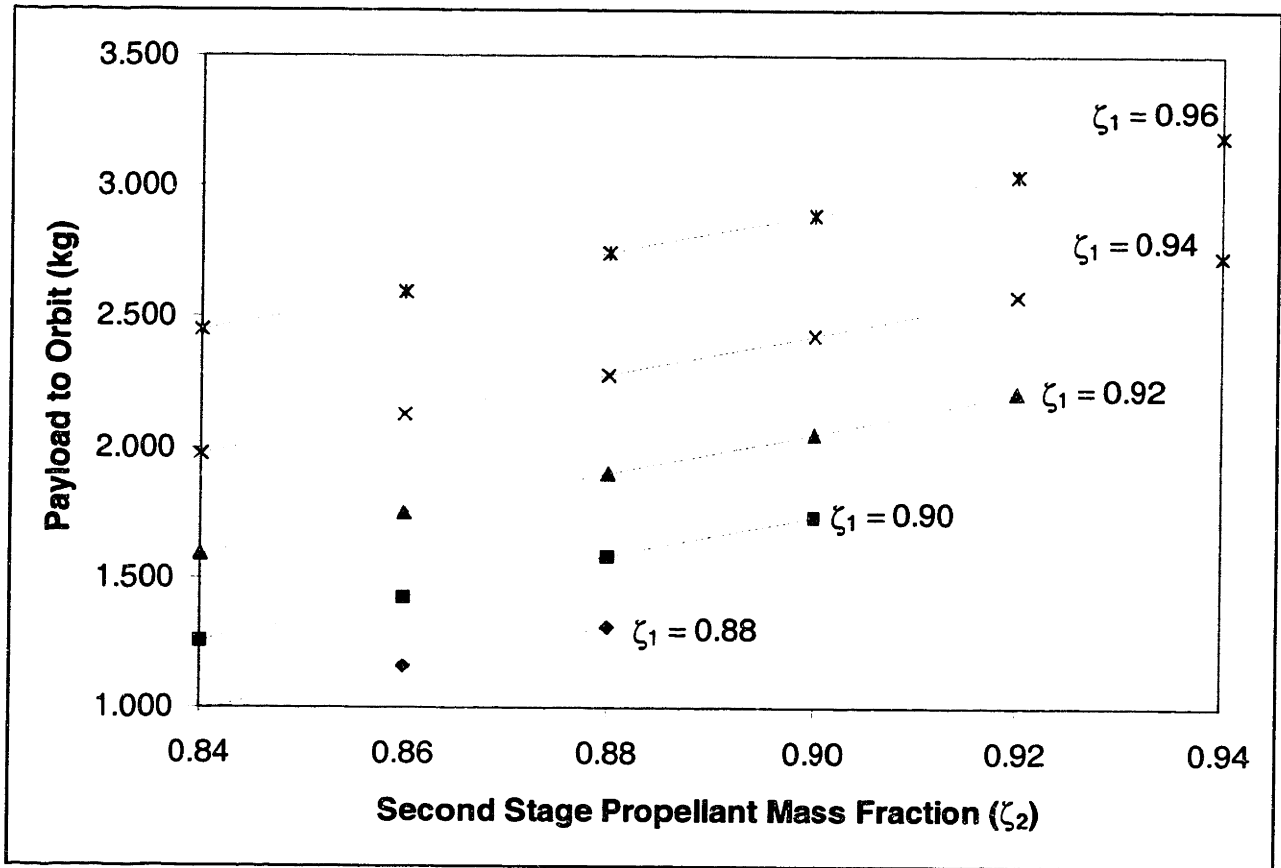
Figure 2.12 - Payload Performance for Varying ζ to 200 km / 28.5 degree orbit

Figures 2.11 and 2.12 are useful in trading off the effect of design choices that might increase the vehicle's inert weight in the more detailed design effort. For example, using a commercial off the shelf (COTS) avionics system might impose a weight penalty on the system, but provide a cost advantage over a lighter system that is designed specificially for this application. The cost savings of the COTS system can be traded off against the payload loss of using a heavier system that would increase inert mass.

2.7.2.5 STACK FRACTIONS

As discussed in Section 2.3.3, the first and second stage stack fractions have significant impact on vehicle performance. With a second stage stack fraction of 0.086 resulting in a stage mass of 6.646 kg, it may be challenging to meet its inert mass target of 532 grams. Decreasing

the first stage stack fraction will result in a larger second stage which may add needed mass margin to the design.

Table 2.15 shows the gross payload performance for a vehicle with stack fractions (f_1/f_2) between 0.850 / 0.150 and the baseline vehicle's 0.914 / 0.086. The loss in payload performance is low for missions that require less ΔV. The air launched 200 km case only experiences a loss in payload of 6% between the baseline case and the 0.850 / 0.150 case. Since the vehicle was optimized for the air launched 770 km polar orbit, the 200 km cases actually have better performance at slightly lower first stage stack fractions. The baseline case shows a 44% loss in payload for the 0.850 / 0.150 case. The ground launched 770 km case is unable to make orbit for neither the 0.875 / 0.125 case nor the 0.850 / 0.150 one.

Table 2.15 – Payload Performance for Varying Stack Fractions

Vehicle	Baseline		Variation 1		Variation 2		Variation 3	
f_1	0.914		0.900		0.875		0.850	
f_2	0.086		0.100		0.125		0.150	
1st Stage Mass (kg)	70.361		69.597		67.302		65.773	
2nd Stage Mass (kg)	6.648		7.413		9.707		11.237	
Performance	(Kg)	(%)	(Kg)	(%)	(Kg)	(%)	(Kg)	(%)
770 km / 90.0 degrees								
Ground-Launched	0.389	0.50%	0.285	0.37%	X	X	X	X
Air-Launched	1.140	1.46%	1.085	1.39%	0.845	1.09%	0.634	0.82%
200 km / 28.5 degrees								
Ground-Launched	1.260	1.61%	1.272	1.62%	1.249	1.60%	1.058	1.36%
Air-Launched	2.580	3.24%	2.600	3.27%	2.598	3.26%	2.414	3.04%

The optimum stack fractions are a strong function of the target orbit (i.e. ΔV requirement). As the ΔV required is increased, the ratio of first to second stage mass increases, as does the sensitivity to this ratio. This can be seen in Figure 2.3 and Table 2.15.

CHAPTER 3
SYSTEMS DESIGN

With the overall performance analysis completed in Chapter 2, it is now important to more closely examine the mass targets (propellant mass fractions) that were assumed in the performance calculations. A brief systems analysis will give an idea of whether any revisions need to be made in these target and illuminate what challenges exist in the fabrication of the launch vehicle. Each of the major subsystems analyzed is discussed in Sections 3.1 through 3.5, and the results of the calculations are summarized in Section 3.6.

Table 3.1 summarizes the vehicle parameters and mass targets that will be examined in this chapter. The inert mass targets will be examined in greater detail. They should contain all of the subsystem mass outlined in this chapter.

Table 3.1 – Summary of Overall Vehicle Parameters

Overall Vehicle Parameters		
Stack Mass (w/o payload)	77.009 kg	169.81 lb_m
Length	362.0 cm	142.4 in
Diameter (Same for Stgs. 1&2)	19.0 cm	7.5 in
L/D	19.1	19.1
Stage 1		
Stage Mass	70.361 kg	155.46 lb_m
Propellant Mass Fraction, ζ	0.94	0.94
Inert Mass Target	4.222 kg	9.31 lb_m
Length	248.5 cm	97.9 in
Stage 2		
Stage Mass	6.648 kg	14.66 lb_m
Propellant Mass Fraction, ζ	0.92	0.92
Inert Mass Target	0.532 kg	1.17 lb_m
Length	54.1 cm	21.3 in
Payload		
Mass (770 km / 90.0 deg Air Launch)	1.140 kg	2.51 lb_m
Length	59.1 cm	23.3 in

3.1 PROPULSION SYSTEM

The propulsion system will consist of an array of microrocket engines. The propulsion system is assumed to contain the following components: thrust chamber, turbopumps, valves, and interface connections.

Each engine is assumed to weigh 2 grams.[63] This includes the thrust chamber, turbopumps, and flow passages. All components are integrated together on a single silicon wafer stack. An additional 2 grams per engine is assumed for micro-valves and interconnects to each engine.

The engines will need to be connected together in some manner. For initial weight and sizing purposes, a 500 μm thick by 19.0 cm (7.5 in) silicon wafer is assumed to be a part of each propulsion system. Figure 3.1 gives a description of the propulsion system including the propellant tanks and pressurization system.

Key:

▷◁	Valve (Fill, Control, Relief)
⊟	Pressure Regulator
◻◻ / ▷◁	Microrocket Engines
- - -	Helium Pressurant Gas Flow
———	Fuel (N_2H_4) Flow
———	Oxidizer (N_2O_4) Flow

Engine Module
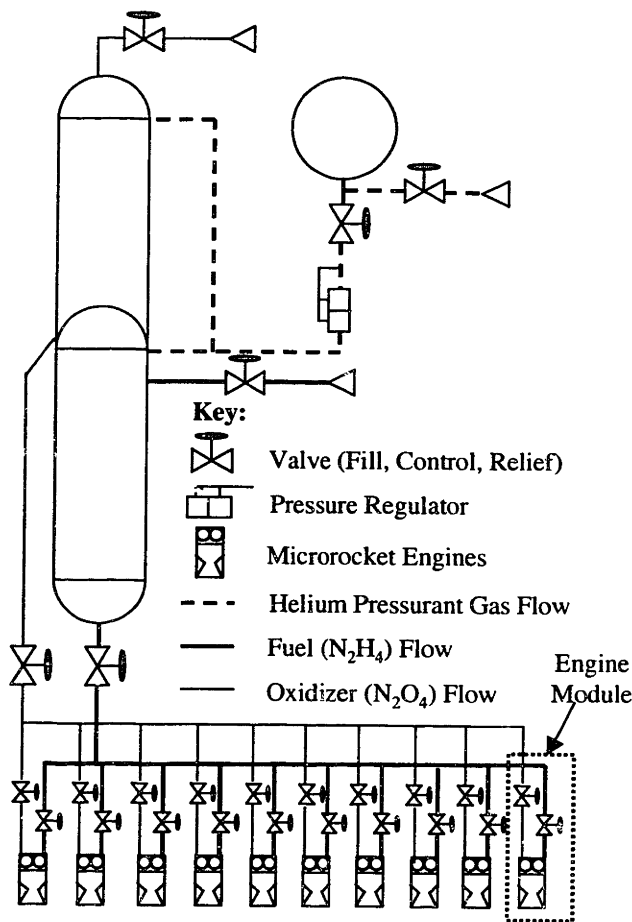
Figure 3.1 – Propellant System Schematic

3.2 PROPELLANT TANKS

Although assuming that the vehicle scaled with the mass of the Titan II vehicle was a reasonable starting place for preliminary performance analysis, a preliminary vehicle design will more accurately estimate component masses. With over 90% of each stage's mass made up of propellant, propellant density drives vehicle size.

3.2.1 TANK SIZING

Since the propellant tanks more or less dictate the size of the entire vehicle, the amount of propellant used by the vehicle will be a key parameter. Since the diameter of the vehicle has been fixed at 7.5 inches (0.190 m), the length of the vehicle will be allowed to vary.

To start with, the amount of propellant (m_{prop}) is known in each stage from the propellant mass fraction (ζ). The mixture ratio (MR) is the ratio of the mass of oxidizer over the mass of fuel. For our vehicle, a mixture ratio of 0.9 is used (Section 2.1). Equations 3.1 and 3.2 allow m_{ox} and m_{fu} for each stage to be determined.

$$m_{ox} = \frac{(MR)m_{prop}}{MR+1}$$
<div align="right">**Equation 3.1**</div>

$$m_{fu} = \frac{m_{prop}}{MR+1}$$
<div align="right">**Equation 3.2**</div>

With the necessary mass of propellants calculated, the amount of actual volume in the tanks needs to be determined. First the density of each propellant is used to calculate the volume ($V_{ox-prop}$, $V_{fu-prop}$) that they require. Then some margin is added on for ullage volume (3% of V_{prop}), and the residual propellant volume that might become trapped in feedlines, etc. (2% of V_{prop}).[27] The sum of the ullage volume, residual propellant volume, and required propellant volume give the total tank volume ($V_{ox-total}$, $V_{fu-total}$).

Now that the total tank volume is known, the tank configuration needs to be configured to determine the length and shape of the tanks. Figure 3.2 shows some alternate tank configurations.

Tandem Tanks   Tandem Tanks
(External Piping)   (Internal Piping)   Concentric Tanks
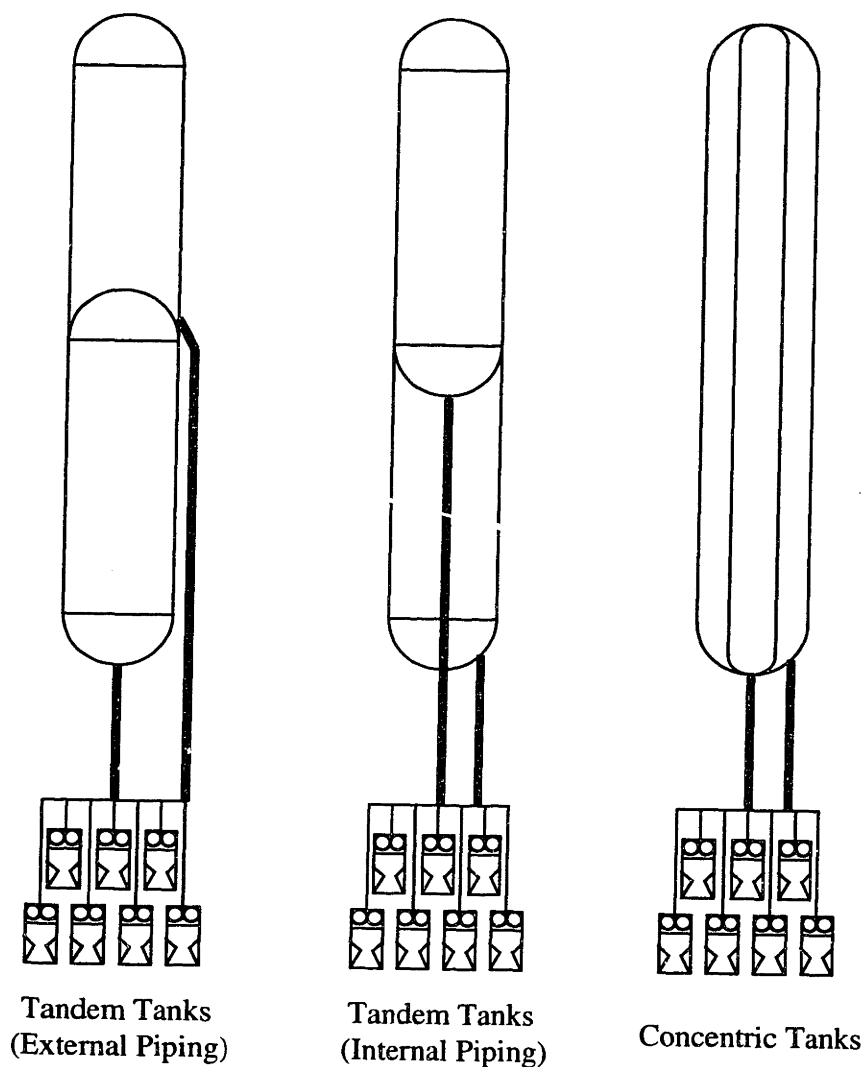
Figure 3.2 – Alternate Tank Configurations[24]

Of the configurations in Figure 3.2, the two tandem tank configurations have about the same weight efficiency, while the concentric tank design will be roughly 18% heavier due to its inefficient structural layout.[24] The concentric tank design has the greatest benefit in simplifying piping considerations between the propellant tanks and propellant manifolds.

Both tandem configurations have their advantages and disadvantages. Internal piping prevents having to attach extra structure to the outside of the vehicle. However, the internal

65

piping arrangement may increase the complexity of tank manufacture. In order to maximize simplicity and minimize weight of the design, the external piping arrangement was chosen.

The propellant tank design chosen appears in Figure 3.3. Stiffening rings will be placed at the intersection of each ellipsoidal end cap with the cylindrical tank structure. The propellant from the fuel (top) tank will be expelled from passageways machined on each side of the middle stiffening ring. The propellant from the oxidizer (bottom) tank will be drawn through the bottom of the tank.

The end caps of the tanks are ellipsoidal with a radius of minor to major diameter (Ellipse Factor, or EF) of 0.75. The reasons for this are discussed in Section 3.2.4.4. A schematic of the main dimensions of the first and second stage tanks appears as Figure 3.4. The dimensions in Figure 3.4 are calculated using Equations 3.3 through 3.5, knowing the volume of each of the tanks and the set diameter of the tanks (7.5 in. / 0.190 m). The results of these calculations for the vehicle appear in Table 3.2.
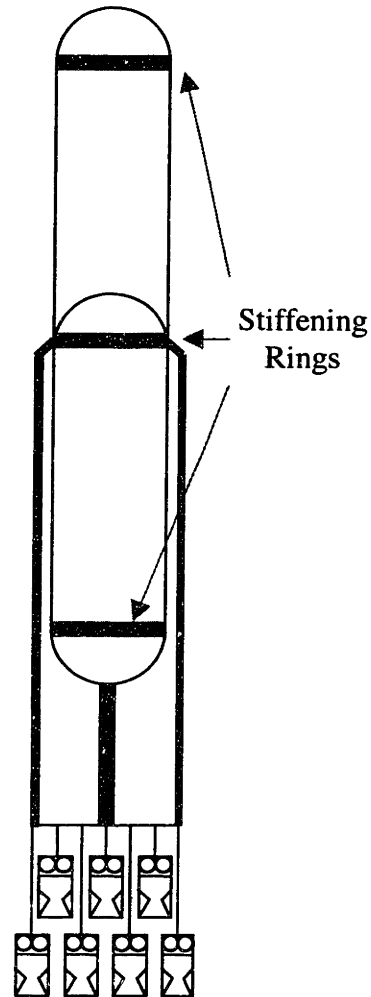
Figure 3.3 – Propellant Tank Design
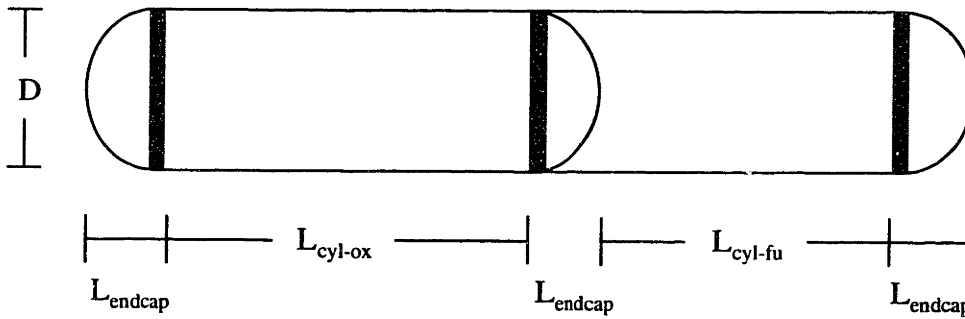
Figure 3.4 – Propellant Tank Dimension Definitions

Table 3.2 – Propellant Tank Dimension Values

Endcap Length, L_{endcap}	2.81 in	7.08 cm	2.81 in	7.08 cm
Length of Fuel Cylinder, L_{cyl-fu}	47.10 in	118.64 cm	1.80 in	4.53 cm
Length of Oxidizer Cylinder, L_{cyl-ox}	29.61 in	74.58 cm	1.04 in	2.62 cm

$$L_{endcap} = (EF)D$$

Equation 3.3

$$L_{cyl-fu} = \frac{8V_{fu-total} - \pi D^3 (EF)}{2\pi D^2}$$

Equation 3.4

$$L_{cyl-ox} = \frac{12V_{ox-total} - \pi D^3 (EF)}{3\pi D^2}$$

Equation 3.5

3.2.2 MATERIAL SELECTION

Once the shape has been established, it is necessary to choose the propellant tank material. This requires consideration of the material's chemical compatibility with the propellants, mechanical properties, and manufacturability. The tanks in this vehicle are also an integral part of the vehicle's structure. Therefore, they must be able to be sustain all vehicle flight loads as well as loads from the propellant.

3.2.2.1 MATERIAL COMPATIBILITY WITH PROPELLANTS

One of the benefits of using propellants such as hydrazine or hydrogen peroxide is that they can be catalytically decomposed and used as a monopropellant. Unfortunately, that can be a problem as well when storing these propellants. The first step in choosing the tank material is determining which materials are compatible with the propellants.

Various sources were consulted to determine compatibility. Some information is a bit conflicting, depending on the test conditions, etc., but a summary of the information gathered appears in Table 3.3. N_2O_4 and N_2H_4 can be stored in selected alloys of aluminum, stainless steel, or titanium. H_2O_2 can be stored in many aluminum and stainless steel alloys, but can not be stored in titanium.[60] Data in Table 3.3 has been reduced to three categories. A rating of G signified that the material was good for indefinite storage in contact with the material. A rating of L signified that the material could be in contact with the material for a limited time. This may be sufficient for some valves and flow components that are only wetted during flight, but for tankage, such materials must be analyzed on a case-by-case basis. Finally, a rating of unacceptable, U, signifies that the material may not be in contact with the fluid. Where two ratings existed for the propellant – material combination, it is noted in Table 3.3. Some compatibility information for hydrogen peroxide was not located. This is denoted by N/A.

Table 3.3 – Material Compatibility Data[9,11,12,55,60,61,65]

	Nitrogen Tetroxide	Hydrazine	Hydrogen Peroxide
Aluminum Alloys			
1100 (> 99% Pure Al)	L	G	G
2024 (Cu)	L	U	U
3003 (Mn)	G	G	G
5052 (Mg)	G	G	G
6061 (Mg, Si)	L	G	G
Inconel	L	L	N/A
Monel	B	L/U	N/A
Stainless Steels			
303	G	G/U	G
304L	G/U	G	G
316	G	U	G
321	G	G/L	G
347	G/U	G	G
410	G/L	L	G
430	G/L	L	G
Titanium Alloys			
6Al - 4V	G	G	U

There is mixed data on the compatibility of nitrogen tetroxide, especially with steels. Older tests seem to show that many stainless steels are incompatible with N_2O_4.[55] However, more recent tests indicate that with careful attention to surface preparation and by limiting the water present in the N_2O_4, many stainless steels listed above are acceptable for flight tankage.[55] Other metals compatible with N_2O_4 are tungsten, tantalum, and beryllium.

Hydrazine will react especially violently with copper oxides. Since the 2000-series of aluminum alloys contains a high amount of alloyed copper, they are incompatible with N_2H_4. Other metals compatible with N_2H_4 are nickel and tantalum. Iron, magnesium, and zinc should be avoided.

Careful surface preparation is important for hydrogen peroxide. H_2O_2 should be kept away from high concentrations of copper and chromium, as these are catalytic. This is why the 2000-series of aluminum alloys are unacceptable. If aluminum alloys are to be used, the surface should be sulfuric acid anodized per Mil. Spec. A-8625.[12] Other compatible metals include tantalum and zirconium. Silver solder and brazing should be avoided.

Limited material compatibility does not necessarily eliminate a material from consideration. A material can be coated with a glass or other nonreactive material to make it acceptable for use. This adds mass to the component being made, which may be a concern in components with small material thicknesses. Damage to the coating could as well cause localized exposure to the original alloy.[64]

The following alloys were selected for further consideration: Al 3003, SS 430, and Ti 6Al-4V. Al 3003 showed good compatibility with all propellants in all of the sources examined. SS 430 showed limited acceptability for hydrazine, but still was ok for limited use. It also has excellent resistance to nitric acid so it should fare well in the presence of N_2O_4. There was mixed data available on stainless steels that seemed to indicate that most of them are actually ok with careful attention paid to surface preparation and propellant purity. Ti 6Al-4V is not acceptable for H_2O_2, but will be considered for the $N_2O_4 - N_2H_4$ propellant combination.

3.2.2.2 MATERIAL MECHANICAL PROPERTY TRADE-OFFS

Having picked three candidate materials (Al 3003, SS 430, and Ti 6Al-4V), it is important to determine which material will provide the lowest weight structure for the propellant

tanks. First we will look at the dominant loading condition of the structure and enunciate the appropriate combination of material mechanical properties and density.

A thin walled cylindrical pressure vessel's wall thickness is determined by its mechanical strength σ_f, which is defined as the 0.2% offset yield strength σ_y. Equation 3.6 shows the relationship to calculate minimum thickness, based on the design burst pressure (P_b), inner diameter of the sphere (D_i), and the yield strength of the material σ_y.

$$t_{min} = \frac{P_b D_i}{2\sigma_y}$$

Equation 3.6

The overall weight of the pressure vessel is determined by the wall thickness and the density. Therefore, the best material for a thin walled pressure vessel dominated by internal pressure can be determined by maximizing the specific strength, the ratio of yield strength (σ_y) to density (ρ).

Structures with other dominant loads will depend on different mechanical properties. The weight of a thin walled cylinder undergoing a compressive load will be dependent on maximizing the ratio of Young's modulus (E) over the density squared. A flat plate in bending will depend on the ratio of E over ρ^3.[26]

The tanks are under a combination of internal pressure loading and compressive loading. Since the propellant tank is also an integral part of the vehicle's structure, it will experience significant axial and bending loads. The expected internal pressure in the propellant tank (on the order of 50 psia / 3.40 atm) is fairly low since we are dealing with a pump-fed propulsion system. However, the internal pressure will introduce a longitudinal tensile stress which works to relieve the compressive and bending stresses introduced by the external loads. The dominant loading mechanism for the tanks will be determined.

The cylindrical structure above and below the tanks will not experience any internal pressure loading. It is assumed that the quasi-static axial and bending loads are the dominant loading condition for sizing the cylindrical structure's walls.

These calculations will assist in the decision of which material to use for the propellant tanks. Table 3.4 shows the three candidate materials, their values for ρ, σ_y, E, and the ratios σ_y/ρ and E/ρ^2.

Table 3.4 – Mechanical Property Data

Material	ρ (kg/m³)	σ_y (MPa)	E (GPa)	σ_y/ρ (Pa-m³/kg)	E/ρ² (Pa-m⁶/kg²)
Aluminum 3003	2,730	145	69	53,114	9,258
Stainless Steel 430	7,800	441	200	56,538	3,287
Titanium 6Al-4V	4,430	880	114	198,646	5,809

From Table 3.4, two possible material choices for the propellant tank are suggested. If the axial and bending loads are dominant, then Al 3003 would be the best material choice due to its higher E/ρ^2 ratio. This case would be referred to as buckling limited. However, if internal pressure loads dominate over the buckling load, than it would be best to make the tank out of Ti 6Al – 4V, since it has the highest value of σ_y/ρ. This condition would be called pressure limited. It turns out that the propellant tanks are pressure limited (to be discussed in Section 3.2.4), and Titanium 6Al-4V is selected as the material that would provide the lowest weight propellant tank structure.

3.2.3 VEHICLE LOADING

A launch vehicle experiences a dynamic environment of rapidly changing acceleration, pressure, aerodynamic, and vibrational loads. These can be grouped into the categories below:[1]

- Static, external loads – Mass loading of the structure itself due to gravity or steady acceleration.

- Static, self-contained loads – Pressure of stored propellant, mechanical preloads, thermoelastic loads (loads from temperature changes).

- Dynamic, external loads – Unsteady engine thrust, sound pressure, gusts of wind during launch.

- Dynamic, self-contained loads – Oscillation of propellants (slosh).

For a first cut analysis, an attempt is made at identifying the dominating static (or quasi-static) loads to size the vehicle structure. Dynamic loads will be neglected in this part of the

analysis. The goal is to determine the distribution of axial and bending loads at the worst case loading condition on the vehicle so as to size the vehicle's walls to protect against buckling.

3.2.3.1 ACCELERATION LOADS

Since the thrust force on the vehicle is greater than the sum of the gravity, drag, and other retarding forces, the vehicle experiences a net acceleration, which exerts a force on the structure. This acceleration is frequently expressed as some multiple of the gravitational acceleration and referred to as a number of "g's." Since the thrust is assumed constant during a stage burn, acceleration will rise during the stage burn, reaching a maximum at the stage burnout

At this point, the engines are still firing at full thrust and the propellant mass has been depleted. If all retarding forces are neglected for the baseline launch vehicle design and the first stage thrust is assumed constant at 1530 N, the vehicle experiences a maximum acceleration of 13 g's at first stage burnout. However, drag and other aerodynamic forces will lower the net acceleration of the vehicle. Figure 3.5 shows the acceleration profile of the baseline vehicle for the 770 km / 90.0° air-launched mission including aerodynamic drag.
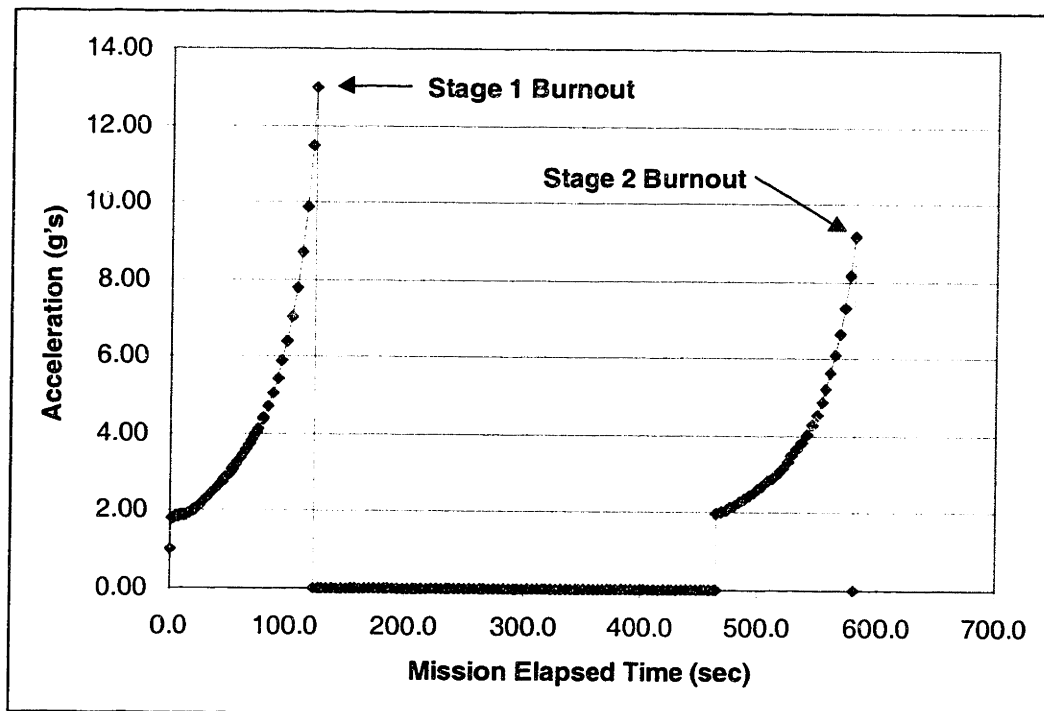
**Figure 3.5 – Acceleration Profile of Baseline Mission
(77 kg vehicle / 770 km / 90.0° Air-Launched)**

The 1st stage burn out point's acceleration matches well with our simple prediction of 13 g's since at that point, the atmospheric density is less than 0.01% of that at sea level.[52] Therefore, in-line aerodynamic drag forces on the vehicle are negligible.

Besides affecting the design of the vehicle, the maximum acceleration can influence the design of the payload, as it must be designed to withstand the maximum acceleration of the vehicle. Conversely, payload requirements can limit the maximum allowable acceleration of a vehicle. The maximum acceleration of the Space Shuttle is 3.2 g's. Expendable launch vehicles such as the Ariane IV and the Titan IV have maximum accelerations of 4.0 g's and 4.2 g's, respectively.[1]

Is the 13 g's of the constant thrust design so large as to adversely compromise the design of the payload? What penalty would accrue from a limit on maximum acceleration during launch? The acceleration can be limited by tailoring the thrust profile. The impact on the vehicle's performance was estimated assuming that total propellant burn (and stage impulse, I_{STAGE}) was constant, i.e. the stage burn time was extended as necessary. Two types of regressive thrust profiles were examined (Figure 3.6). The step profile would result in the most inefficient profile and the largest stage burn. The linear profile would be more efficient.
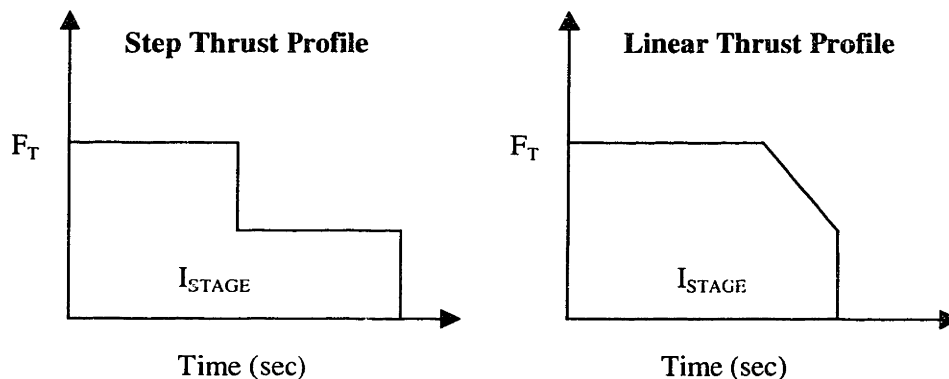
Figure 3.6 – Step and Linear Thrust Profiles

Table 3.5 shows the effect of acceleration limits on the payload performance to orbit. Both step and linear profiles were calculated with acceleration limits down to 5 g's, in line with contemporary launch vehicles. The worst case (step throttling / 5 g's maximum acceleration) shows a loss of payload to orbit of 11%. A linear profile penalizes the payload by only 2%.

Table 3.5 – Payload Performance for Acceleration-Limited Profiles

Acceleration Case	Maximum Acceleration		Step Profile Payload		Smooth Profile Payload	
	1st Stage (g's)	2nd Stage (g's)	Mass (kg)	Fraction (%)	Mass (kg)	Fraction (%)
Baseline	12.99	9.15	1.140	1.46%	1.140	1.46%
10 g Limited	10.00	10.00	1.140	1.46%	1.140	1.46%
7.5 g Limited	7.50	7.50	1.127	1.44%	1.136	1.45%
5.0 g Limited	5.00	5.00	1.001	1.28%	1.119	1.43%

3.2.3.2 AERODYNAMIC LOADS

A launch vehicle will experience a variety of external loads during the course of its travel through the sensible atmosphere. Shock waves, winds, and dynamic pressure will all cause loads on the vehicle with time varying intensity.

For the propellant tank sizing calculations in Section 3.2.4, an axial compressive load and bending moment due to a distribution of side forces must be determined. The acceleration loading conditions described in Section 3.2.3.1 will be used for the axial loading conditions. This leaves the bending moment to be calculated.

Side forces that do not act in line with the thrust vector must be compensated for to keep the vehicle stable. Here, we will assume that this is accomplished by controlling the propellant flow to individual microrocket engines to generate a moment on the vehicle to counteract any aerodynamic side forces. The bending moment due to side forces is going to be assumed to be no greater than the maximum maneuvering moment that the differential engine throttling can provide, to approximate side loading.

Since the engines are arrayed perimeter the outside of the vehicle's base, the maximum moment is assumed to occur when half of the engines are shut off. This is approximated as a point load equal to half of the stage's maximum thrust value acting at a point 3.75 inches (9.5 cm), or one radius, from the vehicle axis.

3.2.4 DESIGNING FOR STRUCTURAL LOADS

With the types of loading being determined, a method for combining that loading to determine the sizing of the vehicle's tank wall is needed. Maximum acceleration loads will not necessarily correspond with the maximum aerodynamic loads. In fact, at stage burnout, where

$F_{inertia} = ma_{max}$

1st Stage:
$F_{inertia} = 1530$ N
$M_B = 73$ N-m

M_B **2nd Stage:**
$F_{inertia} = 150$ N
$M_B = 7$ N-m

F_T
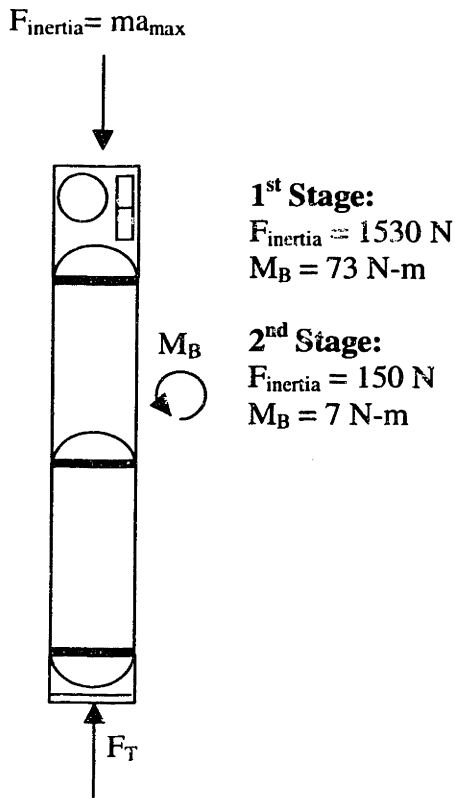
Figure 3.7 – Load Combination for Propellant Tank Sizing

the maximum acceleration occurs in the constant thrust case, the density of the atmosphere is less than 1% of its sea level, which makes the inline aerodynamic drag forces negligible.

A combination of the loading at the point of maximum acceleration combined with the maximum moment that the differentially throttled engines can deliver will be considered as the worst case for loading. Figure 3.7 illustrates the maximum loading condition for the first and second stages.

The inertial force will vary depending on location along the vehicle. In sizing the structure at the time of maximum acceleration we will examine a point at the bottom of the stage structure, which would see the effect of the entire burnout mass of the stage plus all subsequent stages and the payload being accelerated.

3.2.4.1 MAIN STRUCTURE – BUCKLING LIMITED

The cylindrical portion of the vehicle is first modeled as an isotropic, monocoque thin-walled unpressurized cylinder under axial and bending loads. The axial load (F_a) and bending moment (M_b) determined in the previous two sections are used to calculate axial compressive (σ_a) and bending stresses (σ_b) in the cylinder wall using Equations 3.7 through 3.10.[1] D_i is the cylinder inner diameter, D_o is the outer diameter, A_{cyl} is the cylinder cross-sectional area, c is the distance from the outer diameter to the neutral axis for bending, and I is the area moment of inertia.

$$A_{cyl} = \frac{\pi(D_o^2 - D_i^2)}{4}$$

Equation 3.7

$$\sigma_a = \frac{F_a}{A_{cyl}}$$

Equation 3.8

$$I = \frac{\pi(D_o^2 - D_i^2)}{32}$$

Equation 3.9

$$\sigma_b = \frac{M_b c}{I}$$

Equation 3.10

With the stresses in the cylinder calculated, it remains to calculate critical stresses for failure. The critical stresses for buckling can be expressed by Equation 3.11, where t is wall thickness, D_o is outer diameter, E is Young's modulus, η is a plasticity correction factor assumed equal to 1.0 since the stress is below the proportional limit, and γ is a correlation factor used to match theory with test results.[1]

$$\sigma_{cr} = 0.6\eta\gamma\frac{2Et}{D_o}$$

Equation 3.11

The critical stress is different depending on whether axial loads or bending moments are being considered. This difference is expressed through different values of the correlation factor, γ. Equations 3.12 and 3.13 give equations for γ for axial compression (γ_a) and bending (γ_b), respectively.

$$\gamma = 1 - 0.901(1 - e^{-\phi})$$

Equation 3.12

$$\gamma = 1 - 0.731(1 - e^{-\phi})$$

Equation 3.13

The value of ϕ depends on the ratio of the tank's outer radius (r) to its wall thickness, and is valid for both axial compression and bending providing the ratio r/t is less than 1500. Equation 3.14 gives an expression for ϕ.

76

$$\phi = \frac{1}{16}\sqrt{\frac{r}{t}}$$

Equation 3.14

For combined axial compression and bending, Equation 3.15 provides a condition for the failure by local buckling of the cylinder.[1] As long as the sum of the ratios on the right is less than or equal to one, the cylinder will not buckle. A safety factor (FS$_{buckle}$) is included into Equation 3.15. It was set at 1.5 so as to provide some cushion in designing the wall thickness.

$$\frac{(FS_{buckle})\sigma_a}{\sigma_{a-cr}} + \frac{(FS_{buckle})\sigma_b}{\sigma_{b-cr}} \leq 1$$

Equation 3.15

Table 3.6 shows the minimum wall thickness calculated using Equations 3.7 through 3.15. As well, the mass of the resulting cylindrical structure (w/o endcaps) is calculated to verify the assertion made in Section 3.2.2.2 that the material with the highest ratio E/ρ^2 leads to the lowest structure weight.

Table 3.6 – Tank / Cylindrical Structure Sized for Buckling

Minimum Thickness	mils	8.40	6.78	5.37
	mm	0.21	0.17	0.14
Mass of Cylindrical Section	kg	0.704	0.922	1.278
% of Stage Mass	%	1.00%	1.31%	1.82%
Minimum Thickness	mils	3.23	2.61	2.07
	mm	0.08	0.07	0.05
Mass of Cylindrical Section	kg	0.019	0.025	0.035
% of Stage Mass	%	0.29%	0.38%	0.53%

3.2.4.2 MAIN STRUCTURE – PRESSURE LIMITED

Table 3.6 gives minimum tank wall thickness providing that the buckling load is the limiting load for the tank structure. Since the tank is going to hold 50 psi (3.40 atm) of internal pressure, it must be verified that the tank will not fail at the thicknesses specified for buckling.

In reality, the internal pressure in the tanks does not act independently of the loading forces on the tanks. This coupling effect will be discussed in Section 3.2.4.3. First the propellant tanks will be examined for failure due to internal pressure.

Equation 3.16 gives the minimum required thickness of the cylindrical section of the propellant tanks given the maximum expected operating pressure, P, the factor of safety to protect against bursting, FS_{burst}, commonly 1.25, and the material yield strength, σ_y.[24] Table 3.7 gives the required size of the cylindrical section to protect for the internal pressure.

$$t = \frac{P(FS_{burst})D}{2\sigma_y}$$

Equation 3.15

Table 3.7 – Tank Structure Sized for 3.4 atm (50 psi) Internal Pressure

Stage 1 and Stage 2		Ti 6Al-4V	SS 430	Al 3003
Minimum Thickness	mils	1.84	3.66	11.14
Against Internal Pressure	mm	0.05	0.09	0.28
Mass of Cylindrical Section	kg	0.250	0.872	0.934
% of Stage Mass	%	0.35%	1.24%	1.33%

The required thicknesses in Table 3.7 illustrate the trade-offs in using different materials. While an aluminum tank will yield the lowest weight tank for a buckling limited structure, a titanium structure will give the lowest weight tank for a pressure limited structure. The best material choice is going to depend on the internal pressure in the tanks.

3.2.4.3 MAIN STRUCTURE – COUPLING EFFECTS

The internal pressure will have an effect on the required thickness in the wall. In addition to the radial, or hoop stress expressed by Equation 3.16, the internal pressure acting on the projected cross sectional area of each tank endcap will exert a longitudinal tensile stress in the cylindrical tank structure that directly counteracts the compressive stresses due to external loading. This stress, σ_L, is expressed by Equation 3.17. A modified form of 3.15, rewritten as Equation 3.17, includes the longitudinal stress. It is used to calculate the effects of internal pressure on relieving the compressive stresses.

78

$$\sigma_L = \frac{P(FS_{burst})D}{4t}$$

Equation 3.16

$$\frac{FS_{buckle}(\sigma_a - \sigma_L)}{\sigma_{a-cr}} + \frac{(FS_{buckle})\sigma_b}{\sigma_{b-cr}} \leq 1$$

Equation 3.17

Figures 3.8 and 3.9 show two superimposed graphs. One is the solution of Equation 3.17 as a function of the internal pressure. This represents a buckling limited strucutre. As the required thickness (and cylinder mass) decreases, the structure eventually becomes pressure limited and failure due to hoop stress (Section 3.2.4.2 / Equation 3.15) becomes the sizing criterium.
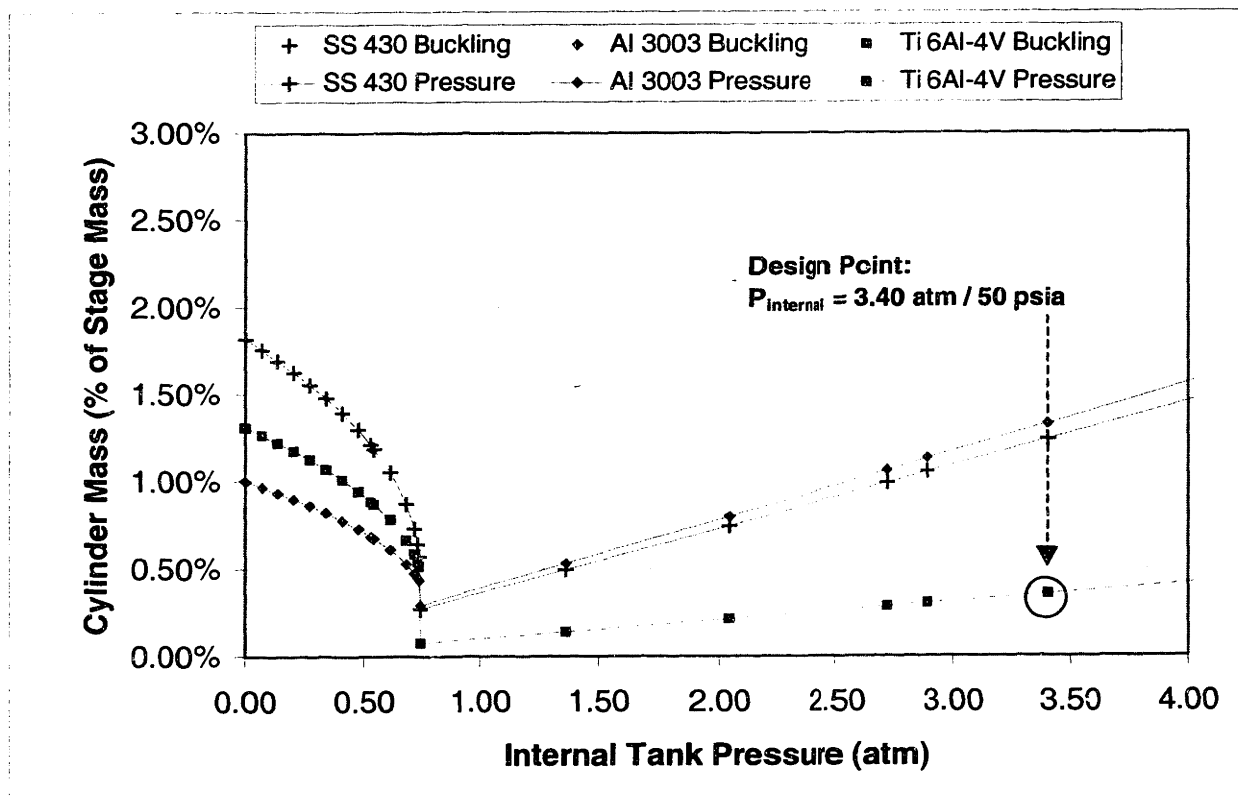
Figure 3.8 – First Stage Tank Structure Sized for Buckling and Internal Pressurization
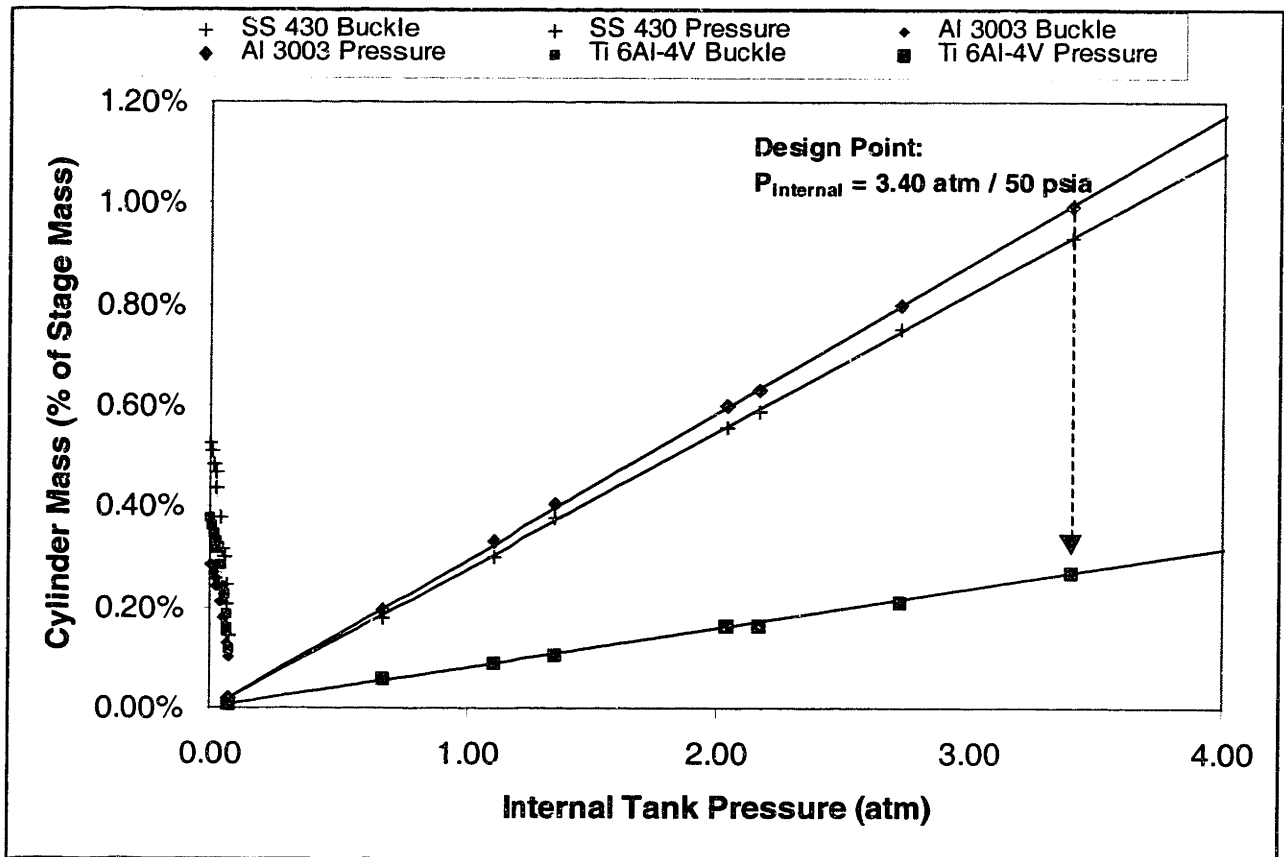
Figure 3.9 – Second Stage Tank Structure Sized for Buckling and Internal Pressurization

Concerning Figures 3.8 and 3.9, it is important to note that the internal tank pressure is really a pressure difference across the tank wall. The exterior pressure will decrease with altitude from 1 atm (14.7 psi) to approximately 0 atm. The most conservative pressure sizing criteria is to assume 0 atm external pressure and use the internal pressure as an absolute pressure for determing stresses and wall thickness.

Looking again at Figures 3.8 and 3.9, it is apparent that the tanks are pressure limited at any internal pressure above 1 atm (14.7 psi). This suggests the choice of Ti 6Al-4V for the tank walls. However, sizing the tanks for internal tank pressure requires that the tanks are always kept above some minimum pressure. According to Figures 3.8 and 3.9, 1 atm (14.7 psi) would be acceptable. Table 3.7 gives wall thicknesses and mass data for the cylindrical section of the pressure tank.

The cylindrical non-tank structure will not be pressurized, and must be sized for the buckling condition of Section 3.2.4.1. This is explained in Section 3.3. Also, if the H_2O_2 –

Ethanol engine cycle is chosen for further development (Section 3.2.2.1), the titanium alloy tank will not be an acceptable material choice. In this event, either a coating will be added to the titanium alloy or SS 430 can be used instead.

3.2.4.4 ENDCAPS

With the cylindrical tank walls sized, it remains to determine a size and configuration for the tank's three endcaps. The major load driving the endcap sizing will be the internal pressure in the tank (50 psia). The design that would create the lowest stress is a hemispherical one, and the equation for minimum wall thickness would be described by Equation 3.18, with P being the maximum expected operating pressure of the tanks, r being the endcaps' radius, and t being the required wall thickness. FS$_{burst}$ is a factor of safety, commonly 1.25,[24] applied to size the tanks for an absolute burst pressure.

$$\sigma_y = \frac{P(FS_{burst})r}{t} \qquad \textbf{Equation 3.18}$$

Although a hemispherical endcap will provide the minimum stress, and hence, the minimum tank thickness, a flatter endcap will lead to less overall material since the vehicle can be a bit shorter. This reduces the length of cylindrical side walls in the vehicle. For this reason, an ellipsoidal endcap is designed for the launch vehicle. This is shown in Figure 3.10.
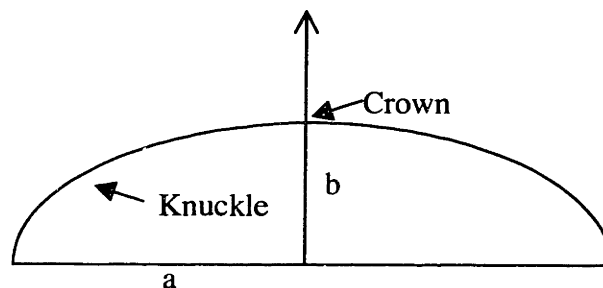
Figure 3.10 – Semiellipsoidal Endcap

A flat end on the tank would save the most length, but would introduce unacceptable bending stresses at the intersection with the outer tank walls. The ratio of the major axis to the

minor axis is defined as the ellipse factor, EF. One needs to determine how high the ellipse factor should reasonably be.

Equations 3.19 and 3.20 give the longitudinal (σ_L) and hoop (σ_h) stresses present in an ellipsoid as a function of major and minor axis as well as the longitudinal (ρ_L) and hoop (ρ_h) radii of curvature.[29]

$$\sigma_L = \frac{P(FS_{burst})\rho_L}{2tb} \qquad\qquad \textbf{Equation 3.19}$$

$$\sigma_h = \frac{P(FS_{burst})}{t}\left(\rho_h - \frac{\rho_h^2}{2\rho_L}\right) \qquad\qquad \textbf{Equation 3.20}$$

At the equator, there is a point, as you increase the ellipse factor, that the tensile hoop stresses for the hemispherical case turn compressive. As the compressive stress gets larger, it creates an unstable loading condition, and it is recommended by the ASME Pressure Vessel Code to keep EF less than 2 in order to avoid this condition.[29] At the equator, $\rho_L = b^2/a$ and $\rho_h = a$. Equation 3.21 shows the hoop stress at the equator. Taking Equation and solving for the point where the hoop stress turns compressive (i.e. equals 0), it is apparent that an ellipse factor greater than 1.42 will cause compressive stresses, and thus should be avoided.

$$\sigma_h = \frac{P(FS_{burst})a}{t}\left(1 - \frac{a^2}{2b^2}\right) \qquad\qquad \textbf{Equation 3.21}$$

In light of the calculations above, an ellipse factor of 1.33 was chosen for the semiellipsoidal endcaps, well below the ASME limit of 2.00. Also, the value of EF is below 1.42, which should prevent any compressive hoop stresses at the equator.

One way of predicting the required wall thickness would be to solve Equation 3.21 for t. However, this would result in a endcap thickness that would likely be too low. The effects of discontinuity stresses at the endcap-cylinder junction need to be taken into account. For this reason, Equation 3.22 is used to solve for the required thickness. Equation 3.22 is a modified

version of Equation 3.21 intended to correspond with empirical data.[30] In Equation 3.22, e_w is the weld joint efficiency, assumed to be 0.90 (average value for groove welds).[30]

$$\sigma_y e_w = \frac{P(FS_{burst})a}{t}\left[\frac{2+\left(\frac{a}{b}\right)^2}{6}\right] + 0.1P(FS_{burst})$$

Equation 3.22

Once the thickness of the endcap is known, the mass of the tank needs to be calculated. Equations 3.23 and 3.24 calculate the eccentricity and surface area of the semiellipsoid, respectively. Multiplying the surface area by the material density gives the mass of the endcap. Table 3.8 gives values for the thickness and masses of endcaps for the three alloys in question.

$$e = \frac{\sqrt{a^2 - b^2}}{a}$$

Equation 3.23

$$A_{surf} = a^2 + \frac{\pi b^2 \ln\left(\frac{1+e}{1-e}\right)}{2e}$$

Equation 3.24

Table 3.8 – Sizing of Ellipsoidal Endcaps for Propellant Tanks

Stage 1		Ti 6Al-4V	SS 430	Al 3003
Minimum Thickness	mils	1.28	2.56	7.80
	mm	0.03	0.07	0.20
Mass of Endcap	kg	0.007	0.024	0.026
% of Stage Mass	%	0.01%	0.03%	0.04%
Stage 2		Ti 6Al-4V	SS 430	Al 3003
Minimum Thickness	mils	1.28	2.56	7.80
	mm	0.03	0.07	0.20
Mass of Endcap	kg	0.007	0.024	0.026
% of Stage Mass	%	0.10%	0.36%	0.39%

3.2.5 PROPELLANT TANK SUMMARY

With Ti 6Al-4V chosen as the structural material, and both the cylindrical section and endcaps sized, it is possible to determine the configuration and weight of the propellant tanks. Tank wall thicknesses given in Tables 3.6 through 3.8 have all been rounded up to the nearest thousandth of an inch (mil), so as not to impose to great of a tolerance on manufacturing of the endcaps. Table 3.9 summarizes the baseline vehicle's propellant tank mass distribution.

Table 3.9 – Propellant Tank Mass Summary

		Stage 1	Stage 2
Cylindrical Structure			
Wall Thickness	mils	2	2
	mm	0.1	0.1
Mass of Cylinder	kg	0.272	0.019
% of Stage Mass	%	1.43%	1.07%
Endcap (x3)			
Wall Thickness	mils	2	2
	mm	0.1	0.1
Mass of One Endcap	kg	0.011	0.011
% of Stage Mass	%	0.02%	0.17%
Total Propellant Tank Mass	**kg**	**0.304**	**0.052**
% of Stage Mass	**%**	**0.43%**	**0.78%**

3.3 VEHICLE STRUCTURE

The vehicle will have two cylindrical structures within which will be contained the semiellipsoidal endcaps of the propellant tanks, the pressurization system, engines, avionics, and power subsytems. These cylinders will be subject to the buckling constraint discussed in Section 3.2.4.1.

The lower cylinder is sized to contain the engine subassembly. Each microrocket engine is 0.63 in (1.60 cm) tall. To allow for this and some room for connectors, etc., the lower cylinder has been sized to be 0.75 in (1.91 cm) tall plus 2.81 in (7.14 cm) and of the same thickness as the propellant tanks. The total length is 3.60 in (9.14 cm). It is assumed to be the same thickness as the propellant tanks in order to be conservative. The lengths are the same for both the first and second stages.

The upper cylinder is sized to contain the top endcap of the propellant tanks, and the pressurization system. The avionics and power subsystems are positioned next to the pressure tank, so they do not serve to increase the cylinder's length. Half of a vehicle diameter length is added on for margin. Once again, the thickness is assumed to be the same as that for the propellant tanks. This yields a first stage upper cylinder length of 9.10 in (23.1 cm) and a second stage length of 5.60 in (14.2 cm).

In addition to the lower and upper cylinders, stiffening rings have been added to the propellant tank. These are intended to serve as hard points for handling loads and as material support for the weld joints between the semiellipsoidal endcaps and the tank cylinder structure. Also, the propellant feed line out of the upper hydrazine fuel tank in the current tank configuration will perforate the middle stiffening ring. The stiffening rings are assumed to be located at the three interfaces between endcaps and cylindrical structure. They are all arbitrarily assumed to be 0.5 mm, which is approximately 10 times the wall thickness. The first stage rings are 2.54 cm (1.00 in) tall, and the second stage rings are 0.64 cm (0.25 in) tall.

Table 3.10 shows specifications for the lower and upper cylinders for both the first and second stages along with the support rings.

Table 3.10 – Vehicle Structure Data

Upper Cylinder		Stage 1	Stage 2
Length	in	9.10	6.40
	cm	23.11	16.26
Thickness	mils	7	7
	mm	0.2	0.2
Mass of Cylinder	kg	0.109	0.033
% of Stage Mass	%	0.15%	0.49%
Lower Cylinder		Stage 1	Stage 2
Length	in	3.60	3.60
	cm	9.14	9.14
Thickness	mils	7	7
	mm	0.2	0.2
Mass of Cylinder	kg	0.043	0.018
% of Stage Mass	%	0.06%	0.28%
Support Rings		Stage 1	Stage 2
Length	in	1.00	0.25
	cm	2.54	0.64
Thickness	mils	20	20
	mm	0.5	0.5
Mass of Three Rings	kg	0.100	0.025
% of Stage Mass	%	0.14%	0.38%

The payload shroud referred to in Table 3.1 and Figure 3.16 is arbitrarily assumed to have a 7.5 in (19.0 cm) diameter cylindrical section of length 15.76 in (40.03 cm). At the end of this section is a conical endcap with a height of 7.5 in (19.0 cm), equal to the vehicle's diameter. These numbers scale with some proposed small missiles and launch vehicles.[63] The mass of this payload shroud is assumed to be a portion of the gross payload mass reported in Chapter 2.

3.4 PRESSURIZATION SYSTEM

Although a pump-fed system has been chosen to feed the propellants into the microrocket engine, a pressurization system is still needed to create enough pressure to deliver the propellant to the pumps without cavitating them. One possibility would be to eliminate the pumps altogether and go with a fully pressure-fed system to reduce the system's complexity. However, instead of the 20-50 psia (1.4 - 3.4 atm) tank pressure typically required of a pump-fed system, a pressure more on the order of 100-300 psia (6.8 - 20.4 atm) would be required for a totally pressure-fed system.[9] The effect on tank mass alone would be significant, as can be seen in Figures 3.9 and 3.10. Since the pumps themselves will be on the same chip as the microrocket engine, they will little mass to the propulsion system.

To develop a pressurization system for the propellant tanks, both the type of system and its size and configuration must be determined. There are many ways to pressurize a gas. Some of the more commonly used methods are:

- Stored Gas System – By far the most common type of pressurization system, high pressure inert gas is used to pressurize and expel the propellant. The gas is stored at much higher pressure than the propellant, and is regulated down in pressure using a pressure regulator, or even just a fixed orifice.
- Evaporated Propellant System – Propellant is heated and reintroduced into the propellant tank to pressurize itself. Since many fuels tend to decompose violently under heating, primarily the oxidizers are pressurized this way.

- Gas Generator System – The gas generator of a pump-fed system is bled off and reintroduced into the propellant tank for pressurization. Compatibility of the hot gas with the propellants must be maintained.

- Polytropic Expansion System – This type of system involves prepressurization of the propellant tank ullage to a high enough initial pressure level so that sufficient propellant flow can be maintained. This eliminates the need for an additional high pressure tank, but results in a nonconstant ullage pressure in the tank.

Each system has specific advantages and disadvantages depending on the type of system being considered. System selection for this launch vehicle is outlined in Section 3.4.2.

3.4.1 PRESSURIZATION REQUIREMENTS

The pressurization system for the launch vehicle will be required to produce enough pressurant gas to displace the entire volume of the propellant tanks with 50 psia (3.4 atm) gas. Table 3.11 outlines the pressurization requirements.

Table 3.11 – Pressurization Requirements

Baseline Launch Vehicle		Stage 1	Stage 2
Oxidizer Tank Volume	in^3	1,391	129
	cm^3	22,792	2,108
Fuel Tank Volume	in^3	2,205	204
	cm^3	36,128	3,341
Total Propellant Tank Volume	in^3	3,396	332
	cm^3	58,920	5,449
Propellant Tank Pressure	psia	50	50
	atm	3.4	3.4

3.4.2 SYSTEM SELECTION

Each type of pressurization system is best suited for particular applications. Each type of system is examined.

The evaporated propellant system is one way to eliminate the need for a separate pressurant gas, potentially saving system mass. One of the important requirements for such a

system is a low boiling point, so that it is easier to boil the propellant.[9] This works especially well with cryogenic oxidizers, such as oxygen, where the boiling point at 1 atm pressure is -298°F (90°K).[27] With an atmospheric boiling point of 70°F (294°K), nitrogen tetroxide is also a good candidate to be pressurized in this way. However, hydrazine does not work with this type of system. Besides the risk of violent boiling and/or decomposition by heating, it has a high boiling point, 236°F (387°K). With a hydrazine – nitrogen tetroxide propellant combination selected, separate pressurization systems would be required for the N_2O_4 and N_2H_4 propellants. This would likely add more system complexity than it would actually save mass, so this option was rejected.

The gas generator system has found some, although not widespread, use. It is used for fuel tank pressurization for the Titan as well as in some other military vehicles.[9] However, the concept is frequently ruled out since the combustion products are hot and often include condensable solids and/or excessive H_2O content. With the N_2O_4 – N_2H_4 system under consideration, it is undesirable to introduce any unburned oxidizer into the fuel tank and vice versa, since the propellants are hypergolic. As well, nitrogen tetroxide is very sensitive to H_2O content and hydrazine becomes unstable at high temperatures. As a result, this type of system was also ruled out.

A polytropic expansion system has potential to eliminate any additional pressurization system hardware. However, it will require an increase in propellant tank length to accommodate the additional pressurant gas and/or an increase in wall thickness to hold the higher initial pressure. However, it is much more difficult to control the flow of propellant in this way since the ullage pressure varies considerably over time. This is a problem in bipropellant systems, since the mixture ratio needs to be well controlled. For this reason, this type of system is commonly used in monopropellant systems, and was also ruled out.[9]

The storable inert gas system is by far the most commonly used pressurization method today. Inert gases such as helium and nitrogen are usually used due to their low molecular weights and the fact that they will not react with any propellants. The particular gas to be used is discussed in Section 3.4.3. Frequently, the gas is stored at cryogenic temperatures to reduce density, and thus storage volume. This method requires some sort of heat exchanger to warm the gas up to be used as a pressurant. In large vehicles, this is frequently worthwhile. Due to its

simplicity and compatibility with the vehicle being designed, a storable inert gas system was chosen for this vehicle.

3.4.3 PRESSURANT GAS SELECTION

The most commonly used pressurant gases are helium and nitrogen. Other gases, especially inert ones like argon and neon can be used as well, although they have higher molecular weights and are therefore less desirable. The main criterion for pressurant gas selection is that the pressurant gas is compatible with the propellant being pressurized.[9]

One consideration with the choice of a pressurant gas is its solubility in the propellants being pressurized. At 77°F (273°K) and 1 atm, the solubility of nitrogen gas in N_2O_4 is more than 6 times that of helium gas.[58] High solubility is going to lead to a greater pressurant demand, and thus a heavier pressurization system. This concern led to the choice of helium over nitrogen gas for the pressurant gas. As a side note, out of ten vehicles selected from the late 1960's and early 1970's which used N_2O_4 as an oxidizer, seven of them used helium as the pressurant gas and three used nitrogen.[9]

3.4.4 VALVES AND REGULATORS

Besides the high pressure tank and propellant tank, the pressurization system must have a way to regulate the high pressure stored helium to the relatively low pressure of the propellant tanks. This can be accomplished merely with an in-line orifice that chokes the gas flow. However, this will produce a steadily decreasing pressure into the tank, which will make propellant mass flow and eventually thrust unsteady as well. More commonly, this is accomplished with a pressure regulator, which, in effect, is an orifice with a controllable area that is set by the upstream pressure. Whether a conventional pressure regulator can be used in this vehicle or some way to keep the pressure more constant than a single fixed orifice must be determined.

In addition to the pressure regulator, valves will be used in the system for filling the high pressure tank and for relief of the propellant tank in case the tank pressure exceeds its limit, which we will assume to be the burst pressure discussed in Section 3.2.4 of 62.5 psia (4.25 atm).

Standard commercial regulators and valves usually contain dynamic O-rings and other seals made from rubber, viton, and other viscoelastic materials. These seals "flow" into crevices, etc. to prevent leakage and/or failure of the device. However, temperature has an effect on the materials' ability to flow correctly. This places a minimum operating temperature limit on those type of regulators and valves. This limit varies depending on the particular material, but a commonly used guideline is -65°F (219°K).[6] Valves have been developed at greater cost and complexity for cryogenic service, operable to much lower temperatures.

In order to minimize system complexity and cost, the minimum temperature of the helium gas will be set at -65°F (219°K) to correspond to the minimum service temperature for commonly available pressure regulators and valves described above.

3.4.5 PRESSURANT TANK SIZING

With some specifications determined for the pressurization system, the next step is to determine the size of the tank that holds the high pressure helium. The volume of the tank and internal pressure must be determined to minimize system mass. Then a material suitable for high pressure helium storage must be selected. Then the tank mass can be determined.

3.4.5.1 THERMODYNAMIC COOLING ISSUES

One issue that comes up with a storable inert gas system is the potential cooling of the propellant as it is discharged from the tank. This effect can be seen by looking at the process of expansion from a fixed control volume (i.e. a spherical tank) from an initial to final state. Assuming an adiabatic, reversible process with negligible potential and kinetic energy losses of a calorically perfect gas, and utilizing the ideal gas equation of state, one can obtain Equations 3.25 and 3.26.

$$\frac{T_2}{T_1} = \left(\frac{P_2}{P_1} \right)^{\frac{\gamma-1}{\gamma}}$$

Equation 3.25

$$\frac{T_2}{T_1} = \left(\frac{m_2}{m_1}\right)^{\gamma-1}$$

Equation 3.26

State 1

T_1

P_1

State 2

T_2

P_2

Discharged Mass $\longrightarrow$ $m_1\text{-}m_2$
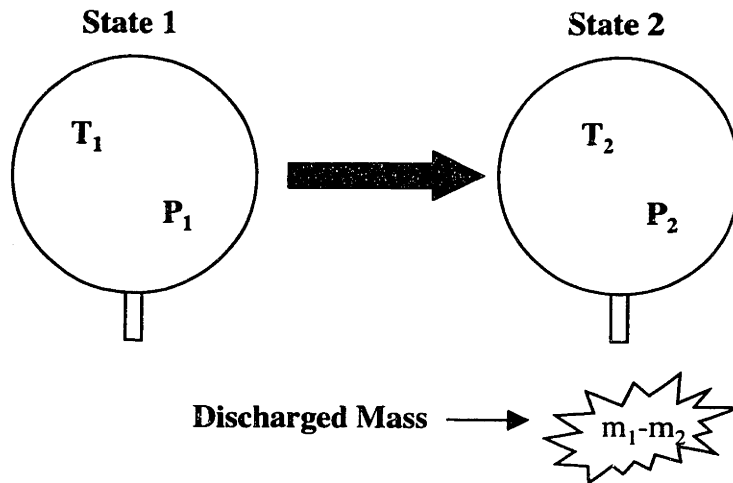
Figure 3.11 – Pressurant Tank Discharge Process

Keeping the idealizations in mind that were used to develop Equations 3.25 and 3.26, it is apparent that the final gas temperature, T_2, could become extremely cold. The questions that must be determined for this system is whether this will have any significant impact, and, if so, what limit should be set on T_2? One important point to realize about Equations 3.25 and 3.26 is that they represent an idealized case. Other effects should be considered. For example, heat transfer will take place between the tank's metal structure and the gas inside. This might negate some or all of the cooling effect. Also, the fact that the gas is not ideal will actually result in colder final temperatures since not as much gas will be in the tank initially as the ideal gas equation of state suggests.

An extremely cold final gas temperature could have a couple of possible effects on the system. First of all, heat transfer from the extremely cold pressurant gas could cool the hydrazine or nitrogen tetroxide below their freezing temperatures, 11.5°F (262.0°K) and 34.4°F (274.7°K) respectively.[27] If either the fuel or oxidizer were allowed to freeze, this could cause clogging of the feed lines or even outright failure of the microrocket engines. A second concern is that if valves and regulators with standard sealing materials are indeed used for the pressurant

flow as described in Section 3.4.4, the temperature of the pressurant gas must be kept above the minimum service temperature for those materials.

The question of freezing is a complex analysis that would require knowledge of the heat transfer coefficient between the propellant and helium pressurant during all stages of the propellant discharge process. Also, heat input from the propellant tank walls to the system should also be considered, whether it is due to aerodynamic heating or just the latent heat capacity of the aluminum tank wall.

To first order, an idea of the severity of the freezing question can be examined. All heat transfer to the system from the tank walls, atmosphere, is neglected. The only heat exchange is assumed to be between a volume of propellant and a volume of pressurant gas. First, take the entire volume of the first stage oxidizer tank at the storage temperature, 77°F (298°K). Then assume that the helium gas pushes the oxidizer out of the tank doing $P\Delta V$ work at the constant tank pressure of 50 psia (3.4 atm). Then, calculate the mass of helium that would occupy the tank at the tank pressure a fixed inlet temperature of -65°F (219°K). Finally, assume that the helium and nitrogen tetroxide end up at the same equilibrium temperature through heat transfer. Assume constant specific heats of 0.42 Btu/lb$_m$°F (1758 J/kg°K) for N_2O_4 and 1.25 Btu/lbm/°F (5190 J/kg°K) for He. Assuming helium is a thermally perfect gas, using the ideal gas equation of state, and Equation 3.27 based on the conservation of energy, it is possible to solve for the ending temperature.

$$m_g c_{pg}\left(T_f - T_{ig}\right) + P_{\tan k}V_{\tan k} = m_l c_{pl}(T_{il} - T_f)$$
  Equation 3.27

Using the above relation and assumptions, the final temperature of the helium and nitrogen tetroxide is 76.6°F (297.8°K). Due to the vast difference in the mass of helium (0.01 kg) and the mass of nitrogen tetroxide (32.89 kg) being considered, the helium gas does not have the heat capacity to appreciably affect the N_2O_4.

One potential temperature limitation was the minimum service temperature of system valves and regulators discussed in Section 3.4.4. This was set at -65°F (219°K), and will be assumed to be the minimum temperature that the gas remaining in the helium tank is allowed to reach. With this minimum limit in mind, it is possible to determine a necessary size of

propellant tank required to pressurize the propellant tanks and leave enough residual mass in the high pressure storage tank so that the helium temperature never drops below the service limit.

One way to calculate the ending temperature of the pressure tank is by using Equations 3.25 and 3.26. This, however, carries with it the assumption of a perfect gas and the ideal gas equation of state. The storage pressure of the high pressure tank could be up to 10,000 psi (680 atm). At high pressures, the intermolecular forces become increasingly significant, causing significant variation from the ideal gas equation of state. For example, at 500 atm (7,350 psia) and 300°K (80°K), the difference between actual data[34] and the ideal gas prediction is 23%. Since high storage pressures will be considered, it makes sense to account for real gas effects in any calculation.

From the First Law of Thermodynamics, assuming quasistatic behavior in the tank and no work done on the system, Equation 3.28 can be developed to calculate the change in internal energy, Δu, over a small increment of time, Δt. The change is mass out of the tank is assumed to be the amount of mass of helium required to fill the volume vacated by the propellant in the same time increment.

$$\Delta u = \frac{P\Delta m_{12}}{\rho_1 m_1} + \frac{\dot{Q}\Delta t}{m_1} \qquad \text{Equation 3.28}$$

Providing the time increment, Δt, is chosen small enough, Equation 3.28 can be iterated over the stage burn time to end up with the final conditions in the propellant tank. The initial volume must be guessed ahead of time. The result of the calculation can be used to determine whether the guess for tank volume was too large or too small.

The discharge of the tank was calculated using Equation 3.28, and real gas property data for helium gas.[34] The real gas data was tabulated and a 2-D linear interpolative look-up function was written to determine one state value with two others as input. Six different tables were created: $P(\rho,T)$, $\rho(P,T)$, $h(P,T)$, $u(P,T)$, $T(P,h)$, and $T(\rho,u)$. The algorithm and code for this calculation appears in Appendix B.

Calculations were carried out to determine the required tank volume and diameter for a variety of initial pressures to protect against the minimum service temperature of -65°F (219°K).

Results for the first and second stage appear in Figures 3.12 and 3.13. The internal diameter of the first and second stage is 19.0 cm (7.5 in).
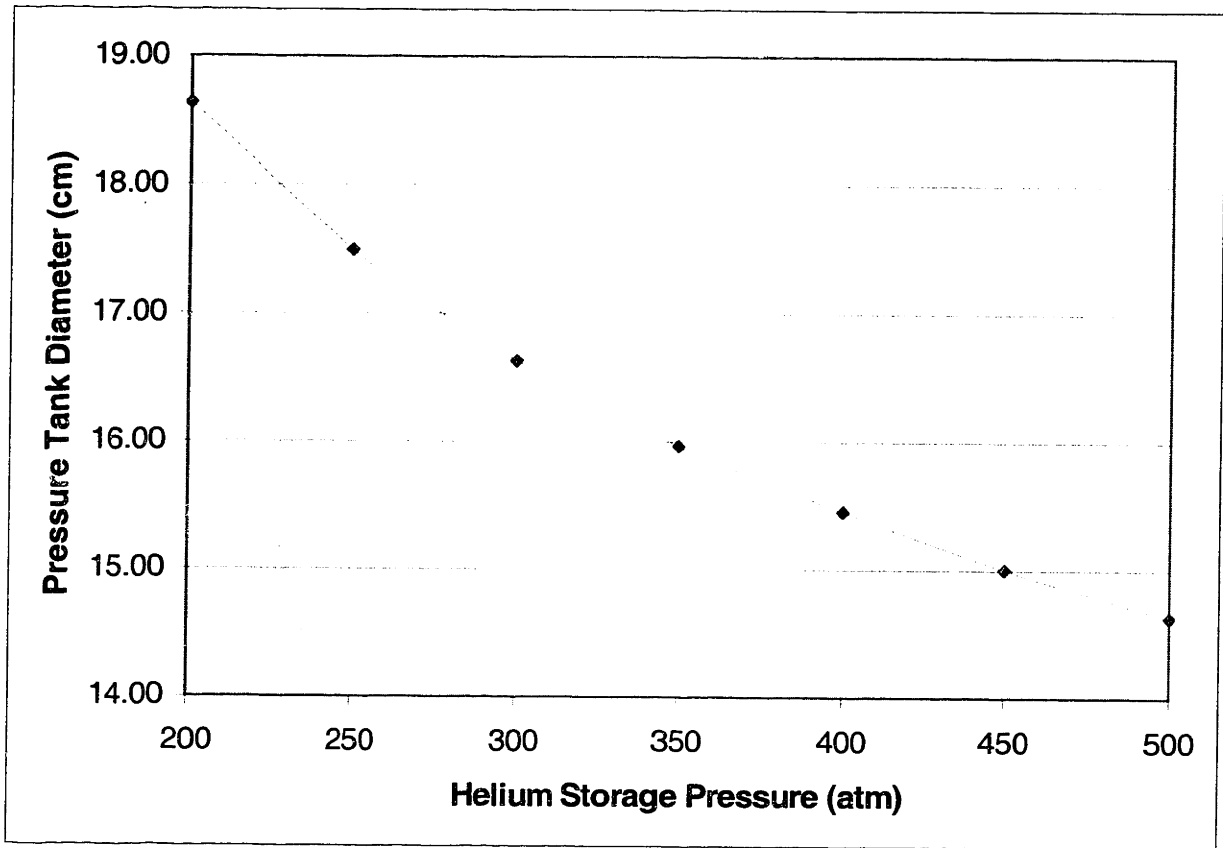
Figure 3.12 – First Stage Pressure Tank Diameter vs. Helium Storage Pressure
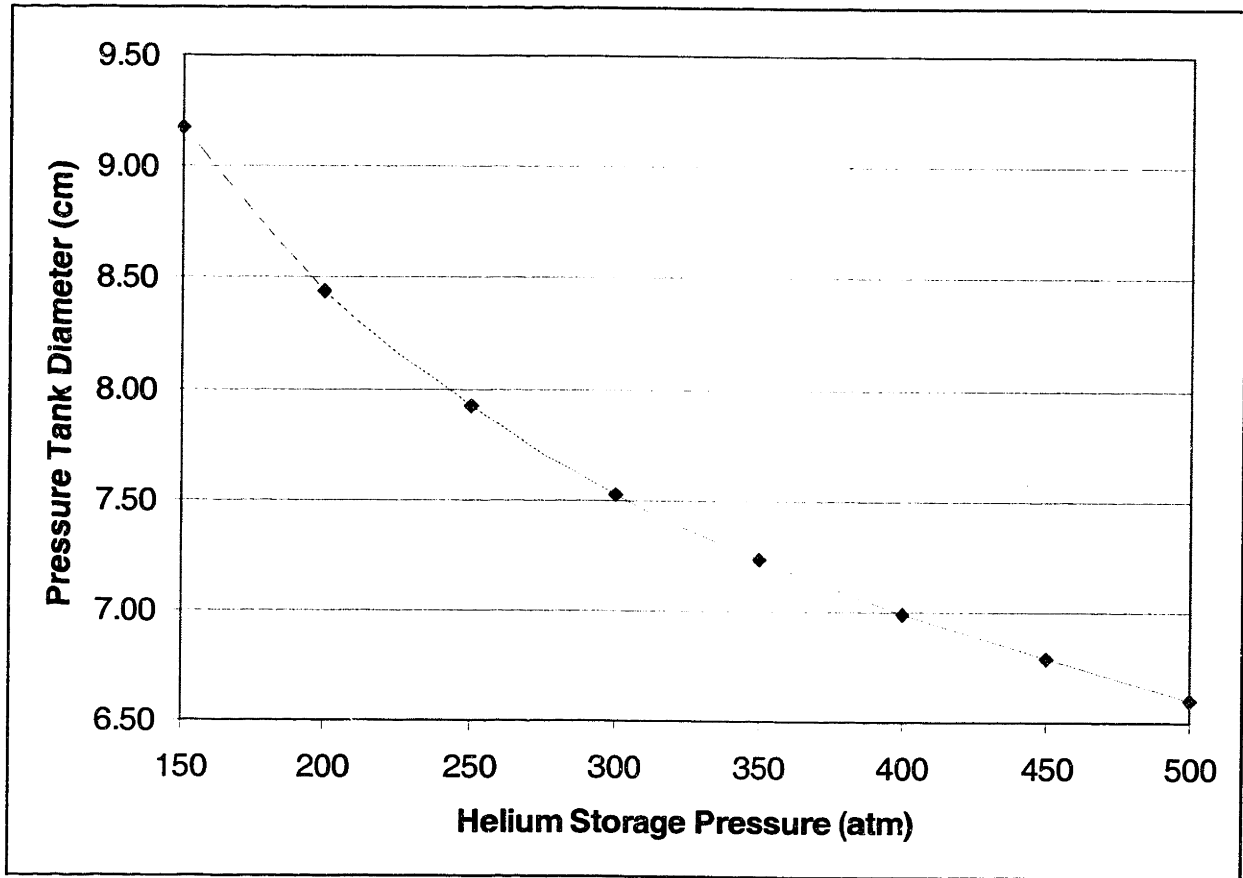
Figure 3.13 – Second Stage Pressure Tank Diameter vs. Helium Storage Pressure

3.4.5.2 MATERIAL SELECTION

The dominant loading condition in the pressurant tanks will be the internal pressure in the tank. As discussed in Section 3.2.2.2, this loading condition is best met by a material with a high specific strength (σ_y/ρ). Titanium 6Al-4V alloy is a good choice for this application, since it has a higher σ_y/ρ ratio than aluminum or stainless steel alloys. There is no concern with material compatibility since helium is an inert gas. Therefore, Ti 6Al-4V was chosen for the high pressure helium storage tank.

3.4.6 SYSTEM MASS

With the material selected, it remains to determine the mass of the tank. To obtain this, Equation 3.29 is used to calculated the required thickness of the tank. P is the storage pressure, FS_{burst} is the factor of safety to protect against bursting, commonly 1.25, and σ_y is the material's yield strength. The mass is then calculated by multiplying the thickness of the tank by the surface area and density. This is seen in Equation 3.30.

$$t = \frac{P(FS_{burst})D}{4\sigma_y}$$
Equation 3.29

$$m_{tan\,k} = \frac{t\rho\pi D^3}{6}$$
Equation 3.30

The thickness of the tank, and thus the mass, will depend on the storage pressure of the tank. Figures 3.14 and 3.15 show the effect of changing the storage pressure on tank mass, subject to the restrictions and assumptions already made.

Figures 3.14 and 3.15 show that the tank mass decreases as the helium tank storage pressure is decreased. This would suggest using as low of a pressure as possible that would still be acceptable to meet minimum inlet conditions for pressure regulators, etc. However, looking at Figures 3.12 and 3.13, a significant constraint is noticable. With only a 19.0 cm (7.5 in) diameter, any pressure tank is going to have to have a diameter that will fit in this envelope. This is not a problem with the second stage, but it is with the first stage. For this reason, the first stage helium tank is designed to be at a relatively high pressure of 500 atm (7348 psia), in order to keep as small of a diameter as possible so that other components can fit alongside the helium tank. This is consistent with modern practice. The second stage tank storage pressure is set at 200 atm (2939 psia), to minimize weight.
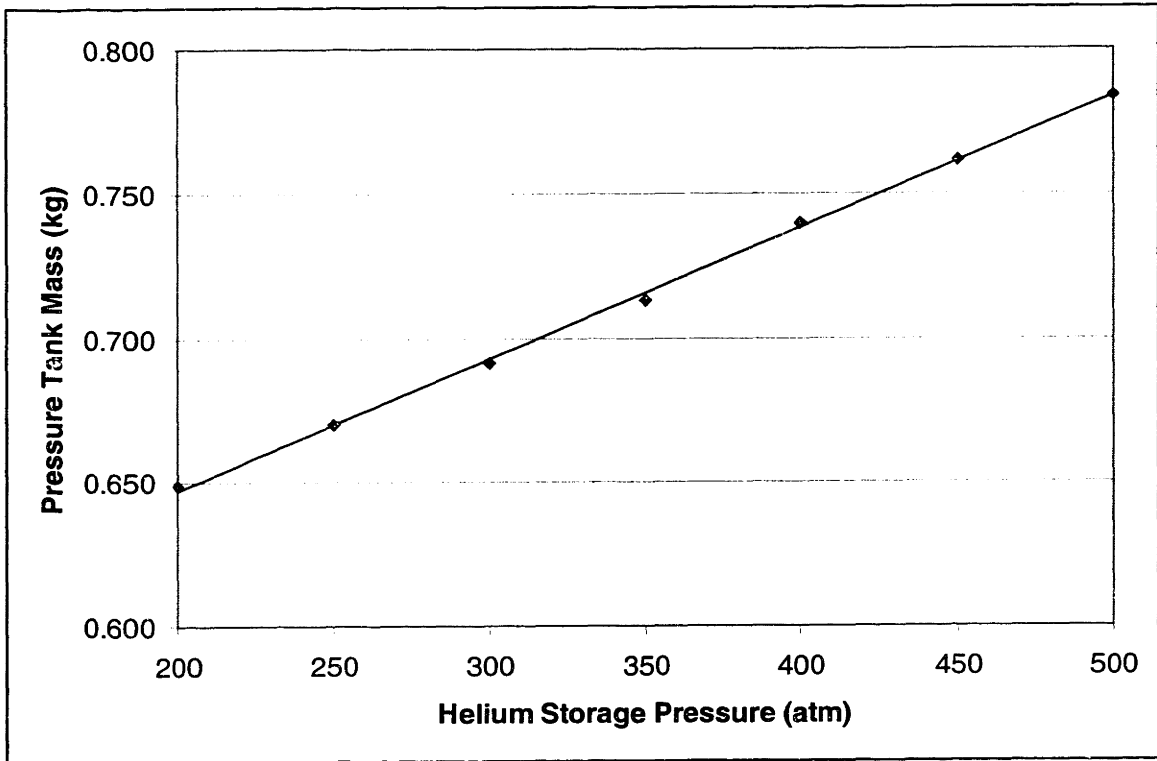
Figure 3.14 – First Stage Pressure Tank Mass vs. Helium Storage Pressure
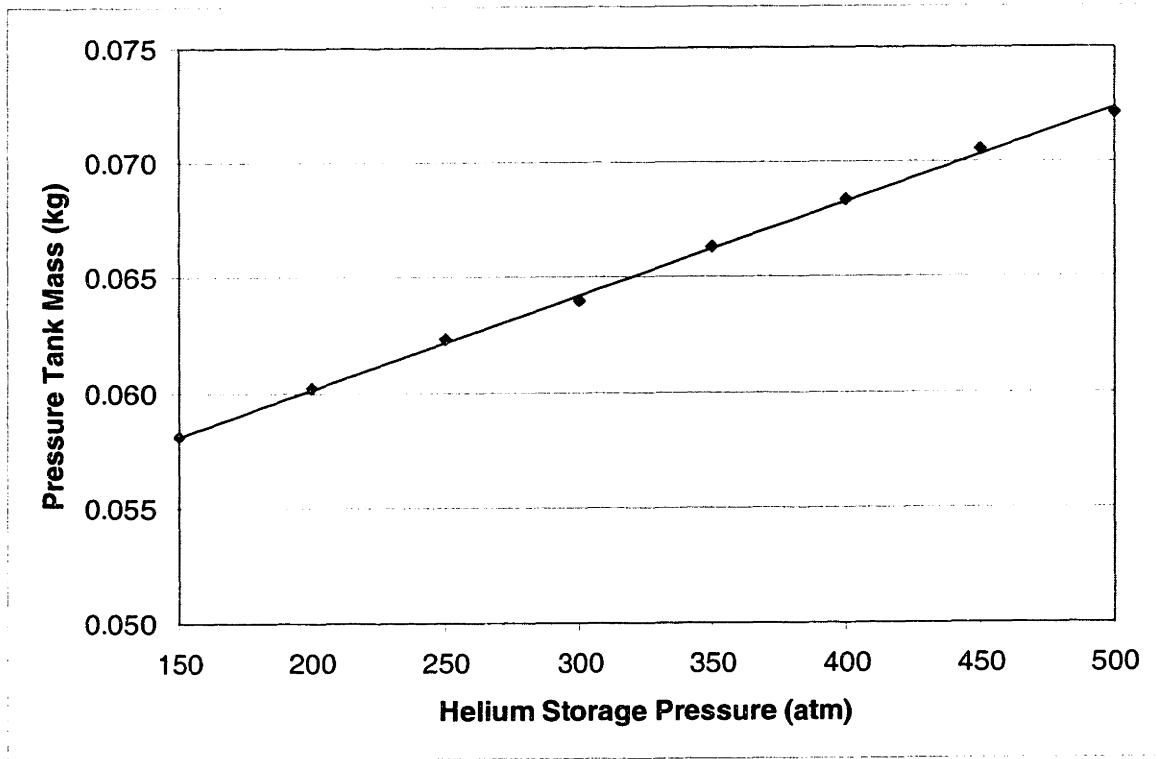
Figure 3.15 – Second Stage Pressure Tank Mass vs. Helium Storage Pressure

In addition to the tank thickness, extra material will be used for support in areas of welding and for attachment and support to the main structure. An estimate of 20% tank mass has been added to the system to account for this additional mass. The helium pressurization system mass is then defined as the mass of the tank at minimum thickness, 20% tank mass for supports, etc., and the actual mass of the helium gas at initial storage conditions. Table 3.12 shows the values for this system.

Table 3.12 – Pressurization System Data

Baseline Launch Vehicle		Stage 1	Stage 2
Storage Tank Pressure	atm	500	200
	psia	7,348	2,939
Storage Tank Diameter	cm	14.63	8.44
	in	5.76	3.32
Storage Tank Mass	kg	0.784	0.060
20% Structural Reserve	kg	0.157	0.012
Helium Gas	kg	0.073	0.006
Total Storage Tank Mass	kg	1.013	0.078

3.5 AVIONICS AND POWER

To control the vehicle's communication, propellant management devices, guidance, navigation, and control, a central computer or avionics subsystem is needed. Likewise to provide power to the avionics subsystem and the other various subsystems, a power generation subsystem is required.

Electronics miniaturization has enabled a tremendous reduction in the size of avionics systems. The current state of the art for an integrated avionics system, complete with a micro-scale GPS navigation system is assumed to weigh 50 grams. It will draw 15 W of power.

Avionics is primarily needed in the second stage for guidance, navigation, communications, control of stage and payload separation, and control of the propellant feed valves in the microrocket engines. Some first stage avionics will be needed to control power distribution to the first stage engines, but the majority of the avionics can be handled by the second stage.

Since it is unknown how much smaller a state of the art avionics system can be with only partial features, it will be assumed that a 50 g avionics system is being used in both the first and second stages.

Power for launch vehicles and spacecraft can be handled by a variety of sources including batteries, chemical fuel cells, gas generators, or even hydrazine decomposing power units. Due to the low power demand of this system and desire for simplicity, batteries will be used. Two more commonly used types of batteries are nickel-cadmium (NiCad) and lithium oxide. Lithium oxide batteries tend to have a higher energy density, and are desirable on spacecraft with long mission times. However, they have a slower power dissipation rate. For the relatively short mission time of this launch vehicle, this will lead to heavier batteries to supply the power needed, even though the total energy density is greater. For this reason, NiCad batteries are selected for the launch vehicle. Looking at some typical application with similar mission lengths, the mass per watt of power delivered by the NiCad batteries is found to be 1 g/W. Thermal batteries were not examined but may hold the promise of reduced mass for this application.

In addition to the 15 W of power required for the avionics system, the engines are assumed to require 2 W of power per engine. Table 3.13 outlines the power and mass requirements of the avionics and power subsystems.

Table 3.13 – Avionics and Power Subsystem Data

Power Demand		Stage 1	Stage 2
Avionics Subsystem	W	15	15
Engines and Valves	W	204	20
Number of Engines		102	10
Power per Engine	W	2	2
Total Power Requirement	W	219	35
Subsystem Mass		Stage 1	Stage 2
Avionics Subsystem	kg	0.050	0.050
Power Subsystem	kg	0.219	0.035
Total Avionics and Power Mass	kg	0.269	0.085

3.6 VEHICLE SUMMARY

With the systems study in Sections 3.1 through 3.6 in mind, a preliminary design of the launch vehicle is obtained.

3.6.1 MASS BUDGET

The trajectory analysis and mission performance calculations in Chapter 2 made assumptions about the inert mass in each stage. The systems study of Chapter 3 checks the reasonableness of those assumptions. Table 3.14 shows the mass budget for the vehicle based on the calculations and assumptions in Sections 3.1 through 3.5.

Table 3.14 - Baseline Launch Vehicle Mass Budget

	Stage 1 Mass	Fraction	Stage 2 Mass	Fraction
Propulsion System	**0.474 kg**	**0.67%**	**0.106 kg**	**1.59%**
Engines	0.204 kg	0.29%	0.020 kg	0.30%
Valves and Flow Controllers	0.204 kg	0.29%	0.020 kg	0.30%
Support Structure	0.066 kg	0.09%	0.066 kg	0.99%
Propellant Tanks	**0.304 kg**	**0.43%**	**0.052 kg**	**0.78%**
Cylinder	0.272 kg	0.39%	0.019 kg	0.29%
End Caps	0.032 kg	0.05%	0.032 kg	0.49%
Structure	**0.253 kg**	**0.36%**	**0.076 kg**	**1.15%**
Lower Cylinder	0.043 kg	0.06%	0.018 kg	0.28%
Upper Cylinder	0.109 kg	0.15%	0.033 kg	0.49%
Support Rings	0.100 kg	0.14%	0.025 kg	0.38%
Avionics & Power	**0.269 kg**	**0.38%**	**0.085 kg**	**1.28%**
Avionics	0.050 kg	0.07%	0.050 kg	0.75%
Batteries / Power	0.219 kg	0.31%	0.035 kg	0.53%
Pressurization System	**1.049 kg**	**1.49%**	**0.080 kg**	**1.20%**
Pressurant Gas	0.109 kg	0.15%	0.008 kg	0.11%
Tank Mass	0.784 kg	1.11%	0.060 kg	0.91%
Tank Connections (20%)	0.157 kg	0.22%	0.012 kg	0.18%
ACTUAL INERT SYSTEM MASS	**2.348 kg**	**3.34%**	**0.398 kg**	**5.99%**
TARGET INERT SYSTEM MASS	**4.222 kg**	**6.00%**	**0.532 kg**	**8.00%**
INERT MASS RESERVE	**1.874 kg**	**80% of m_{inert}**	**0.134 kg**	**33% of m_{inert}**

From Table 3.14, it is shown that the calculated inert mass falls within the estimates made for the trajectory analysis of Chapter 2. The margin in this mass is significantly less in the second stage than the first. As well, the sensitivity of the second stage to increases in mass is

high due to its low stage mass. From an inert mass perspective, it is critical that stage 2 remains as light as possible and extraneous inert mass is not added. If the mass reserve were not sufficient for stage 2, the performance numbers for a vehicle with a lower second stage mass fraction, either 0.90 or 0.88, could be determined from Figure 2.12.

3.6.2 SYSTEM LAYOUT

With the major subsystems designed, the vehicle can be configured. Figure 3.16 shows the vehicle with its major subsystems.

Overall Vehicle

Length:	3.62 m (142.4 in)
Diameter:	0.19 m (7.5 in)
Mass:	77.01 kg

Propellants: N_2O_4 / N_2H_4
Mixture Ratio (Oxidizer/Fuel): 0.90
Vacuum Specific Impulse: 290 sec.

First Stage:

Length:	2.49 m (97.9 in)
Diameter:	0.19 m (7.5 in)
Mass:	70.36 kg
$m_{prop}/m_{stage}(\zeta)$:	0.94
Engines:	102

Second Stage:

Length:	0.54 m (21.3 in)
Diameter:	0.19 m (7.5 in)
Mass:	6.65 kg
$m_{prop}/m_{stage}(\zeta)$:	0.92
Engines:	10

Payload Shroud:

Length:	0.59 m (23.3 in)
Diameter:	0.19 m (7.5 in)

Engines
N_2O_4 Oxidizer Tank
N_2H_4 Fuel Tank
Power Unit
Avionics Unit
Helium Pressure Tank
Power Unit
Avionics Unit
Payload Shroud
N_2H_4 Fuel Tank
N_2O_4 Oxidizer Tank
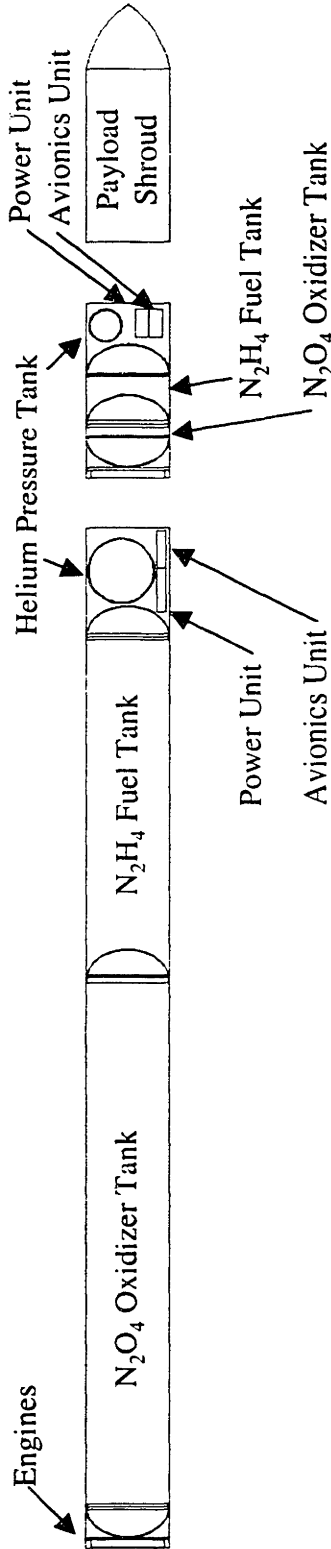
Figure 3.16 - Very Small Launch Vehicle System Schematic

CHAPTER 4
CONCLUSIONS AND FUTURE WORK

The performance analysis and systems study suggest that it is technically feasible to produce a very small launch vehicle (15 - 2000 kg liftoff mass) in order to deliver nano and micro scale payloads (0.1 - 20 kg) to orbital and ballistic targets. Vehicles of this size incur performance penalties due to increased relative aerodynamic drag and challenges in scaling down of certain components. However, recent developments in micro-scale technologies, such as MEMS / micropropulsion and electronics miniaturization could provide a weight savings on the same order as the gross payload loss resultant from scaling down the vehicle. Also, by air launching, much of the performance loss from the aerodynamic drag can be mitigated.

4.1 SMALL LAUNCH VEHICLE CHALLENGES

The scaling down of a launch vehicle presents design challenges that must be overcome. Some of the most significant challenges are increased relative aerodynamic drag, individual component scaling, mass sensitivity of upper stages, and fixed operations costs. However, micro-scale technologies and innovative operations concepts may overcome these limitations.

4.1.1 AERODYNAMIC DRAG VS. AIR LAUNCH

The relative effect of inline aerodynamic drag on a launch vehicle roughly increases as the inverse of the vehicle's length. This suggests a performance penalty for smaller vehicles, which is significant for vehicles smaller than 10,000 kg (Figure 1.2). However, this effect does not prevent vehicles larger than 15 kg from reaching orbit (Section 1.3). As a result, a smaller vehicle must accept a smaller payload fraction or use other technologies and/or operational methods to mitigate the effect.

One way to avoid the performance penalties of aerodynamic drag is to avoid the atmosphere. Air launching the vehicle, as is planned for the baseline 77 kg version, is one way of mitigating the increased relative drag losses incurred by scaling the vehicle down.

Table 4.1 illustrates this effect. Using the baseline 77 kg launch vehicle to its 770 km polar reference orbit, the ground and air launched cases are compared with the ground launched case with the drag coefficient, C_D, set to 0 to simulate no inline aerodynamic drag acting on the vehicle.

Table 4.1 – Comparision of Air Launch vs. Ground Launch
(77 kg Vehicle / 770 km Orbit / 90.0° Inclination / Ground Launched)

		770 km Polar Ground Launched	770 km Polar Ground Launched No Drag	770 km Polar Air Launched
Gross Payload, m_{pl}	kg	0.389	0.890	1.140
Payload Fraction	%	0.50%	1.14%	1.46%

Table 4.1 suggests that air launch can mitigate the performance loss due to increased aerodynamic drag on a small launch vehicle. The baseline 77 kg vehicle is intended to be air launched.

Besides the advantage of flexibility in launch location gained from air launching the vehicle, there is a potential economic advantage as well. Air launching could reduce or eliminate range costs, which do not scale with the size of the vehicle.[63]

4.1.2 COMPONENT SCALING AND MASS SENSITIVITY

Scaling down a component can introduce manufacturing and design complexity at very small sizes. Since very small launch vehicles do not yet exist, components for them have not been developed as well. Fortunately, the miniaturization of electronics has enabled the production of small, powerful computers. This technology makes possible an avionics system for the vehicle's second stage that weighs only 50 grams (Section 3.5).

However, meeting second stage inert mass targets is a significant challenge when designing launch vehicles of this size range (15 - 2000 kg). A first stage vehicle with a vacuum Isp of 290 seconds is unable to reach low earth orbit with any mass fraction (Section 2.3.1).

Therefore, at least two stages are necessary. In order for a two stage vehicle to reach both of the orbits considered in the performance analysis (200 km / 28.5° and 770 km / 90.0°) with a significant payload fraction, the second stage must be approximately 20% or less of the overall vehicle mass (Section 2.3.3). Larger second stages can reach the 200 km / 28.5° orbit, but not the 770 km / 90.0° orbit. For the 77 kg vehicle carried through the preliminary design, this suggests possible second stages sized at 12 kg or less. If the first stage is assumed to have a propellant mass fraction, ζ_1, of 0.94, the second stage needs to have a ζ_2 greater than 0.75 (extrapolation of Figure 2.11) to reach an air launched polar orbit of 770 km. This suggests the inert mass of the second stage must be less than 3 kg. With these targets for second stage inert masses, there is considerable sensitivity of the system to added mass.

The baseline 77 kg vehicle was sized with a 6.646 kg second stage. With a ζ_2 of 0.92, this sets an inert mass target of 532 grams. The 50 g avionics system is an example of some of the challenges of non-scalable components. Assuming that that is the smallest system available to perform the necessary function, it represents 9.4% of the inert mass budget for the baseline vehicle designed. The same 50 g avionics system would only represent 1.7% of the mass budget of a 77 kg vehicle with f_1 and ζ_2 of 0.80 and 0.75, respectively.

This suggests that the second stage's mass targets are critical for the vehicle's success or failure in reaching orbit. Changing the stack fractions or propellant mass fractions, with a resulting loss in payload fraction can compensate for growth in the preliminary inert mass estimates.

Although significant challenges arise by scaling down the size of a launch vehicle, new technologies in combination with changes in operational techniques offer promise to meet these challenges to produce a viable small launch vehicle.

4.1.3 MICROPROPULSION AND ELECTRONICS MINIATURIZATION

As described in Section 1.4.3, micropropulsion technology may produce lower propulsion system mass than would result from scaling down current technology. Table 4.2 suggests this trend. The fraction of total stage made up on engines for various vehicles is listed. This percentage is considerably lower for the microrocket engine powered baseline 77 kg launch vehicle than for other vehicles using conventional engine technology. With most current launch

vehicles having inert mass fractions per stage less than 15% of total stage mass (Table 2.5), microrocket engines may allow for improved performance by significantly lowering the inert mass fraction.

Table 4.2 – Data for Various Rocket Engines[32,33,67]

Engine	Launch Vehicle	Stage	Propellants	Mass (kg)	Thrust to Weight Ratio	% Stage Mass
Microrocket Engine	Very Small Launch Vehicle	1st	N_2O_4 / N_2H_4	0.002	765	0.29%
Microrocket Engine	Very Small Launch Vehicle	2nd	N_2O_4 / N_2H_4	0.002	765	0.30%
RD-253	Proton	1st	N_2O_4 / UDMH	1280	130	1.70%
RD-210	Proton	2nd	N_2O_4 / UDMH	566	105	1.35%
RS-27A	Delta 3	1st	LO_2 / Kerosene	1091	99	1.05%
F-1	Saturn V	1st	LO_2 / Kerosene	8391	94	1.84%
Vulcain	Ariane V	1st	LO_2 / LH_2	1300	84	0.76%
LR 91-7	Titan II	2nd	N_2O_4 / Aerozine-50	565	80	1.89%
RD-180	Atlas III	1st	LO_2 / Kerosene	5393	79	2.76%
J-2	Saturn V	2nd	LO_2 / LH_2	1438	73	1.47%
RL-10A-4	Atlas IIAS	3rd	LO_2 / LH_2	168	56	1.76%
L7	Ariane V	2nd	N_2O_4 / MMH	110	25	1.17%

The ability to produce computers, communications, and electronic navigation devices that weigh on the order of the tens of grams is critical in the development of very small launch vehicles. If electronic systems continue to get smaller (Figure 1.3), these systems are likely to scale better with the vehicle size.

4.1.4 ECONOMIC CHALLENGES

As they become smaller, modern launch vehicles tend to have a higher cost per kilogram of payload. Figure 4.1 is another representation of the data in Table 1.1, and shows, for US and European launch vehicles, cost per kilogram of payload as a function of the payload size. The cost rises significantly with smaller vehicles. Some of this cost may be due to fixed costs such as range operations and component costs that do not scale down linearly with size.

An example of this type of fixed cost would be the cost of operating the carrying aircraft for an air launched vehicle. A F-15 has a hourly operations cost of roughly $2,000 per hour.[63] This cost would be fixed regardless of the size of vehicle or payload and would have to be absorbed in the per kilogram cost. These types of fixed costs are a challenge for the viability of a small launch vehicle.
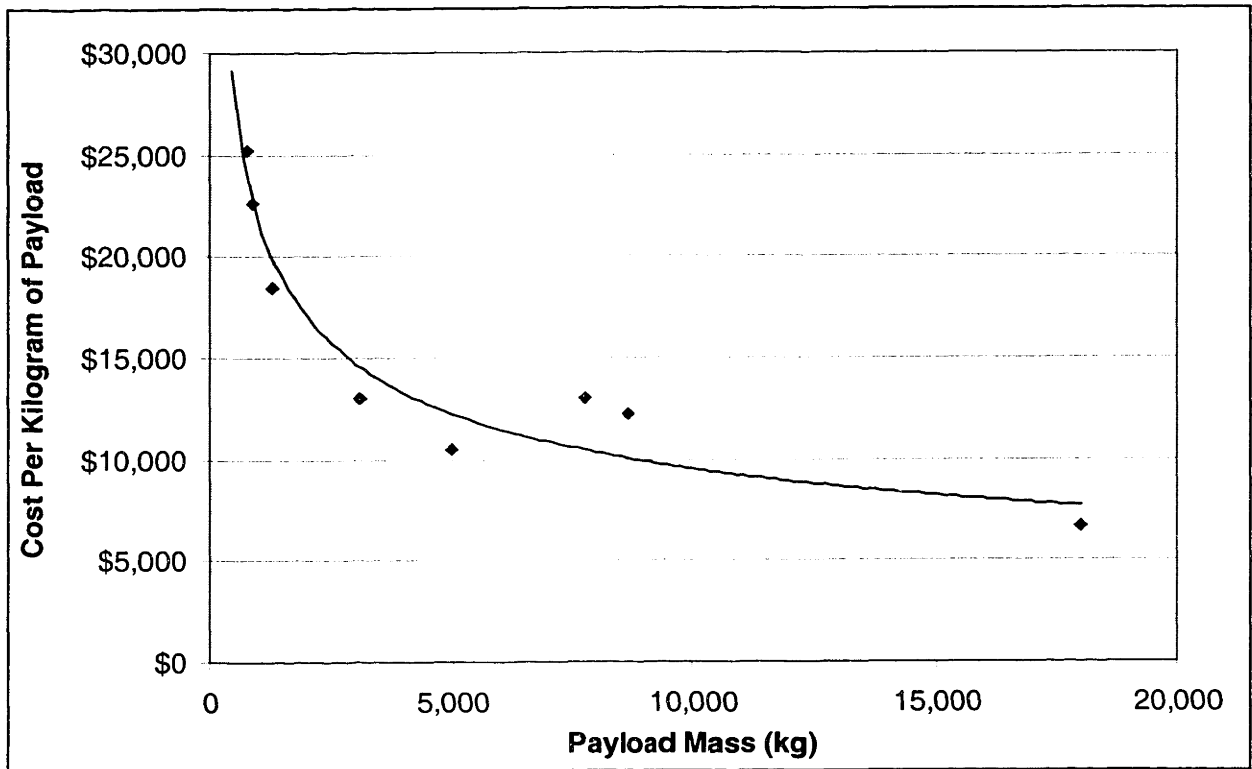
Figure 4.1 – Launch Cost vs. Payload Mass for US and European Launch Vehicles[32,33,67]

4.2 FUTURE WORK

Further work remains to be done in modeling of the vehicle's external environment, defining the subsystems in greater detail, economic analysis, and determining the interfaces between the microrocket engines and the larger scale subsystems they interface with.

4.2.1 VEHICLE LOADS

For structural sizing purposes, it was assumed that differential throttling of the microrocket engines would compensate for any aerodynamic loads on the vehicle. As a result, aerodynamic loads were approximated by considering the maximum bending moment the engines would be able to produce on the vehicle.

A complete determination of the loads, static and dynamic, acting on the vehicle must be determined. All of the static or quasistatic loads need to be determined over the mission time. Where appropriate, they need to be coupled with the dynamic loading.

Loading is different at different stages of flight. For typical ground launched vehicle, the most significant loads to the primary structure at liftoff are loads produced by engine ignition (thrust and acoustic noise), tank pressurization, and launcher release.[8]

For aerodynamic loading, the most complex loading usually occurs when the vehicle is passing through the period of transonic flight.[1] The most significant loading at this time is unsteady shock waves and air pressure changes combined with wind shears and gusts.[8] For many launch vehicles, this region imparts the worst loading conditions on the vehicle.[1]

For an air launched vehicle, the launch environment is different than for a ground launched vehicle and must be examined. Loads resulting from separation with the carrier aircraft must be combined with ignition loads, initial maneuvering loads, and significant aerodynamic loads from the aircraft's initial velocity.

4.2.2 ENGINE CYCLE REQUIREMENTS

The results from the cycle analysis on the N_2O_4 / N_2H_4 microrocket must be finalized and those results used to size critical vehicle subsystems.[42] Significant among the results will be the propellant combination the vehicle will use and the required inlet pressure to the micro-turbopumps. The inlet pressure will set the required ullage pressure in the propellant tanks. The combination of this information will finalize the tanks' structural material (Section 3.2.2).

4.2.3 FLUIDIC CONNECTIONS AND INTERFACES

Methods for delivering the propellant from the tanks to the microrocket engines need to be determined. Flow paths to separate the propellant flow to each engine and to control the flow need to be determined. Appropriate pressure losses upstream of the micro-turbopumps must be estimated and translated into increased ullage pressure requirements.

A method for introducing the helium pressurant gas into the propellant tanks must be determined. Also, tank perforations for the draining of propellant must be designed. Any mass buildup for such perforations that exceeds the current estimates must be determined. As well, valves and regulators for the helium pressurization system must be specified and selected or designed.

Leakage issues with the N_2O_4 and N_2H_4 propellants must be addressed. Appropriate safety requirements must be followed so as to avoid inadvertent contact and ignition of the hypergolic propellants.

4.2.4 INTERNAL SUPPORT STRUCTURE

Any necessary support structure for the appropriate subsystems (avionics, power, pressurization, etc.) must be designed following the loading analysis (Section 4.3.1) and its mass estimated. With this designed, assumptions such as the 20% mass margin built into the pressurization system can be revised (Section 3.6).

4.2.5 THERMAL MANAGEMENT

Careful analysis is required to ensure that the storable propellants do not freeze. Nitrogen tetroxide and hydrazine freeze at 11.5°F (262.0°K) and 34.4°F (274.2°K), respectively, at atmospheric pressure.[27]

For an air launched vehicle, the external air temperature at launch can be less than the freezing temperature of the propellants.[52] This effect must be looked into in the design of the launch tube so that the propellant isn't allowed to freeze before launch.

4.2.6 Payload Shroud

Gross payload performance calculated in the performance analysis (Chapter 2) was assumed to include the payload shroud / fairing. The size and mass of this fairing and any accompanying payload interfaces must be estimated so as to know the actual payload performance.

4.2.7 Launch Tube

The launch tube for the air launched 77 kg vehicle based on the AIM-7 air-to-air missile (Section 2.6.3) must be designed. Thermal considerations mentioned in Section 4.3.5 must be taken into account.

4.2.8 Economic Analysis

As important as the technical viability of a small launch vehicle is the economic viability of such a project. A detailed economic analysis needs to be conducted to determine the projected launch cost of such a vehicle. Fixed costs that do not scale down with vehicle size should be delineated from variable costs, which do. This will produce a better picture of launch cost for a range of vehicle sizes.

References

1. T. Sarafin (editor), <u>Spacecraft Structures and Mechanisms From Concepts to Launch</u>, *Space Technology Series*, Microcosm Inc., 1995.

2. National Aeronautics and Space Administration, <u>Buckling of Thin-Walled Circular Cylinders</u>, NASA SP-8007.

3. National Aeronautics and Space Administration, <u>Models of Earth's Atmosphere (120 to 1000 km)</u>, NASA SP-8021.

4. National Aeronautics and Space Administration, <u>Aerodynamic and Rocket-Exhaust Heating During Launch and Ascent</u>, NASA SP-8029.

5. National Aeronautics and Space Administration, <u>Wind Loads During Ascent</u>, NASA SP-8035.

6. National Aeronautics and Space Administration, <u>Liquid Rocket Pressure Regulators</u>, NASA SP-8080.

7. National Aeronautics and Space Administration, <u>Liquid Rocket Valve Components</u>, NASA SP-8094.

8. National Aeronautics and Space Administration, <u>Combining Ascent Loads</u>, NASA SP-8099.

9. National Aeronautics and Space Administration, <u>Pressurization Systems for Liquid Rockets</u>, NASA SP-8112.

10. National Aeronautics and Space Administration, <u>The 1997 NASA Aerospace Battery Workshop</u>, NASA CP-1998-208536.

11. <u>Liquid Propellant Engine Manual</u>, Chemical Propulsion Information Agency, 1982.

12. J.C. McCormick, <u>Hydrogen Peroxide Rocket Manual</u>, FMC Corporation, New York, 1967.

13. J. Becklake, "The British Black Knight Rocket," *Journal of the British Interplanetary Society*, Vol. 43, pp. 283-290, 1990.

14. S. Frazier and D. Moser, "Low Cost Liquid Upper Stage for Small Launch Vehicles," AIAA 94-3024.

15. S. Frazier and D. Moser, "Low Cost First Stage for Small Launch Vehicles," AIAA 95-3088.

16. E. Keith, "Low Cost Space Transportation: Hurdles of Implementation," AIAA 91-2048.

17. E. Keith, "Low Pressure Liquid Propulsion for Very Low Cost Space Transportation," AIAA 92-3648.

18. K. Gavitt, et. al., "TRW's Ultra Low Cost LOX/LH$_2$ Booster Liquid Rocket Engine," AIAA 97-2818.

19. W. Anderson, et. al., "Low Cost Propulsion Using a High Density, Storable, and Clean Propellant Combination," AIAA 98-3679.

20. P. Wagner and E. Cleveland, "Low Cost Rocket Motor Technology Program," AIAA 91-1959.

21. J. Anderson, Modern Compressible Flow With Historical Perspective, Second Edition, McGraw Hill, 1990.

22. F. Beer, E.R. Johnston, Mechanics of Materials, McGraw-Hill, 1981.

23. K. Wark, Tables and Figures to Accompany Thermodynamics, McGraw-Hill, 1988.

24. D. Huzel and D. Huang, Modern Engineering for Design of Liquid-Propellant Rocket Engines, Progress in Astronautics and Aeronautics Series, Volume 147, American Institute of Aeronautics and Astronautics, 1992.

25. R. Craig, Mechanics of Materials, John Wiley & Sons, 1996.

26. M. Ashby, Materials Selection in Mechanical Design, Pergamon Press, 1992.

27. G. Sutton, Rocket Propulsion Elements, Sixth Edition, John Wiley & Sons, 1992.

28. F. Incropera and D. DeWitt, Fundamentals of Heat and Mass Transfer, Fourth Edition, John Wiley & Sons, 1996.

29. D. Fryer and J. Harvey, High Pressure Vessels, International Thompson Publishing, 1998.

30. H. Bednar, Pressure Vessel Design Handbook, Second Edition, Van Nostrand Reinhold Company, 1986.

31. H. Ashley and M. Landahl, Aerodynamics of Wings and Bodies, Dover Publications, 1965.

32. S. Isakowitz, International Reference Guide to Space Launch Systems, Second Edition, American Institute of Aeronautics and Astronautics, 1995.

33. M. Wade, "Encyclopedia Astronautica," http://solar.rtd.utk.edu/~mwade/spaceflt.html

34. E. Lemmon, M. McLinden, and D. Friend, "Thermophysical Properties of Fluid Systems" in NIST Chemistry WebBook, NIST Standard Reference Database Number 69, W. Mallard and P. Linstrom (Editors), National Institute of Standards and Technology, Galthersburg, MD, http://webbook.nist.gov, November 1998.

35. National Aeronautics and Space Administration, Consumer Price Index Inflation Calculator, http://www.jsc.nasa.gov/bu2/inflateCPI.html.

36. Ledebuhr et. al., "Autonomous, Agile, Micro-Satellites and Supporting Technologies for Use in Low-Earth Orbit Missions," 12th AIAA/USU Conference on Small Satellites, 1998.

37. A. Epstein, et. al., "Micro-Heat Engines, Gas Turbines, and Rocket Engines – The MIT Microengine Project," American Institute of Aeronautics and Astronautics, 1997.

38. E. Flinn, "Micromachines Gear Up For Smallsat Applications," Aerospace America, Vol. 36, No. 10, American Institute of Aeronautics and Astronautics, October 1998.

39. K. Lohner, Microfabricated Refractory Ceramic Structures for Micro Turbomachinery, S.M. Thesis in Aeronautics and Astronautics, Massachusetts Institute of Technology, May 1999.

40. G. Watson, "Moore's Law for Intel CPU's," http://www.physics.udel.edu/scen103/intel.html.

41. CNET News.com Report, "Moore says Moore's Law to hit wall," September 30, 1997, http://www.news.com/News/Item/0,4,14751,00.html.

42. C. Protz, Systems Analysis of a Microfabricated Storable Bipropellant Rocket Engine, S.M. Thesis in Aeronautics and Astronautics, Massachusetts Institute of Technology, 1999.

43. O. Al-Midani, Preliminary Design of a Liquid Bipropellant Microfabricated Rocket Engine, S.M. Thesis in Aeronautics and Astronautics, Massachusetts Institute of Technology, May 1998.

44. The MIT Microengine Project, 1998 Annual Technical Report, MIT Proprietary, Cambridge, MA, 1998.

45. Micro Gas Turbine Generators and Technology Foundations for Micro Heat Engines, ARO Annual Presentation, MIT Proprietary, Cambridge, MA, April 1999.

46. National Aeronautics and Space Administration - Lewis Research Center, Chemical Equilibrium Code.

47. A. London, Research Assistant, Massachusetts Institute of Technology, Personal Communications, 1998-99.

48. Autometric Inc., User's Guide for Ascent v. 2.0, January 1999.

49. UTS Technologies Inc., *TK Solver 2.0 Computer Program.*

50. S. Hoerner, <u>Fluid Dynamic Drag</u>; Hoerner, New Jersey, 1958.

51. T. Middendorf, Autometric Inc., Personal Communications, 1998-99.

52. National Aeronautics and Space Administration, "1976 Standard Atmosphere."

53. Orbital Sciences Corporation, <u>Pegasus Users Manual</u>, 1998.

54. <u>USAF Rocket Propellant Handbook</u>, Volume II, Martin Marietta, 1977.

55. H. Heubush and T. Pugmire, "Acceptability of Stainless Steel for Nitrogen Tetroxide Propellant Management Devices and Flight Tankage," AIAA 88-3024.

56. H. Boyer and T. Gall (Editors), <u>Metals Handbook</u>, American Society for Metals, 1985.

57. <u>Metals Handbook Vol. 2 – Properties and Selection: Nonferrous Alloys and Special Purpose Materials</u>, ASM International 10th Edition, 1990.

58. E. Chang and N. Gokcen, "Thermodynamic Properties of Gases in Propellants and Oxidizers. Solubilities of He, N_2, O_2, Ar, and N_2O_3 in Liquid N_2O_4," *Journal of Physical Chemistry*, Volume 70, pp. 2394-2399, July, 1966.

59. R. Humble, G. Henry, W. Larson (Editors), <u>Space Propulsion Analysis and Design</u>, McGraw Hill, 1995.

60. S. Heister, Professor of Aeronautics and Astronautics, Purdue University, Personal Communications, 1998-99.

61. T. Galati, Engineer, USAF Rocket Propulsion Laboratory, Personal Communications, 1999.

62. J. Kerebrock, Professor Emeritus of Aeronautics and Astronautics, Massachusetts Institute of Technology, Personal Communications, 1998-99.

63. A. Epstein, R.C. Macclaurin Professor of Aeronautics and Astronautics, Massachusetts Institute of Technology, Personal Communications, 1999.

64. M. Spearing, Professor of Aeronautics and Astronautics, Massachusetts Institute of Technology, Personal Communications, 1999.

65. M. Martinez-Sanchez, Professor of Aeronautics and Astronautics, Massachusetts Institute of Technology, Personal Communications, 1998-99.

66. P. Young, Professor of Aeronautics and Astronautics, Massachusetts Institute of Technology, Personal Communications, 1998-99.

67. Andrews Space and Technology, *Aerospace Database*, http://www.spaceandtech.com.

68. Commercial Alcohols Inc., http://www.comalc.com.

69. S. Yuan, FMC Corporation, Personal Communications, 1999.

Appendix A - Performance Analysis Results

The performance results referred to in Chapter 2 are summarized on the following page. Results were obtained using the DAB Ascent 2.0 three degree of freedom trajectory software program, explained in Section 2.2.

Vehicle								Launch			Orbit		Performance	
mass (kg)	Isp (s)	f₁	c₁	Engines	f₂	c₂	Engines	Air/Ground	Alt (km)	Vinit (m/s)	Alt (km)	Inc (deg)	mass (kg)	Payload Fraction
5,000,000	290	0.914	0.94	6,603,043	0.086	0.92	627,616	Air	12.2	250.81	770	90.0	83151	1.64%
								Ground	0.0	0.00			56783	1.12%
1,000,000	290	0.914	0.94	1,320,609	0.086	0.92	125,523	Air	12.2	250.81	770	90.0	16594	1.63%
								Ground	0.0	0.00			11203	1.11%
500,000	290	0.914	0.94	660,304	0.086	0.92	62,762	Air	12.2	250.81	770	90.0	8286	1.63%
								Ground	0.0	0.00			5554	1.10%
100,000	290	0.914	0.94	132,061	0.086	0.92	12,553	Air	12.2	250.81	770	90.0	1650	1.62%
								Ground	0.0	0.00			1079	1.07%
50,000	290	0.914	0.94	66,030	0.086	0.92	6,276	Air	12.2	250.81	770	90.0	822.4	1.62%
								Ground	0.0	0.00			529.5	1.05%
10,000	290	0.914	0.94	13,206	0.086	0.92	1,255	Air	12.2	250.81	770	90.0	162.8	1.60%
								Ground	0.0	0.00			99.42	0.98%
5,000	290	0.914	0.94	6,603	0.086	0.92	628	Air	12.2	250.81	770	90.0	80.93	1.59%
								Ground	0.0	0.00			47.80	0.95%
2,000	290	0.921	0.94	2,615	0.079	0.92	224	Air	12.2	250.81	200	28.5	55.99	2.72%
								Ground	0.0	0.00			34.76	1.71%
								Air	12.2	250.81	770	90.0	32.07	1.58%
								Ground	0.0	0.00			17.55	0.87%
1,000	290	0.914	0.94	1,321	0.086	0.92	126	Air	12.2	250.81	770	90.0	15.93	1.57%
								Ground	0.0	0.00			8.390	0.83%
500	290	0.914	0.94	660	0.086	0.92	63	Air	12.2	250.81	770	90.0	7.862	1.55%
								Ground	0.0	0.00			3.842	0.76%
188	290	0.901	0.94	265	0.099	0.92	44	Air	12.2	250.81	200	28.5	6.210	3.20%
								Ground	0.0	0.00			2.630	1.38%
								Air	12.2	250.81	770	90.0	2.120	1.12%
								Ground	0.0	0.00			0.300	0.16%
100	290	0.914	0.94	132	0.086	0.92	13	Air	12.2	250.81	770	90.0	1.481	1.46%
								Ground	0.0	0.00			0.518	0.52%
77.0	290	0.914	0.94	102	0.086	0.92	10	Air	12.2	250.81	200	28.5	2.580	3.24%
								Ground	0.0	0.00			1.260	1.61%
								Air	12.2	250.81	770	90.0	1.140	1.46%
								Ground	0.0	0.00			0.389	0.50%
77.0	290	0.914	0.94	102	0.086	0.92	10	Air	12.2	0.00	200	28.5	2.103	2.66%
										73.77			2.255	2.84%
										147.54			2.397	3.02%
										221.30			2.529	3.18%
										295.07			2.653	3.33%
										368.84			2.773	3.48%
										442.61			2.894	3.62%
										516.37			3.008	3.76%
										590.14			3.115	3.89%

		Vehicle						Launch			Orbit		Performance	
mass (kg)	Is (s)	Stage 1 f1	S	Engines	Stage 2 f2	S	Engines	Alt/ Ground	Alt. (km)	V (m/s)	Alt. (km)	Inc. (deg)	m payload (kg)	Payload Fraction
77.0	290	0.914	0.94	102	0.086	0.92	10	Air	12.192	0.00	770	90.0	0.855	1.10%
										73.77			0.943	1.21%
										147.54			1.026	1.31%
										221.30			1.108	1.42%
										295.07			1.187	1.52%
										368.84			1.272	1.62%
										442.61			1.365	1.74%
										516.37			1.460	1.86%
										590.14			1.557	1.98%
77.0	290	0.914	0.94	102	0.086	0.92	10	Air	0.000	289.41	200	28.5	1.713	2.18%
									1.524	284.39			1.856	2.35%
									3.048	279.29			1.991	2.52%
									6.096	268.80			2.232	2.82%
									9.144	257.89			2.428	3.06%
									15.240	250.81			2.697	3.38%
									18.288	250.81			2.779	3.48%
									21.336	251.68			2.839	3.56%
									24.384	253.42			2.883	3.61%
									27.432	255.15			2.917	3.65%
									30.480	256.87			2.943	3.68%
77.0	290	0.914	0.94	102	0.086	0.92	10	Air	0.000	289.41	770	90.0	0.671	0.86%
									1.524	284.39			0.753	0.97%
									3.048	279.29			0.828	1.06%
									6.096	268.80			0.958	1.23%
									9.144	257.89			1.061	1.36%
									15.240	250.81			1.201	1.54%
									18.288	250.81			1.244	1.59%
									21.336	251.68			1.276	1.63%
									24.384	253.42			1.301	1.66%
									27.432	255.15			1.321	1.69%
									30.480	256.87			1.337	1.71%
77.0	260	0.914	0.94	102	0.086	0.92	10	Air	12.192	250.81	200	28.5	1.574	2.00%
											770	90.0	0.459	1.46%
	270										200	28.5	1.895	0.50%
											770	90.0	0.675	0.87%
	280										200	28.5	2.228	2.81%
											770	90.0	0.899	1.15%
	290										200	28.5	2.580	3.24%
											770	90.0	1.140	1.46%
	300										200	28.5	2.970	3.71%
											770	90.0	1.411	1.80%
	310										200	28.5	3.362	4.18%
											770	90.0	1.684	2.14%
	320										200	28.5	3.792	4.69%
											770	90.0	1.988	2.52%
	330										200	28.5	4.220	5.20%
											770	90.0	2.291	2.89%
	350										200	28.5	5.144	6.26%
											770	90.0	2.952	3.69%

117

m_stack (kg)	Isp-vac (s)	f₁	ζ₁	Engines	f₂	ζ₂	Engines	Air/Ground	Alt (km)	V_initial (m/s)	Alt (km)	Inc (deg)	m_payload (kg)	Payload Fraction
77.0	290	0.914	0.96	102	0.086	0.94	10	Air	12.192	250.81	200	28.5	3.189	3.98%
											770	90.0	1.631	2.07%
			0.96			0.92					200	28.5	3.043	3.80%
											770	90.0	1.496	1.91%
			0.96			0.90					200	28.5	2.891	3.62%
											770	90.0	1.356	1.73%
			0.96			0.88					200	28.5	2.743	3.44%
											770	90.0	1.220	1.56%
			0.96			0.86					200	28.5	2.596	3.26%
											770	90.0	1.084	1.39%
			0.96			0.84					200	28.5	2.447	3.08%
											770	90.0	0.948	1.22%
77.0	290	0.914	0.94	102	0.086	0.94	10	Air	12.192	250.81	200	28.5	2.729	3.42%
											770	90.0	1.275	1.63%
			0.94			0.92					200	28.5	2.580	3.24%
											770	90.0	1.140	1.46%
			0.94			0.90					200	28.5	2.424	3.05%
											770	90.0	0.998	1.28%
			0.94			0.88					200	28.5	2.274	2.87%
											770	90.0	0.862	1.11%
			0.94			0.86					200	28.5	2.123	2.68%
											770	90.0	0.725	0.93%
			0.94			0.84					200	28.5	1.972	2.50%
											770	90.0	0.587	0.76%
77.0	290	0.914	0.92	102	0.086	0.92	10	Air	12.192	250.81	200	28.5	2.205	2.78%
											770	90.0	0.853	1.10%
			0.92			0.90					200	28.5	2.048	2.59%
											770	90.0	0.711	0.91%
			0.92			0.88					200	28.5	1.896	2.40%
											770	90.0	0.575	0.74%
			0.92			0.86					200	28.5	1.744	2.21%
											770	90.0	0.438	0.57%
			0.92			0.84					200	28.5	1.591	2.02%
											770	90.0	0.300	0.39%
77.0	290	0.914	0.90	102	0.086	0.90	10	Air	12.192	250.81	200	28.5	1.732	2.20%
											770	90.0	0.467	0.60%
			0.90			0.88					200	28.5	1.580	2.01%
											770	90.0	0.332	0.43%
			0.90			0.86					200	28.5	1.426	1.82%
											770	90.0	0.196	0.25%
			0.90			0.84					200	28.5	1.254	1.60%
											770	90.0	0.059	0.08%
77.0	290	0.914	0.88	102	0.086	0.88	10	Air	12.192	250.81	200	28.5	1.313	1.68%
											770	90.0	0.118	0.15%
			0.88			0.86					200	28.5	1.160	1.48%
											770	90.0	X	X
			0.88			0.84					200	28.5	0.988	1.27%
											770	90.0	X	X

Note: "X" in the m_payload or Payload Fraction column signifies that the vehicle did not reach orbit.

118

Vehicle								Launch			Orbit		Performance	
		Stage 1			Stage 2			Air /	Alt.	$V_{initial}$	Alt.	Inc.	$m_{payload}$	Payload
m_{stack} (kg)	$I_{sp\text{-}vac}$ (s)	f_1	ζ_1	Engines	f_2	ζ_2	Engines	Ground	(km)	(m/s)	(km)	(deg)	(kg)	Fraction
77.0	290	0.900	0.94	102	0.100	0.92	11	Air	12.192	250.81	200	28.5	2.600	3.27%
								Ground	0.000	0.00	200	28.5	1.272	1.62%
								Air	12.192	250.81	770	90.0	1.085	1.39%
								Ground	0.000	0.00	770	90.0	0.285	0.37%
77.0	290	0.875	0.94	102	0.125	0.92	14	Air	12.192	250.81	200	28.5	2.598	3.26%
								Ground	0.000	0.00	200	28.5	1.249	1.60%
								Air	12.192	250.81	770	90.0	0.845	1.09%
								Ground	0.000	0.00	770	90.0	X	X
77.0	290	0.850	0.94	102	0.150	0.92	16	Air	12.192	250.81	200	28.5	2.414	3.04%
								Ground	0.000	0.00	200	28.5	1.058	1.36%
								Air	12.192	250.81	770	90.0	0.634	0.82%
								Ground	0.000	0.00	770	90.0	X	X
55.1	290	0.917	0.94	72	0.083	0.92	6	Air	12.192	250.81	200	28.5	1.753	3.09%
								Ground	0.000	0.00	200	28.5	0.719	1.29%
								Air	12.192	250.81	770	90.0	0.781	1.40%
								Ground	0.000	0.00	770	90.0	0.194	0.35%
27.5	290	0.917	0.96	36	0.083	0.90	3	Air	12.192	250.81	200	28.5	0.845	2.98%
								Ground	0.000	0.00	200	28.5	0.303	1.10%
								Air	12.192	250.81	770	90.0	0.375	1.34%
								Ground	0.000	0.00	770	90.0	0.053	0.19%

Appendix B - Pressure Tank Discharge Calculations

The Visual Basic macros written to calculate the discharge in the pressure tank are included. One of the six functions written to perform two-dimensional linear interpolation with real gas property data is also included, along with one of the spreadsheets containing the data.

```
'Function Name        : Presstest()
'Created              : June 14, 1999
'Description              : This function estimates (by time steps) an gas discharge
'                     process including heat transfer effects due to heat input
'                     to the tank.  The entire discharge procedure is contained
'                     in a loop and iterated for steadily increasing pressure tank
'                     volumes until the desired ending tank temperature is reached.


'Declare All Variables
Dim P_1i As Single          'Initial Tank Pressure  (Pa)
Dim P_1A As Single          'Tank pressure after discharge step (Pa)
Dim P_1B As Single          'Tank pressure after heating step (Pa)
Dim rho_1i As Single        'Initial Gas Density (kg/m^3)
Dim rho_1A As Single        'Gas Density after discharge step (kg/m^3)
Dim rho_1B As Single        'Gas Density after heating step (kg/m^3)
Dim T_1i As Single          'Initial Gas Temperature (deg K)
Dim T_1A As Single          'Gas temperature after discharge step (deg K)
Dim T_1B As Single          'Gas temperature after heating step (deg K)
Dim u_1i As Single          'Initial gas internal energy (J/kg)
Dim u_1A As Single          'Gas internal energy after discharge step (J/kg)
Dim u_1B As Single          'Gas internal energy after heating step (J/kg)
Dim m_1i As Single          'Initial mass of gas (kg)
Dim m_1A As Single          'Mass of gas after discharge step (kg)
Dim m_1B As Single          'Mass of gas after heating step (kg)
Dim m_1AB As Single         'Average gas mass over time step (kg)
Dim t_discharge As Single   'Duration of discharge process (s)
Dim dt As Single            'Time step length (s)
Dim h_1i As Single          'Initial gas enthalpy (J/kg)
Dim h_1A As Single          'Gas enthalpy after discharge step (J/kg)
Dim h_1B As Single          'Gas enthalpy after heating step (J/kg)
Dim mdot As Single          'Mass flow rate of gas out of tank (kg/s)
Dim V_tank As Single        'Volume of pressurant tank (m^3)
Dim clock As Single         'Time elapsed in discharge process (s)
Dim Qdot1 As Single         'Heat rate into tank (W)
Dim j As Integer            'Counter
Dim K As Integer            'Counter
Dim steps As Integer        'Number of time steps
```

```
Dim V_press As Double          'Volume of pressure tank (m^3)
Dim du As Double               'Differential change in int. energy (J/kg)
Dim V_step_US As Single        'Increment in tank volume (in^3)
Dim V_step As Double           'Increment in tank volume (m^3)
Dim T_limit_US As Single       'Desired ending tank temperature (deg F)
Dim T_final_US As Single       'Actual ending tank temperature (deg F)
Dim m As Integer               'Counter
Dim dm As Double               'Differential change in mass (kg)
Dim dQ1 As Double              'Unit of heat entering gas in time step (J)
Dim V_press_US As Double 'Volume of pressure tank (in^3)

'Set inital conditions
V_step_US = 0.1
V_step = V_step_US / (39.372 ^ 3)
T_limit_US = -30
T_final_US = -100
m = 1


Do While T_final_US < T_limit_US

'Retrieve Initial Tank Conditions from Spreadsheet "Discharge"
mdot = Worksheets("Discharge").Range("mdot").Value
t_discharge = Worksheets("Discharge").Range("t_discharge").Value
steps = Worksheets("Discharge").Range("steps").Value
T_1i = Worksheets("Discharge").Range("T_1i").Value
P_1i = Worksheets("Discharge").Range("P_1i").Value * 101325
m_1i = Worksheets("Discharge").Range("m_1ir").Value
V_press = Worksheets("Discharge").Range("V_press").Value
Qdot1 = Worksheets("Discharge").Range("Qdot1").Value

'Calculate Initial Variables
dt = t_discharge / steps
dm = mdot * dt
dQ1 = Qdot1 * dt
K = 1
j = 1

'Initial Tank Conditions
T_1A = T_1i
P_1A = P_1i
rho_1A = Density(P_1A / 101325, T_1A)
m_1A = rho_1A * V_press
u_1A = Intenergy(P_1A / 101325, T_1A) * 1000

'Loop until expansion is over
Do While (j <= steps)
```

Time tracking
clock = j * dt

Blowdown Process w/Heat Input, Real Gas Effects (Steps A-B)
m_1B = m_1A - dm
m_1AB = (m_1A + m_1B) / 2
du = (((P_1A) * dm) / (rho_1A * m_1AB)) - dQ1 '(Negative dQ1 accounts for heat input!)
u_1B = u_1A - du
rho_1B = m_1B / V_press
T_1B = T_ru(rho_1B, u_1B / 1000)   'Input for u must be in kJ/kg (thus the /1000 factor!)
P_1B = Pressure(rho_1B, T_1B) * 101325

Increment counter
j = j + 1

T_1A = T_1B
P_1A = P_1B
rho_1A = rho_1B
m_1A = m_1B
u_1A = u_1B
Loop

Placing of Final Tank Conditions Into Spreadsheet
Worksheets("Discharge").Cells(m + 4, 12) = V_press * 39.372 ^ 3
Worksheets("Discharge").Cells(m + 4, 13) = T_1B * 1.8 - 459.67
Worksheets("Discharge").Cells(m + 4, 14) = m_1B
Worksheets("Discharge").Cells(m + 4, 15) = (P_1B / 101325) * 14.696
Worksheets("Discharge").Cells(m + 4, 16) = rho_1B

Update V_press
T_final_US = T_1B * 1.8 - 459.67
V_press = V_press + V_step
V_press_US = V_press * 39.372 ^ 3
Worksheets("Discharge").Range("V_press_US").Value = V_press_US
m = m + 1
Loop

End Sub

122

```
'Function Name       : Pressure(ByVal rho As Single, ByVal Temp As Single)
'Created             : June 1, 1999
'Description          : This function uses two dimensional interpolation to return
'                       to the calling program the pressure, given the density (rho)
'                       and the temperature.

Function Pressure(ByVal rho As Single, ByVal Temp As Single)

'Declare Variables
Dim T(21) As Double              'Temperature (deg K)
Dim r(21) As Double              'Density (kg/m^3)
Dim P(21, 21) As Double          'Pressure (atm)
Dim i As Integer                 'Rows index for interpolation
Dim j As Integer                 'Columns index for interpolation
Dim v As Integer                 'Row location of value
Dim w As Integer                 'Column location of value
Dim Corner As Boolean            'Boolean variable to determine whether
                                 'point is lower right corner
Dim P_vw As Double               'Selected Pressure value (atm)
Dim P_vjp1 As Double
Dim P_vj As Double

For i = 1 To 21
  T(i) = Worksheets("P(rho,T)").Cells(i + 4, 2)
Next i

For j = 1 To 21
  r(j) = Worksheets("P(rho,T)").Cells(4, j + 2)
Next j

For i = 1 To 21
  For j = 1 To 21
    P(i, j) = Worksheets("P(rho,T)").Cells(i + 4, j + 2)
  Next j
Next i

'Find v and w

If (Temp < T(1)) Then MsgBox "Temperature Too Low"
If (rho < r(1)) Then MsgBox "Density Too Low"
If (Temp > T(21)) Then MsgBox "Temperature Too High"
If (rho > r(21)) Then MsgBox "Density Too High"

For i = 1 To 21
  If (Temp >= T(i)) Then v = i
Next i
```

```
For j = 1 To 21
    If (rho >= r(j)) Then w = j
Next j

Find rho(v,j)

i = v
j = w

Determine if point is lower right corner
Corner = i = 21 And j = 21

If Corner = True Then
    P_vw = P(21, 21)
ElseIf i = 1 Then
    P_vw = (rho - r(j)) / (r(j + 1) - r(j)) * (P(i, j + 1) - P(i, j)) + P(i, j)
ElseIf i = 21 Then
    P_vw = (rho - r(j)) / (r(j + 1) - r(j)) * (P(i, j + 1) - P(i, j)) + P(i, j)
ElseIf j = 1 Then
    P_vw = (Temp - T(i)) / (T(i + 1) - T(i)) * (P(i + 1, j) - P(i, j)) + P(i, j)
ElseIf j = 21 Then
    P_vw = (Temp - T(i)) / (T(i + 1) - T(i)) * (P(i + 1, j) - P(i, j)) + P(i, j)
Else
    P_vj = (Temp - T(i)) / (T(i + 1) - T(i)) * (P(i + 1, j) - P(i, j)) + P(i, j)
    P_vjp1 = (Temp - T(i)) / (T(i + 1) - T(i)) * (P(i + 1, j + 1) - P(i, j + 1)) + P(i, j + 1)
    P_vw = (rho - r(j)) / (r(j + 1) - r(j)) * (P_vjp1 - P_vj) + P_vj
End If

Pressure = P_vw

End Function
```

Pressure Data for Helium Gas (atm)

Temperature °F	°K	: Density, kg/m³																				
		0.14	0.5	1	2	4	5	10	15	20	30	40	50	60	70	80	90	100	110	120	130	140
-190	150	0.431	1.540	3.085	6.19	12.45	15.61	31.72	48.33	65.48	101.5	139.9	181.0	225.0	272.2	322.7	377.0	435.4	498.1	565.5	638.0	715.9
-172	160	0.459	1.643	3.290	6.60	13.28	16.65	33.83	51.55	69.83	108.2	149.2	193.0	239.9	290.1	344.0	401.8	463.8	530.4	602.0	678.9	761.6
-154	170	0.488	1.745	3.496	7.01	14.11	17.69	35.94	54.76	74.18	115.0	158.5	205.0	254.7	308.0	365.1	426.4	492.1	562.7	638.4	719.7	807.0
-136	180	0.517	1.848	3.701	7.42	14.94	18.73	38.05	57.97	78.53	121.7	167.7	216.9	269.5	325.9	386.3	451.0	520.4	594.8	674.7	760.4	852.3
-118	190	0.546	1.951	3.907	7.84	15.77	19.77	40.16	61.18	82.87	128.4	177.0	228.8	284.3	343.7	407.3	475.5	548.6	626.9	710.9	800.9	897.5
-100	200	0.574	2.053	4.112	8.25	16.60	20.81	42.26	64.39	87.21	135.1	186.2	240.8	299.1	361.5	428.8	500.0	576.7	658.9	747.0	841.4	942.5
-82	210	0.603	2.156	4.318	8.66	17.43	21.85	44.37	67.59	91.55	141.8	195.4	252.6	313.8	379.3	449.3	524.4	604.7	690.8	782.9	881.7	986.9
-64	220	0.632	2.258	4.524	9.07	18.26	22.89	46.48	70.80	95.88	148.5	204.6	264.5	328.5	397.0	470.3	548.7	632.7	722.6	818.8	921.9	986.9
-46	230	0.660	2.361	4.729	9.49	19.09	23.93	48.58	74.00	100.22	155.2	213.8	276.4	343.2	414.7	491.2	573.0	660.6	754.3	854.7	962.0	986.9
-28	240	0.689	2.464	4.935	9.90	19.91	24.97	50.69	77.20	104.55	161.9	223.0	288.2	357.9	432.4	512.1	597.3	688.5	786.0	890.4	986.9	986.9
-10	250	0.718	2.566	5.140	10.31	20.74	26.01	52.79	80.41	108.88	168.6	232.2	300.1	372.6	450.1	532.9	621.5	716.3	817.7	926.0	986.9	986.9
8	260	0.747	2.669	5.346	10.72	21.57	27.04	54.90	83.61	113.20	175.2	241.4	311.9	387.2	467.7	553.7	645.7	744.1	849.2	961.6	986.9	986.9
26	270	0.775	2.772	5.551	11.14	22.40	28.08	57.00	86.80	117.53	181.9	250.5	323.7	401.8	485.3	574.5	669.8	771.8	880.7	986.9	986.9	986.9
44	280	0.804	2.874	5.757	11.55	23.23	29.12	59.11	90.00	121.85	188.6	259.7	335.5	416.4	502.9	595.2	694.0	799.5	912.2	986.9	986.9	986.9
62	290	0.833	2.977	5.962	11.96	24.06	30.16	61.21	93.20	126.17	195.3	268.8	347.3	431.0	520.4	616.0	718.0	827.1	943.6	986.9	986.9	986.9
80	300	0.861	3.080	6.168	12.37	24.89	31.20	63.31	96.40	130.49	201.9	278.0	359.1	445.6	538.0	636.7	742.1	854.7	975.0	986.9	986.9	986.9
98	310	0.890	3.182	6.373	12.78	25.71	32.23	65.42	99.59	134.81	208.6	287.1	370.8	460.2	555.5	657.4	766.1	882.3	986.9	986.9	986.9	986.9
116	320	0.918	3.285	6.579	13.20	26.54	33.27	67.52	102.79	139.13	215.2	296.3	382.6	474.7	573.0	678.0	790.1	909.8	986.9	986.9	986.9	986.9
134	330	0.948	3.387	6.784	13.61	27.37	34.31	69.62	105.98	143.45	221.9	305.4	394.4	489.3	590.5	698.7	814.1	937.3	986.9	986.9	986.9	986.9
152	340	0.976	3.490	6.990	14.02	28.20	35.35	71.72	109.17	147.76	228.6	314.5	406.1	503.8	608.0	719.3	838.0	964.8	986.9	986.9	986.9	986.9
170	350	1.005	3.593	7.195	14.43	29.03	36.39	73.82	112.37	152.07	235.2	323.6	417.9	518.3	625.5	739.9	861.9	985.9	986.9	986.9	986.9	986.9

THESIS PROCESSING SLIP

FIXED FIELD: ill. _____ name _____

index _____ biblio _____

▶ **COPIES:** (Archives) (Aero) Dewey Eng Hum

Lindgren Music Rotch Science

TITLE VARIES: ▶☑ _____

_____

NAME VARIES: ▶☑ James _____

_____

IMPRINT: (COPYRIGHT) _____

_____

▶ **COLLATION:** _____ 125 P _____

_____

▶ **ADD: DEGREE:** _____ ▶ **DEPT.:** _____

SUPERVISORS: _____

_____

___ __ _____

___ __ _____

___ __ _____

___ __ _____

___ __ _____

___ __ _____

NOTES:

	cat'r:	date:
		page:
▶ **DEPT:** Aero		▶ S35

▶ **YEAR:** 1919 ▶ **DEGREE:** S. M.

▶ **NAME:** FRANCIS, Richard J.

_____ ▶X